# EFFECT OF LIVER X RECEPTOR TARGET GENES APOLIPOPROTEIN E AND ATP-BINDING CASSETTE TRANSPORTER A1 ON BETA-AMYLOID DEPENDENT PATHOLOGY IN ALZHEIMER'S DISEASE MODEL MICE

by

**Alexis Yvonne Carter**

BS, Clarion University of Pennsylvania, 2012

Submitted to the Graduate Faculty of

Graduate School of Public Health in partial fulfillment

of the requirements for the degree of

Doctor of Philosophy

University of Pittsburgh

2016

UNIVERSITY OF PITTSBURGH

Graduate School of Public Health

This dissertation was presented

by

Alexis Yvonne Carter

It was defended on

December 5th, 2016

and approved by

Claudette St. Croix, PhD, Associate Professor, Department of Environmental and
Occupational Health, Graduate School of Public Health, University of Pittsburgh

Iliya Lefterov, MD, PhD, Research Associate Professor, Department of Environmental and
Occupational Health, Graduate School of Public Health, University of Pittsburgh

F. Yesim Demirci, MD, Associate Professor, Department of Human Genetics, Graduate
School of Public Health, University of Pittsburgh

Donald DeFranco, PhD, Professor, Department of Pharmacology and Chemical Biology,
School of Medicine, University of Pittsburgh

**Dissertation Advisor:** Radosveta Koldamova, MD, PhD, Associate Professor, Department of
Environmental and Occupational Health, Graduate School of Public Health,
University of Pittsburgh

Radosveta Koldamova, MD, PhD

# EFFECT OF LIVER X RECEPTOR TARGET GENES APOLIPOPROTEIN E AND ATP-BINDING CASSETTE TRANSPORTER A1 ON BETA-AMYLOID DEPENDENT PATHOLOGY IN ALZHEIMER'S DISEASE MODEL MICE

Alexis Yvonne Carter, PhD

University of Pittsburgh, 2016

**ABSTRACT**

Alzheimer's disease (AD) is a progressive neurodegenerative disorder that overtime interferes with daily tasks. Late-onset Alzheimer's disease (LOAD) is a multifactorial disease with a combination of genetic and environmental risk factors. The *APOEε4* allele of Apolipoprotein E (*APOE)* is the major genetic risk factor for LOAD. However, *APOEε3* patients still account for the majority of LOAD cases, suggesting additional genetic, environmental, and lifestyle factors as risk modifiers.

We examined the effect of high-fat diet (HFD) and liver x receptor (LXR) agonist T0901317 (T0) in representative mouse models of AD phenotype. LXRs regulate cholesterol and lipoprotein metabolism. ATP-binding cassette transporter A1 (*ABCA1*) and *APOE* are major LXR target genes involved in lipid and cholesterol generation and transport and are implicated in AD pathology. We determined that *Abca1*$^{ko}$ mice have cognitive deficits. Lack of *ABCA1* impaired neurite morphology in the CA1 region of the hippocampus. We then examined the effect of HFD on memory deficits and microglia morphology in AD model mice expressing either mouse *Apoe* or human *APOE* isoforms. HFD exacerbated cognitive deficits in APP23 mice. Microglia morphology resembled activation state in HFD fed female APOE4 mice, suggesting differential response to diet. Lastly, we examined the effects of T0 on the phenotype

and transcriptome of APP/E3 and APP/E4 *Abca1* haplo-deficient mice, revealing the ability of T0 to ameliorate APOE4-driven pathological phenotype.

These findings suggest that disturbances in cholesterol metabolism may negatively impact AD-related patholoy, HFD exacerbates AD-related pathology, and that T0 treatment ameliorates APOE4-induced AD pathogenesis. These results could have clinical implications on lifestyle or dietary and pharmacological interventions for AD patients. The public health significance of this research supports efforts in developing primary prevention techniques, with the end goal of inhibiting or delaying disease onset, AD-related pathology, and promoting healthy brain aging. Targeting the LXR-ABCA1-APOE regulatory axis could be an effective therapy for individuals at risk of dementia and to treat AD patients regardless of *APOE* genotype. Further developing studies that better assess cholesterol metabolism genes in AD pathology are essential for modifying guidelines and therapies for those at risk of dementia.

**TABLE OF CONTENTS**

# LIST OF TABLES

# LIST OF FIGURES

## ACKNOWLEDGEMENT

allowed me to maintain positivity throughout this arduous journey. Thank you for bringing me late-night dinners and being by my side when I needed you the most, including riding to the laboratory in the middle of the night because I forgot keys or laptop. Without you, this journey would not have been possible. Thank you, Mom.

# ABBREVIATIONS

ABCA1/ABCG1            Adenosine triphosphate binding cassette transporters A1/G1

Aβ                     Beta-amyloid

AβO                    Beta- amyloid oligomers

AD                     Alzheimer's disease

AICD                   APP intracellular domain

APLP                   APP-like protein

APL-1                  APP-like 1

APOE/APOA-I/APOA-II    Apolipoprotein E/A-I/A-II

APP                    Amyloid precursor protein

APPL                   APP-like

BACE1                  β-site APP-cleaving enzyme 1

BBB                    Blood brain barrier

CNS                    Central nervous system

CSF                    Cerebrospinal fluid

CTF                    C-terminal fragment

FAD/EOAD               Familial Alzheimer's disease/Early-onset Alzheimer's disease

HDL                    High-density lipoprotein

HFD                    High-fat diet

| | |
|---|---|
| ISF | Interstitial fluid |
| LOAD | Late-onset Alzheimer's disease |
| LXR | Liver x receptor |
| MCI | Mild cognitive impairment |
| NFT | Neurofibrillary tangles |
| PSEN1/PSEN2 | Presenilin 1/Presenilin 2 |
| RXR | Retinoid x receptor |
| T0901317 | T0; LXR agonist |

# 1.0    INTRODUCTION

## 1.1    OVERVIEW OF ALZHEIMER'S DISEASE

### 1.1.1   History, Definitions, and Criteria

In the early 1900s, Auguste Deter – commonly known as Auguste D. – was admitted to the Frankfurt mental asylum in her 50s for rapid changes in personality accompanied by memory weakness, disorientation, unpredictable behavior, paranoia, and auditory hallucinations. German neuropathologist Alois Alzheimer documented August D.'s mental and psychosocial deterioration. After Auguste D.'s death in 1906, Alzheimer published his lecture detailing the clinical aspects and histological findings from the cerebral cortex of his former patient. In 1910, a Clinical Psychiatry textbook first introduced the eponym Alzheimer's disease (AD), now characterized by neurofibrillary tangles (NFT) and beta-amyloid (Aβ) plaques, as distinguishable from historically familiar senile dementia [1-3]. Extracellular Aβ plaques result from the abnormal proteolytic processing of amyloid precursor protein (APP). Intraneuronal hyperphosphorylated tau results from the abnormal addition of phosphate molecules and dissociation of tau protein from microtubules, which form tangles within the cell.

The National Institute of Neurological and Communicative Disorders and Stroke and the Alzheimer Disease and Related Disorders Association developed the first set of criteria for AD

diagnosis based on clinical symptoms only. Diagnostic criteria included patient and family history, clinical examination, neuropsychological testing, and assessment of symptoms over time [4]. However, the National Institute of Aging and Alzheimer's Association revised the diagnostic framework to update the diagnostic guidelines of AD. 'Preclinical AD' represents pathological changes in cognitively healthy individuals that can progress to the pre-dementia stage and manifest as prodromal AD for upwards of ten years. Cerebrospinal fluid (CSF) biomarker evidence of Aβ, tau, neurodegeneration and mild cognitive impairment (MCI) are indicative of pre-dementia. Additionally, individuals who have undergone magnetic resonance imaging and identify as amyloid positive by amyloid positron emission tomography are at an increased risk of clinical AD progression. Furthermore, cerebrospinal Aβ is a strong predictive indicator of subsequent clinical progression in individuals with subjective complaints of cognitive decline [5-8].

A definitive AD diagnosis occurs postmortem. The National Institute on Aging/Reagan Institute of the Alzheimer Association Consensus Recommendations for the Postmortem Diagnosis of AD, published in 1997, was updated because some older individuals classified as cognitively intact before death had significant AD neuropathological changes. Quantification and distribution of Aβ, NFT, and neuritic plaques receive Amyloid [9], Braak [10, 11], and the Consortium to Establish, a Registry for AD [12] scores respectively to correlate clinicopathological findings and neuropathological changes. The revisions also include assessing non-AD brain lesions to recognize co-morbidities in cognitively impaired elderly [13], illustrating the scope and complexity of AD.

Aβ pathology occurs synonymously with the hierarchial organization of brain regions, first appearing in cortical regions responsible for complex, high-ordered thinking. As AD

2

progresses, Aβ pathology lastly affects the brainstem, which regulates vital processes such as heart rate, body temperature, and blood pressure. Observations show that Aβ may drive tau pathology although these proteins have fundamentally different patterning in AD [9, 14, 15].

## 1.1.2 Epidemiology of Alzheimer's disease

According to the Alzheimer's Association, AD is the most common cause of dementia accounting for 60 to 80 percent of cases. Age is the greatest risk factor for AD. The likelihood of having AD increases with age, except for individuals who harbor rare genetic mutations. AD is not a normal part of aging, and age alone is not sufficient to cause disease. For those who do not harbor genetic abnormalities, AD is a multifactorial disease. The ε4 allele of apolipoprotein E (APOE4) is the major genetic risk factor for "sporadic" late-onset AD (LOAD). Although age and genetics are risk factors that cannot change, cardiovascular disease, obesity, diabetes, and lifestyle factors may also increase dementia risk. The prevalence, or existing cases, of Americans who have AD, is approximately 5.4 million, 5.2 million people age 65 and older, and 200,000 people under age 65 with familial AD (FAD). Further indicating the magnitude of AD, approximately one in nine people age 65 and older (11 percent) has AD. Of people age 85 and older, described as the "oldest-old", the number increases to one-third (32 percent). 4.2 million people (81 percent) who have AD are age 75 or older [16].

The incidence, or rate, of the United States population age 65 or older developing AD is approximately 476,000 in 2016. Of these incidences, the number of new cases of AD is estimated to be 63,000 among people age 65 to 74, 172,000 among people age 75 to 84, and 241,000 among people age 85 and older, considered the "oldest-old." The number of Americans

living with AD is expected to escalate as the "baby boomer" generation continues to age. By 2050, the number of new AD and dementia cases is projected to double [17].

According to the National Center for Health Statistics of the Centers for Disease Control and Prevention, AD is the sixth-leading cause of death in the United States, killing 84,767 people in 2013 [18]. Variations in case definitions and recording mortality on death certificates result in underreported AD deaths in part because of intercurrent infection like pneumonia that occurs in advanced stages of AD. Between 2000 and 2013, deaths attributed to HIV, stroke, heart disease, breast, and prostate cancer decreased, while deaths attributed to AD increased 71 percent [18]. On average, people age 65 and older survive 4 to 8 years after AD diagnosis, with some living up to 20 years with the disease [19-24], reflecting the slow progression of and morbidity associated with AD [16].

## 1.2 FAMILIAL ALZHEIMER'S DISEASE SUSCEPTIBILITY GENES

### 1.2.1 Amyloid Precursor Protein Domain Structure and Processing

Human APP belongs to the APP family of single-pass transmembrane proteins and includes APP-like proteins 1 and 2 (APLP1 and APLP2) in mammals [25, 26], APP-like 1 (APL-1) in *C. elegans*, and APP-like (APPL) in *D. melanogaster*. The extracellular N-terminus of APP contains the conserved E1 and E2 domains with heparin- and copper-binding regions. The Kunitz protease inhibitor domain in human APP can undergo alternative splicing. The short intracellular C-terminus has the highest homology due to the highly conserved YENPTY

4

(Tyrosine-Glutamic Acid-Asparagine-Proline-Threonine-Tyrosine) sorting motif. The Aβ domain is present only in human APP. APP domain structure illustrated in Figure 1.
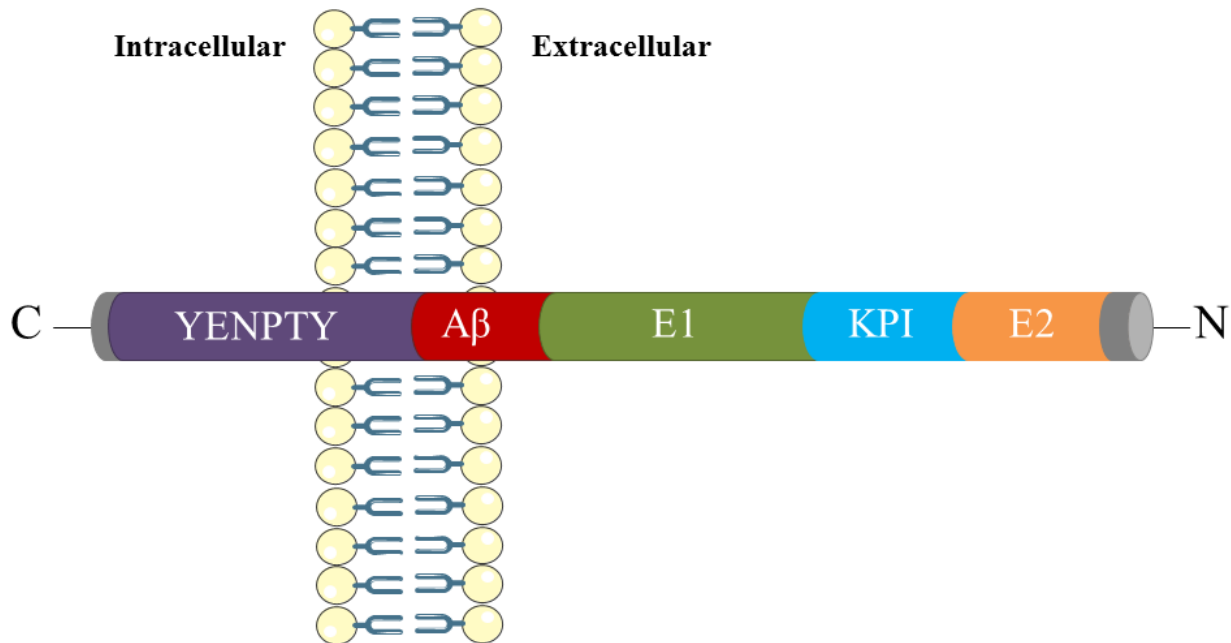


**Figure 1: Domain structure of human APP**
The extracellular N-terminus contains E1 and E2 domains. The KPI domain, also part of the N-terminus, serves as the site for alternative splicing. The C-terminus is intracellular and contains the highly conserved YENPTY sorting motif. Only human APP contains the Aβ domain.

The human *APP* gene on chromosome 21q21.3 contains 18 exons and is approximately 240 kilobases [27]. Alternative splicing of human APP yields three major isoforms with 695, 751 and 770 amino acids. APP695, the major brain isoform predominantly expressed in neurons, was the first cloned APP splice variant [28]. Unlike APP695 isoform, APP770 and APP751 expression is in non-neuronal cells [29] and peripheral tissues like the thymus, heart, muscle, lung, kidney, adipose tissue, liver, spleen, skin, and intestine [30-32]. APP714 isoform expression is in peripheral tissues like APP770 and APP751. The shorter APP639 isoform expression is exclusive to fetal tissue and the adult liver [33].

APP undergoes amyloidogenic and non-amyloidogenic processing. In the non-amyloidogenic pathway, APP on the cell surface is cleaved by α-secretase [34] in the Aβ domain (also known as α-cleavage) producing sAPPα released into the extracellular environment and prevents Aβ generation. APP α-cleavage also yields membrane-associated C-terminal fragment (CTF) C83 also known as αCTF. Sequential cleavage of C83 occurs by the multiprotein complex γ-secretase at two potential intracellular sites: the late endosome/lysosomal compartment or in the TGN. Cleavage of C83 by γ-secretase yields pathologically irrelevant p3 fragment, released through the secretory pathway or exocytosis. Cleavage of C83 by γ-secretase also yields APP intracellular domain (AICD) fragment. APP processing illustrated in Figure 2.
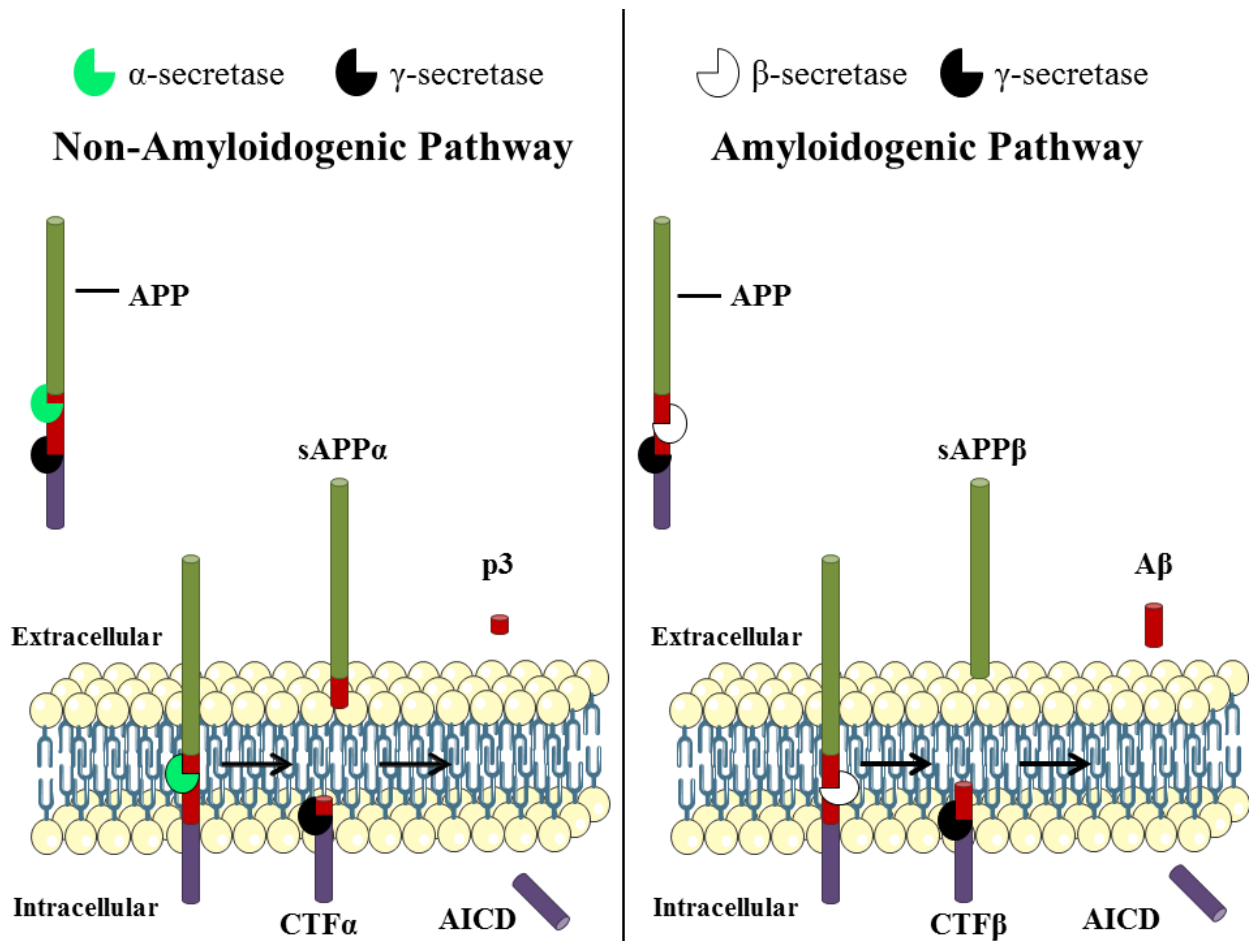
**Figure 2: Amyloid Precursor Protein Metabolism**
Metabolism of APP occurs by two competing pathways. APP is cleaved by the red Aβ domain first by α-secretase, followed by subsequent cleavage by γ-secretase to produce non-pathogenic fragments. Autosomal dominant mutations in APP, mutations in presenillins 1 and 2, which are components of the γ-secretase complex cause early-onset AD and lead to the amyloidogenic pathway. The amyloidogenic pathway involves APP cleavage by β- and γ- secretase that yields amyloid-beta peptides the length of 40 and 42 amino acid residues.

APP located on the cell surface undergoes amyloidogenic processing. APP on the cell surface is endocytosed and translocated to the early endosome containing the major β-secretase known as β-site APP-cleaving enzyme 1 (BACE1; the process also known as β-cleavage). APP cleavage by BACE1 yields sAPPβ in the endosomal lumen and targeted to the lysosome for degradation. The sAPPβ fragment released into the extracellular environment occurs after being exocytosed from the lysosome or sorted into recycling endosomes. Similar to α-cleavage, β-

cleavage of sAPPβ yields a CTF C99 or βCTF that is sequentially cleaved by γ-secretase in the late endosome/lysosomal compartment or trans-Golgi network. Cleavage of C99 by γ-secretase also yields AICD. Similar to the p3 fragment, Aβ is either released via the secretory pathway or exocytosis. Only 16 amino acids differ between the fragments generated by α- or β-cleavage (non-amyloidogenic versus amyloidogenic processing); however, only amyloidogenic processing is thought to lead to AD pathology [31, 35-37].

APP putative functions include neurite outgrowth, neural stem cell proliferation and differentiation, and synaptogenesis. Early studies showed that sAPPα stimulates proliferation of neural stem or progenitor cells isolated from embryonic rat neocortex [38, 39]. More recently, recombinant sAPPα added to cell medium rescued neural stem or progenitor cells proliferation after α-secretase inhibition [40]. Because early APP expression corresponds to the timing of neuronal differentiation, APP, sAPPα and sAPPβ may increase neural [41] and glial cell differentiation [42]. Although results from *in vitro* studies are inconsistent, sAPPα, sAPPβ, and AICD participate in the induction of neurite outgrowth [43, 44]. By fast axonal transport, APP translocates to the synaptic terminals after delivery to the axon [31, 45].

APP gene knock-out studies enhanced understanding of APP molecular and cellular functions. APL-1 knockout in *C. elegans* is lethal because it prevents the exoskeleton from shedding, a process known as molting [46, 47]. APPL knockout in *D. melanogaster* are viable, but have behavior deficits [48] and defects at the neuromuscular junction [49]. APP, APLP1, or APLP2 knockout mice [50] are viable and fertile but possess phenotype defects. APP knockout mice have reduced body (15 to 20 percent) and brain weight, reduced locomotor activity, disturbed forelimb strength, gliosis, altered long-term potentiation responses and performance in the Morris Water Maze, and defects in axonal growth, transport and white matter [51-58]. APP

and APLP2 or APLP1 and APLP2 double knockouts are postnatally lethal [59], suggesting that APP and APLP2 functions may be related or overlap in mammals [35].

## 1.2.2 The Genetic Etiology of Familial Alzheimer's disease

Familial AD (FAD), also known as early-onset AD (EOAD), is practically a genetically determined disease caused by high-penetrant mutations in *APP* and presenilins 1 and 2 (*PSEN1* and *PSEN2*) genes with an autosomal dominant mode of inheritance. Mutations in 18 of the 770 amino acid residues of APP affect substrates for APP proteolytic processing and cause FAD. The majority of APP mutations are a combination of single dominant amino acid substitutions. Identification of APP mutations in FAD stemmed from Down syndrome patients [60]. Aβ plaques from the cerebral vascular walls in DS and AD brains were purified and sequenced [61]. Along with whole-genome-linkage studies in AD families, it became evident that *APP* was the genetic defect on chromosome 21q [62-64], encouraging segregation studies to identify mutations in AD patients and their families. However, some families participating in the segregation studies were negative for *APP* mutations, indicating the involvement of other genes in FAD.

Segregation studies [65-68], genetic mapping, gene cloning and mutation screening identified *PSEN1* on chromosome 14q24.3 as a FAD gene [69-71]. Based on protein homology, *PSEN2* was identified and mapped to chromosome 1q31-q42 [72, 73]. Once discovered, the function of presenilin was unknown. We now know that presenilin is one of four different, necessary and sufficient integral membrane proteins of the γ-secretase protease complex. During maturation of the complex, the 9-TMD of presenilin is proteolytically processed, with amino and carboxyl termini that are oriented to the cytoplasmic and luminal/extracellular sides respectively

[74]. One transmembrane catalytic aspartic acid residue resides in each terminus. Presenilins provide the catalytic subunits to γ-secretase. Along with presenilin, nicastrin, Aph-1, and Pen-2 subunits complete the γ-secretase complex.

Missense mutations in *PSEN1* and *PSEN2* affect Aβ generation by skewing the cleavage of CTF C99 and altering the ratio of $A\beta_{42}$ (Aβ with 42 amino acid residues) to $A\beta_{40}$ (Aβ with 40 amino acid residues) peptides that are susceptible to aggregation [75]. An increase in $A\beta_{42}$ in plasma and fibroblasts from carriers of *PSEN1*, *PSEN2,* and *APP* mutations has been observed [76]: *In vitro,* overexpressing mutant presenilins in N2a neuroblastoma [77] and 293 cells [78] lead to an increase in $A\beta_{42}$. *In vivo*, transgenic mice overexpressing mutant presenilin in the brain with various promoters [77-80] or knock-in mutations in the endogenous mouse presenilin gene have an increase in $A\beta_{42}$ [81, 82].

To date, there are 52 pathogenic *APP* mutations in 119 probands, 215 pathogenic *PSEN1* mutations in 475 probands, and 15 pathogenic *PSEN2* mutations in 24 probands of autosomal dominant families ([http://www.molgen.vib-ua.be/ADMutations](http://www.molgen.vib-ua.be/ADMutations)). The estimated mutation frequency in FAD patient cohort is less than one percent for *APP*, six percent for *PSEN1*, and one percent for *PSEN2*, accounting for 5 to 10 percent of FAD patients [83], suggesting that there is still unknown genetic etiology of FAD.

## 1.3    BETA-AMYLOID PROPAGATION AND TOXICITY

Because Aβ plaque pathology occurs in both FAD and the common sporadic late-onset AD (LOAD), there is an association between Aβ and AD pathogenesis. The Amyloid Cascade Hypothesis formed in 1992 by John Hardy marked amyloid plaques as the earliest lesion in the

etiology of AD. The hypothesis proposed excessive Aβ accumulation and deposition of either Aβ itself or APP cleavage products as the causative agent of AD. NFT, progressive neuronal loss, and cognitive decline were a direct result of insoluble Aβ filaments and caused AD [84-86]. However, as reflected in the revised AD diagnostic framework, individuals considered cognitively intact present advanced AD neuropathology and significant Aβ plaque burden that does not correspond to impaired memory, degeneration, or change in brain volume. Also, individuals diagnosed with AD may not show pathological changes. Therefore, a paradigm shift in AD pathology proposes that soluble Aβ oligomer (AβO) intermediates, not Aβ plaques, are the toxic Aβ species that correlate with the manifestation of AD [87-90].

As previously described, C99 cleavage by γ-secretase produces monomeric Aβ peptides released into the extracellular space as a four kilodalton (kDa) peptide. Aβ monomers range from 39 to 43 amino acids ($A\beta_{39}$ to $A\beta_{43}$) and have different solubility, stability, biological and toxic properties. $A\beta_{40}$ is the major Aβ peptide identified in healthy and diseased brains (approximately 90 percent). The production of other Aβ peptides occurs at lower levels. Studies utilizing thermodynamic solubility models of Aβ peptides illustrate that longer Aβ peptides are less stable [91]. Lack of stability is characteristic of $A\beta_{42}$ compared to $A\beta_{40}$ and therefore is more prone to aggregation and fibril formation [92]. Aβ plaque formation illustrated in Figure 3.
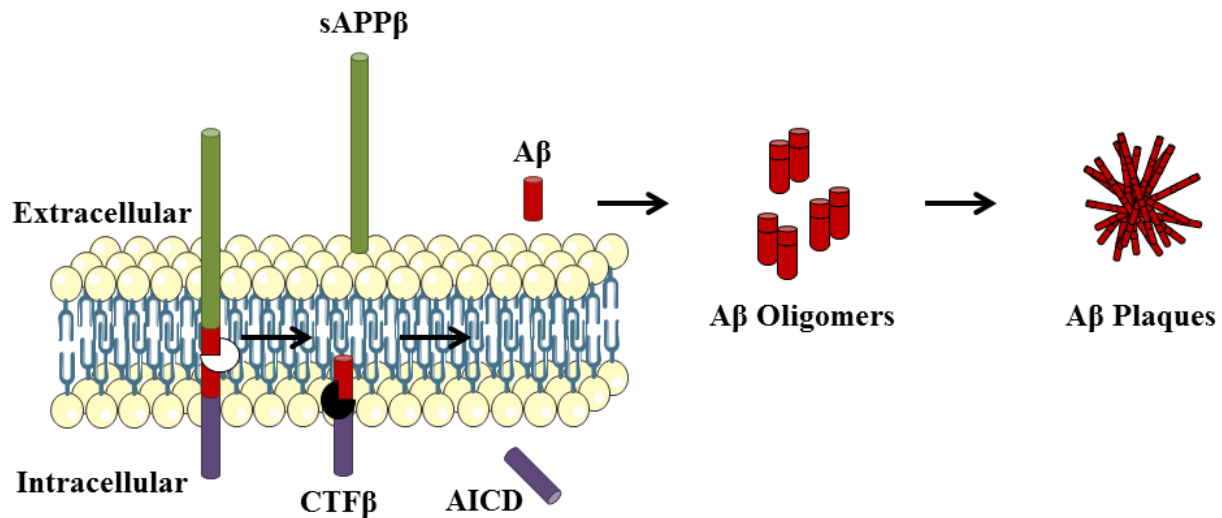
**Figure 3: Generation of Aβ Plaques**
Aβ peptide released into the extracellular space as a monomer can self-assemble to create intermediate structures such as oligomers due to "aggregation" of the peptide. The continued aggregation event leads to the formation of insoluble Aβ plaques, which represents one of the neuropathological hallmarks of AD identified during autopsy.

Nucleation-dependent polymerization, an unordered, abnormal polymerization event, leads to the formation of three Aβ assemblies comprised as monomers, AβO, and insoluble fibrils in three parallel steps *in vitro*. In the lag phase, soluble Aβ monomers first slowly create a thermodynamically unfavorable assembly of nuclei and then undergo a conformational change from α-helical to β-sheet conformation. The exponential or growth phase drives the fast and thermodynamically favorable addition of newly conformed Aβ monomers to the nuclei, creating soluble ordered aggregates known as AβO. As identified by electron and atomic force microscopy, toxic AβOs are spherical and are between 3 to 10 nm in size [89]. AβOs give rise to larger ordered protofibrils and completely formed fibrils during the final saturation phase [89, 93].

A "seeding effect" can accelerate nucleation-dependent aggregation mechanism that occurs during the growth phase. This event leads to rapid aggregation of Aβ by circumventing

12

nucleus formation and utilizing established kinetics of pre-formed fibrils. A seed may result from an admixture of Aβ species to accelerate amyloid formation. Before aggregating into fibrils, $A\beta_{40}$ *in vitro* remains monomeric, whereas $A\beta_{42}$ remains in a combination of monomer, trimer, and tetramer. Therefore, the $A\beta_{42}/A\beta_{40}$ ratio may propagate the formation of smaller, stable toxic structures [94]. Therefore, seeding rather than the major Aβ peptide constituent may influence AβO and plaque formation [93, 95-97].

## 1.4    AMYLOID PRECURSOR PROTEIN TRANSGENIC MICE

APP23 and APP/PS1 transgenic mice are widely used in AD research because they recapitulate the Aβ-dependent pathology seen clinically [98]. APP23 mice express the 695 amino acid isoform of the Swedish human mutation (APP$_{swe}$) commonly associated with FAD. Found in two families from Sweden with FAD, APP$_{swe}$ is a double mutation that substitutes leucine and lysine for asparagine and methionine at codons 670 and 671 (KM670/671NL) near the β-cleavage site [99, 100]. Therefore, APP$_{swe}$ is a better substrate for BACE1, increasing total Aβ generation [101, 102]. Aβ-dependent pathology driven by the murine Thy-1 promoter drives neuron-specific APP expression [103, 104]. Cognitive deficits progress in an age-dependent manner, with recognition and spatial working memory apparent at three moths of age [105]. At the age of six months, APP23 mice have Aβ deposits [103]. Activated glia and degeneative neurites and synapses are commonly identified near Aβ plaques [103, 106]. APP23 mice develop moderate neuronal loss in the neocortex and hippocampus brain region responsible for learning and memory [103, 107, 108].

APP/PS1 mice express mouse *App* and human APP$_{swe}$ mutation. APP$_{swe}$ mice crossed with mice harboring mutant human PSEN1 gene carrying exon 9 deletion (PS1dE9) lead to excessive Aβ plaque formation [98]. APP/PS1 mice present with plaque deposition and amyloid burden at 6 and 18 months respectively. Well characterized cognitive deficits begin at three and six months of age in the radial arm water maze (RAWM) and Morris water maze (MWM) spatial working memory tasks respectively [105, 109, 110]. Reference memory impairments begin at six months of age and persist through the life of the mouse [105, 111]. Aβ pathology in APP/PS1 mice by 18 months correspond to behavioral deficits [112]. Further supporting the role of AβOs, APP/PS1 mice present increased low-n-oligomers (dimers, trimers, and tetramers) and high-ordered oligomeric assemblies (approximately 50 to 150 kDa) in the CSF [113]. AβOs may impair memory and cognition due to their accumulation in the brains and CSF of AD patients [114-116]. AβOs impair microglial phagocytosis, which is important for preventing early Aβ deposition and contribute to brain damage by stimulating an inflammatory response [114]. Overall, these findings implicate smaller soluble Aβ oligomers, not larger aggregates or Aβ plaques, as the toxic Aβ species in AD.

## 1.5 CHOLESTEROL METABOLISM AND ALZHEIMER'S DISEASE PATHOGENESIS

### 1.5.1 Apolipoprotein E Isoforms Structure and Function

Apolipoproteins are the proteinaceous component required for the assembly, structure, function, and metabolism of lipoproteins. The apolipoprotein E (*APOE*) gene, located on chromosome

14

19q13.2, encodes three polymorphic 34 kDa glycoproteins each with 299 amino acids. The ε2, ε3, and ε4 alleles of APOE (*APOE2*, *APOE3*, and *APOE4* respectively) occur at different frequencies in the human population: ε2, 5 to 10 percent; ε3, 65 to 70 percent; ε4, 15 to 20 percent. The three alleles result in six phenotypes: APOE2/2, APOE3/3, *APOE4/4*, *APOE3/2*, *APOE4/2*, and *APOE4/3* [117-119].

The hinge region of ApoE contains approximately 20 to 30 amino acids separating the amino- (amino acid residues 1 to 191) and carboxy-terminal (approximate amino acid residues 225 to 229) domains. Residues 112 and 158 distinguish the three ApoE isoforms. Amino acid residues 136 to 150 in the amino-terminal house 6 to 8 arginine and lysine and a histidine residue critical for the interaction between ApoE and the ligand binding domain of the low-density lipoprotein receptor. A domain interaction unique to the ApoE4 enables an ionic interaction between an arginine at residue 61 (Arg-61) and Glu-255 on the amino- and carboxy-terminal domains respectively. Arg-112 instigates the domain interaction by causing the Arg-61 side chain to extend away from the amino-terminal domain. Because ApoE2 and ApoE3 possess Cys-112, the Arg-61 side chain remains tucked into the helical domain of the amino terminus. Amino acid residue 158 in the amino-terminal has various implications for each ApoE isoform. ApoE2 has Cys-158 which alters the conformation of the side chains of amino acid residues 136 to 150 causing defective binding to the low-density lipoprotein receptor. Although ApoE4 also has Cys-158, disruption of the salt bridge causes an interaction between Asp-154 and Arg-150 completely altering the receptor binding region. In ApoE3, salt bridge formation with Arg-158 and Asp-154 results in normal binding to low-density lipoprotein receptor. The lipid-binding region resides in the carboxy-terminal domain and ranges from amino acid residues 240 to 260 [119-121].

ApoE, discovered in the early 1970s, is important in controlling lipoprotein metabolism and cholesterol homeostasis [119, 122]. Liver hepatocytes are the primary site for ApoE synthesis, accounting for approximately 75 percent of ApoE production in the human body. Peripherally, ApoE participates in the endogenous pathway aiding transportation of triglycerides from the liver, through the plasma, and to sites of utilization such as adipose tissue or muscle critical for meeting energy demands. Defective receptor binding as seen with *APOE2* homozygosity, along with pre-existing conditions like diabetes or obesity, can precipitate hyperlipidemia. Overproduction of triglyceride- and cholesterol-rich very low-density lipoprotein accumulates in the plasma, causes cholesterol accumulation, and increases the risk of atherosclerosis in the peripheral arteries [119].

The brain is the most cholesterol-rich organ in the body containing 25 to 30 percent of total body cholesterol and the second most common organ that synthesizes ApoE [119, 123, 124]. The central nervous system (CNS) relies heavily on ApoE for cholesterol homeostasis and maintenance of myelin sheaths and neuronal membranes and synapses [125, 126]. ApoE and cholesterol are unable to cross the blood-brain barrier from the peripheral circulation; therefore ApoE and cholesterol synthesis occurs *in situ* [119]. Glial cells in the brain, primarily astrocytes, synthesize cholesterol *de novo* and ApoE. Astrocytes secrete cholesterol and ApoE via Adenosine triphosphate binding casette transporters A1 (ABCA1) and G1 (ABCG1), that together with phospholipids generate high-density lipoprotein (HDL)-like nascent particles. Low-density liporptein receptor family members expressed on neurons facilitate uptake of nascent HDL-like particles to maintain physiological functions [127, 128]. ApoE is abundant in the CSF, lymph, and interstitial fluid (ISF).

In the 1980s and 1990s, the Duke University Alzheimer's Disease Research Center pioneered the discovery between the genetic association of *APOE* genotypes and AD. In the mid-1980s, the Alzheimer's Disease Research Center performed a genetic linkage study in individuals who had first- or second-degree relatives with an AD diagnosis and found a linkage on chromosome 19q13 [129-131]. One decade later, Aβ-binding studies consistently presented an impurity, which after sequencing was *APOE*. In 1993, the Alzheimer's Disease Research Center published three papers once realizing that *APOE* is on chromosome 19. The earliest submission reported the association between FAD and APOE4 [130, 132]. The second report indicated that *APOE4* carriers had an increased risk of AD and lower age of disease onset [130, 133]. The third report demonstrated the association between APOE4 and LOAD [133, 134].

*APOE4* is the major genetic risk factor for LOAD [134]. Approximately 40 to 65 percent of individuals afflicted with AD carry one APOE4 allele. Age of disease onset decreases in a dose-dependent manner with APOE4 allele. Compared to APOE3 homozygosity, the risk of developing AD increases 3-fold if heterozygous for APOE4 and 15-fold if homozygous APOE4. The APOE2 is thought to be protective against AD and delay age of onset.[135]. Unlike the role of *APP*, *PSEN1*, and *PSEN2* in FAD, *APOE4* is neither necessary nor sufficient to cause disease, nor can it be used alone to diagnose AD [136-138]. ApoE isoform, structure, and function illustrated in Figure 4.
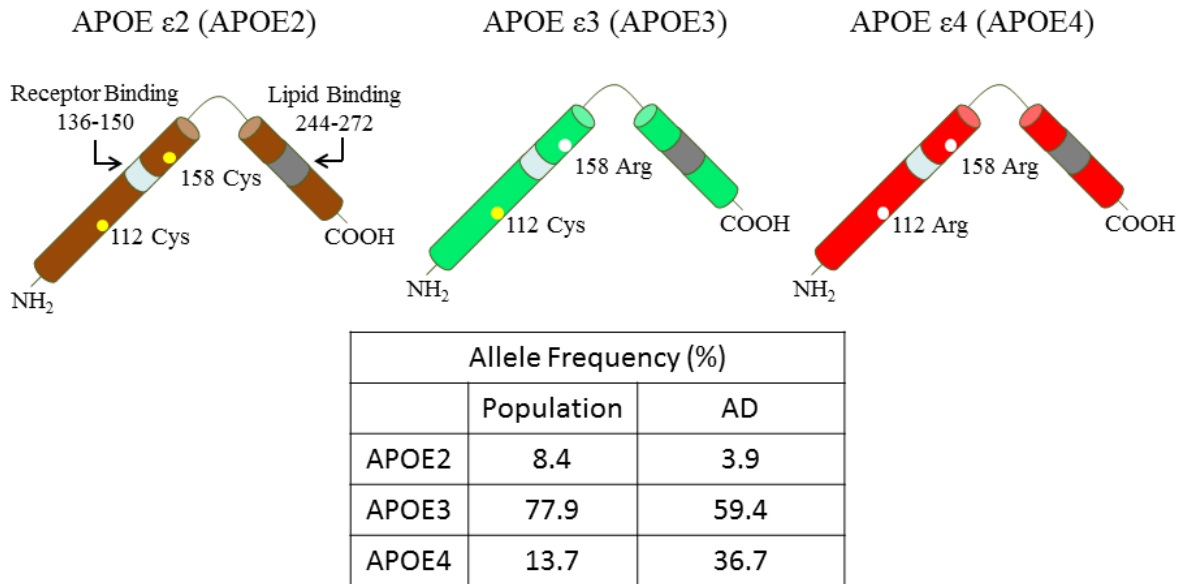
**Figure 4: ApoE isoforms, protein structure, and function**
ApoE is the major cholesterol carrier in the brain. The three ApoE isoforms have structural differences. The hinge region of ApoE separates the receptor-binding domain in the amino-terminal and the lipid-binding domain in the carboxy-terminal. ApoE2 is defective in receptor binding activity due to the cysteine at amino acid residue 158 resulting in defective low-density lipoprotein receptor binding. ApoE3 is the most common variant with function receptor and lipoprotein binding activity with an arginine at amino acid residue 158 in the N-terminus. ApoE4, the strongest genetic risk factor for LOAD, has arginine at both 112 and 158 amino acid residues with altered protein confirmation and binding preference to lipoprotein.

### 1.5.2   Apolipoprotein E Isoforms and Beta-Amyloid

Some individuals considered cognitively intact before death present with significant plaque burden. Research suggests that ApoE influences Aβ aggregation, degradation, and efflux in an isoform-dependent manner. However, the molecular mechanisms of ApoE isoforms and AD pathogenesis are not fully understood. *APOE4* carriers and CSF from AD patients have fewer ApoE/Aβ complexes and higher levels of AβO [139]. ApoE4/Aβ complexes are less stable than complexes formed with ApoE2 or ApoE3, suggesting that ApoE4 has a poor lipidation status. ApoE prefers to interact with Aβ that has conformed to β-sheets [139-141]. Therefore, ApoE4

likely promotes Aβ aggregation by accelerating the formation of ApoE4/Aβ complexes. Aβ fibrils that result from nucleation-dependent polymerization bind to ApoE4/Aβ complexes creating larger ApoE4/Aβ complexes. These large co-aggregates deposit as Aβ plaques. [139, 142]

*In vivo* experiments illustrate how amyloid model mice with gene targeted replacement human *APOE* (APOE-TR) influence Aβ deposition. APOE4-TR mice had more Aβ deposition than APOE3-TR on an amyloid mouse model background [139, 143, 144]. In 5x familial AD mutations (FAD) mice crossed with APOE4-TR, APOE3-TR, and APOE2-TR mice, Aβ deposits as compact plaques in E4FAD mice, which aggressively develop Aβ pathology, compared to E2FAD and E3FAD mice that deposit Aβ as diffuse plaques [145]. Overall, ApoE4 may promote Aβ fibrillogenesis, ineffectively prevent Aβ aggregation, or both. APP transgenic mice lacking mouse ApoE have a reduction in Aβ deposition in the form of amyloid plaques, which illustrates how critical ApoE is for Aβ deposition [139, 146, 147].

Impaired clearance of soluble Aβ consequentially leads to Aβ accumulation in the brain. Proteolytic degradation, microglia phagocytosis, and cerebrovascular system-mediated clearance through the interstitial fluid and BBB are the three major pathways for Aβ clearance from the brain. Proteases neprilysin (NEP) and insulin-degrading enzyme (IDE) degrade soluble Aβ and produce smaller enzymatic products [148]. Microglia clears soluble Aβ through either an NEP-mediated pathway or microglial phagocytosis in the interstitium [139, 149]. Aβ uptake also occurs by neurons and astrocytes in the interstitium. However, in the perivascular space, smooth muscle cells, perivascular macrophages, and astrocytes uptake Aβ. Aβ clearance across the BBB through low-density lipoprotein receptor-related protein 1, a major pathway, enters the blood and systemically cleared in the kidney and liver [150]. APOE mediates Aβ clearance in an isoform-

dependent manner (APOE4 > APOE3 > APOE2), with APOE4 being the least efficient [139]. Clearance of Aβ aggregates through microglial phagocytosis and migration are slower in APOE4-TR mice compared to E3-TR mice [151]. APOE4/Aβ complexes at the BBB clear through low-density lipoprotein receptor-related protein 1 and very low-density lipoprotein receptors at a much slower rate compared to APOE3/Aβ and APOE2/Aβ complexes [139, 152]. Although APOE4 contributes to AD pathogenesis, it is debatable if APOE4 allele confers insufficient protection towards Aβ or if it has deleterious effects. Therefore, it is also debatable if drugs should inhibit APOE4-stimulated Aβ deposition or increase the APOE4 activity.

### 1.5.3   Cholesterol and Alzheimer's disease Pathology

In addition to ApoE4 as the major genetic risk factor for LOAD, cholesterol affects AD pathogenesis by influencing APP processing although the mechanism remains unclear. Cholesterol metabolism and transport are crucial to the brain because the BBB prevents exchange between brain and plasma lipoproteins [123, 153, 154]. *De novo* synthesis of cholesterol from the endoplasmic reticulum produces active, "free" unesterified cholesterol necessary for myelin sheaths and glial and neuronal cell membranes [123, 153]. Free cholesterol converted to cholesteryl esters either accumulate in intracellular lipid droplets or effluxed through the plasma membrane by ATP-binding cassette transporter A1 (ABCA1) to extracellular lipid acceptors like un-lipidated APOE [123, 155, 156]. The role of cholesterol and ApoE illustrated in Figure 5.
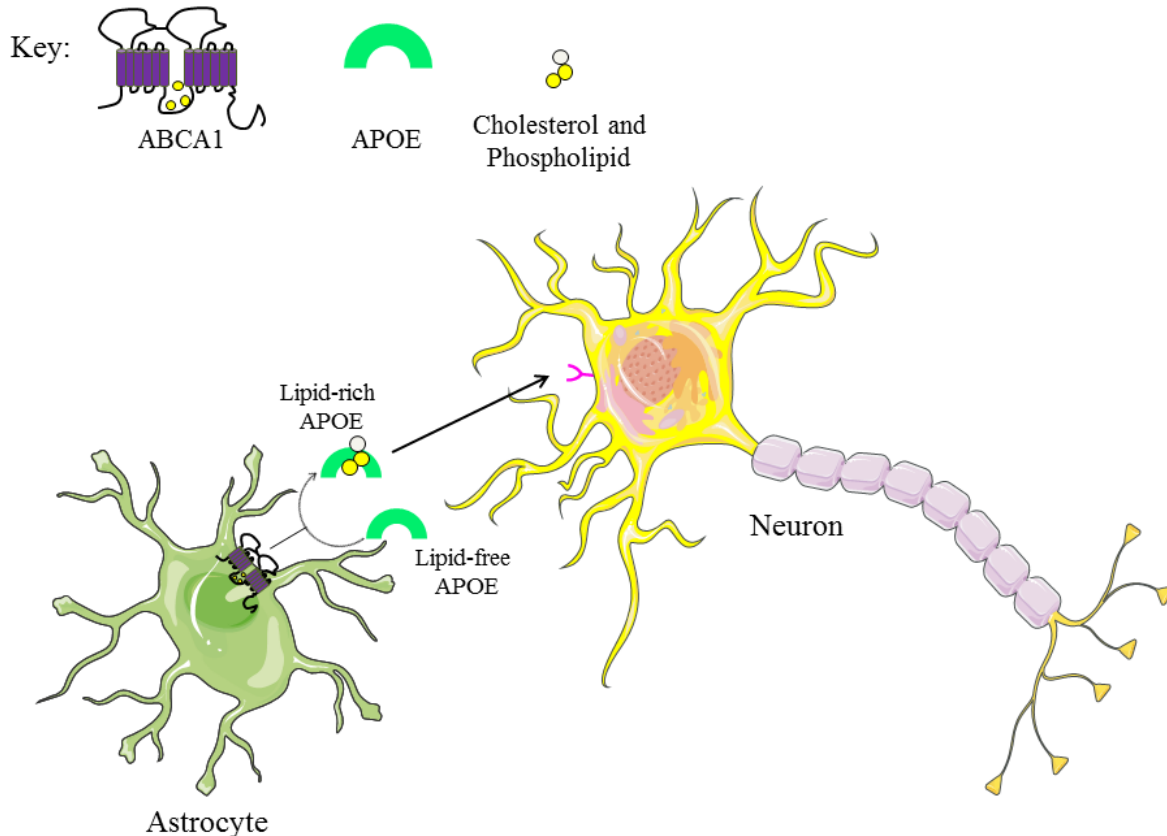
**Figure 5: The role of cholesterol in the brain**
In the adult brain, cholesterol and ApoE synthesis occurs in astrocytes. Efflux of cholesterol and ApoE occurs in an ABCA1-dependent process. ABCA1 is responsible for cholesterol efflux and ApoE lipidation to form discoidal HDL-like particles. ApoE mediates neuronal lipoprotein uptake to supply cholesterol to neurons for various neuronal functions.

The first piece of evidence showing the impact of cholesterol on Aβ production demonstrated dietary cholesterol increasing amyloid production in rabbits [157, 158]. Researchers now investigate how cholesterol levels and distribution alter APP processing that influences Aβ generation. Cholesterol-enriched in membrane microdomains known as 'lipid rafts' at the plasma membrane directly modulate secretase activity. APP is present in both raft and non-raft regions of the membrane. APP processing occurring within lipid rafts appears to be amyloidogenic, whereas APP processing occurring outside lipid rafts favors the non-amyloidogenic, α-secretase pathway [123, 159, 160]. The use of cholesterol-extracting

compounds *in vitro* reduces membrane cholesterols and decreases the activity of both BACE1 and γ-secretase leading to reduced Aβ generation [123, 159-161]. Cholesterol depletion decreases BACE1 association with lipid rafts and correlates to decreased amyloidogenic APP processing [123, 162-164]. However, acute cholesterol exposure *in vitro* promotes APP and BACE1 co-clusters in lipid raft domains which encourage rapid endocytosis. Components of the γ-secretase complex, including presenilins, associate with lipid raft, suggesting cholesterol-enriched microenvironments could directly influence secretase activity and modulate proteolytic processing of APP [160, 165-167].

### 1.5.4   ATP-Binding Cassette A1 and Alzheimer's disease

Members of the ABC transmembrane transporter superfamily shuttle lipids, sterols, metabolic products, and drugs across intracellular and extracellular membranes [168-171]. For example, ABCA1 translocates phospholipids and cholesterol primarily to lipid-free apolipoprotein A-I (ApoA-I), and to a lesser extent ApoA-II and ApoE, for generation of discoidal HDL particles peripherally [168, 172]. ATP-binding and hydrolysis cause conformational changes within the two large extracellular domains or loops of ABCA1 that are connected by intramolecular disulfide bonds and allow direct binding to ApoA-I. Intracellular lipids and cholesterol translocate and undergo 'loading' onto ApoA-I bound to ABCA1. Lipid loading occurs when lipid-free ApoA-I undergoes a conformational change to become lipidated. Lipidated ApoA-I dissociates from ABCA1 to generate discoidal HDL [173]. HDLs, primarily synthesized in the liver, participate in reverse cholesterol transport, which is a function to remove and transport excess cholesterol to the liver from cells for excretion [168, 171].

The frequency of *ABCA1* heterozygosity in the general population is 3:1,000 resulting in decreased HDL cholesterol levels [168, 174]. *ABCA1* heterozygotes with missense mutations have an increased incidence of atherosclerosis. However, not all *ABCA1* functional mutations associate with increased risk of cardiovascular disease. With over 180 mutations, missense mutations in *ABCA1* can lead to a relatively small reduction of HDL or Tangiers disease, a rare, monogenic disorder characterized by impaired cellular cholesterol efflux, extremely low HDL levels, and inefficient reverse cholesterol transport [168]. Mice lacking whole body ABCA1 demonstrated a reduction in HDL and ApoA-I, a decrease of low-density lipoprotein, and foam cell accumulation in the lungs [168, 175].

ApoE was the first genetic link between LOAD and lipid metabolism, prompting the search to associate genes involved in cholesterol metabolism and transport as AD susceptibility genes [133]. Since ABCA1 modulates apolipoproteins ApoA-I in the periphery, the significance of ABCA1 in AD originates from its ability to lipidate and stabilize APOE. ApoE modulates Aβ aggregation, toxicity, and clearance, therefore, the thought is that ABCA1 modulates ApoE metabolism in AD pathogenesis.

All brain cells express ABCA1. The presumptive role of ABCA1 in the brain is to maintain cholesterol transport primarily from astrocytes and other glial cells to neurons [168]. Research supports the role of ABCA1 in amyloid deposition, clearance, and memory deficits in representative mouse models of AD. Along with others, we demonstrated that lack of ABCA1 increases amyloid deposition, cognitive decline, and decreases soluble APOE levels in APP transgenic mice [168, 176-179]. Overexpressing brain *Abca1* in transgenic mice resulted in fewer amyloid plaques [180]. Targeted disruption of *Abca1* in mice lead to a significant reduction of

23

APOE in CNS and a drastically low level of APOE-HDL in CSF [181]. These results make ABCA1 and APOE attractive therapeutic interventions for AD.

## 1.6    APOE DIRECTED THERAPEUTICS

Nuclear receptors are master regulators of transcriptional programs involved in whole body homeostasis. The two liver x receptors (LXR) LXRα and LXRβ, which are members of the nuclear receptor family, physiologically regulate lipid and cholesterol homeostasis. LXRα expression in the liver, kidney, small intestine, spleen, and adipose tissue is critical for peripheral lipid metabolism. LXRβ expression is more common in the liver and brain. In the presence of endogenous and synthetic ligands like oxysterols and LXR/RXR agonists T0901317 (T0) and Bexarotene respectively, LXRs form obligate heterodimers with retinoid x receptors (RXRs) and peroxisome proliferator-activated receptors along with a coactivator complex to directly regulate the transcription of APOE and ABCA1.

Numerous studies confirm the beneficial effect of LXR agonists on AD pathology. Importantly, LXR agonists consistently mediate cognitive improvements in various AD mouse models and treatment paradigms [149, 182-190]. LXR agonists are beneficial by reducing Aβ plaques and soluble Aβ [149, 168, 182, 183, 185, 187-189, 191, 192]. Since LXR forms heterodimers with RXR, APP-expressing mice treated with an FDA approved Bexarotene showed a decrease in plaque load, increase in Aβ clearance, and cognitive improvement [193]. However, follow-up studies using Bexarotene confirmed cognitive improvement [194, 195], but lacked an effect on amyloid deposition [196, 197].

Two main concerns arise from the use of LXR and RXR agonists. Because RXR agonists increase plasma triglycerides, the assumption is that LXR agonist would produce a similar side effect [168, 198, 199]. However, the only published clinical trial with an LXR agonist only reported adverse CNS effects [192]. Secondly, the mechanisms underlying the ApoE4 and AD risk are still unknown, and therefore using an LXR or RXR agonist to increase ApoE levels may not be equally beneficial for *APOE3* and *APOE4* carriers. Although Bexarotene decreases AβOs and restores cognitive deficits effectively in both transgenic mice expressing human APOE3 and APOE4 [194, 200], additional research is needed to determine if LXR and RXR activation are worth targeting for AD therapies.

## 1.7    HIGH-FAT DIET AS A MODIFIABLE RISK FACTOR FOR ALZHEIMER'S DISEASE

Chronic exposure to high-energy diets may induce cognitive deficits. Readily available, low cost, energy dense, and nutrient poor foods create an obesogenic environment. Obesity and being overweight increases the risk of metabolic syndrome, type 2 diabetes, cardiovascular disease, certain cancers, respiratory conditions, fatty liver disease, and reproductive disorders. Obesity and being overweight also negatively affect mental health conditions like depression [201].

Saturated fats and simple carbohydrates are the principal components of a modern Western diet and linked to the development of obesity and AD [202]. Four major categories exist for saturated fats: saturated (SFA), trans, monounsaturated, and polyunsaturated fatty acids [203]. The composition of fatty acids, which are essential for normal physiological function, influences lipoprotein levels in the body. Although saturated fatty acid compositions vary in

natural foods, meats, and dairy products tend to have higher saturated fatty acid composition, meaning that these fatty acids lack double bonds in their composition. However, fruits and vegetables tend to be lower in total fatty acids, which are predominantly unsaturated [203].

Human epidemiological studies address fatty acid composition and cognitive decline and dementia. Population-based prospective studies evaluating the relationship between dietary fat intake and the development of age-related cognitive change over a four- and six-year timespan reported that subjects aged 65 years and older had a greater risk of developing MCI and AD due to consuming a diet with high SFAs [202, 204, 205]. A longitudinal study spanning a 21 year period examined the relationship between SFA intake and development of clinical MCI. The authors found that consumption of dietary SFA midlife increases the risk of MCI and impact specific learning and memory tasks rather than impairing global cognition [206]. Although a limitation of these studies arises from a lack of measuring body mass index (BMI) or adiposity, a relationship between SFA intake and cognitive decline became relevant after adjusting for measures like hypertension and type II diabetes which strongly correlates with BMI [202, 206, 207].

Results from rodent models are parallel to epidemiological studies and tend to support the hypothesis that high SFA intake leads to cognitive impairment. Chronically feeding high levels of SFA and trans fatty acids to rodents induces BBB dysfunction, increase Aβ aggregation, and poor cognitive performance. APP transgenic mice fed either a high SFA diet or high cholesterol diet had decreased BBB integrity and increased cerebrovascular inflammation [208]. *In vitro* administration of trans fatty acids increased amyloidogenic APP and decreased non-amyloidogenic APP compared to administration of polyunsaturated fatty acids [209].

Rodents fed a Western diet demonstrated impaired hippocampal-dependent learning and memory. Importantly, this brain region is vulnerable to toxicity and insults. The MWM behavior paradigm assesses spatial learning and memory in rodents. This task requires mice to learn to find an escape platform hidden below the surface of the pool. Visual cues placed outside the pool serve as spatial landmarks. Trials given differ depending on the spatial location at the edge of the pool. Mice with damage to brain regions vital to learning and memory such as the hippocampus will not learn to use the cues efficiently across trials and therefore will not remember the location of the platform in the MWM task [202]. Several studies illustrate that consuming high levels of SFA, a component of a Western diet disrupts learning and memory in the MWM behavior paradigm. HFD disrupts memory retention component of MWM tasks as well, which requires animals to learn to swim to the location of the hidden escape platform [202].

## 1.8    STATEMENT OF PUBLIC HEALTH SIGNIFICANCE

Although FAD involves a large genetic component, the risk for developing sporadic LOAD is largely dependent on modifiable risk factors like lifestyle and environment. Diets high in fat may alter cholesterol metabolism and increase the risk of a multitude of diseases such as obesity, cardiovascular disease, diabetes, metabolic syndrome and even AD. It is important to reiterate that AD is not a normal part of aging. Cholesterol metabolism is tightly regulated process throughout the body, including the brain. Altered cholesterol metabolism, implemented in cardiovascular disease, influences AD pathogenesis. Therefore the public health significance is that knowledge gained from this research could potentially support efforts in developing primary prevention techniques, which is imperative to the field of public health, to help reduce

modifiable risk factors for AD. This research also supports the possibility of using LXR or RXR agonists to treat AD patients regardless of *APOE* genotype. Overall, the hope is that these interventions, whether dietary, lifestyle or pharmacological will inhibit or delay disease onset and AD-related pathology and promote healthy brain aging.

# 2.0    ABSTRACT

LXRs regulate cholesterol and lipoprotein metabolism. ABCA1 and APOE are major LXR target genes involved in lipid generation and transport. APOE4, the major genetic risk factor for LOAD, is less lipidated compared to the APOE3 isoform. ABCA1 mediates cholesterol efflux to lipid-free apolipoproteins and regulates HDL generation. Previously, we showed that lacking *Abca1* significantly increases amyloid deposition and cognitive deficits in AD model mice expressing human APP. However, it is conceivable that transcriptional control of LXR target genes APOE and ABCA1 combined with environmental factors influence AD pathogenesis in mouse models representative of AD phenotypes.

To determine if ABCA1 is involved in memory deficits caused by AβOs, *Abca1*ko and WT mice were intracerebrally infused with AβOs in the hippocampus, compared to control infusion of scrambled Aβ peptide. We found a statistically significant difference between WT and *Abca1*ko mice infused with control peptide, suggesting that *Abca1*ko mice are vulnerable to the effect of mild stressors. Examination of hippocampal neurite architecture revealed a significant decrease in neurite length, number of neurite segments, and branches in *Abca1*ko mice compared to WT mice. We conclude that mice lacking ABCA1 have basal cognitive deficits preventing coping from additional stressors that do not affect WT mice.

We then examined the effect of high-fat diet (HFD) on memory deficits and microglia morphology in AD model mice expressing mouse *Apoe* or human *APOE* isoforms respectively.

29

HFD exacerbated cognitive deficits. Microglia morphology resembled activation state in HFD fed female APOE4 mice, suggesting differential response to diet. Lastly, we examined the effects of T0 on the phenotype and transcriptome of APP/E3 and APP/E4 *Abca1* haplo-deficient mice, revealing the ability of T0 to ameliorate the APOE4-driven pathological phenotype. T0 increased ABCA1 and ABCG1 mRNA expression. These findings were associated with restoration of APOE4 lipidation, cognition and reduced soluble Aβ levels. After identifying "biological processes" by GSEA, we found up-regulated genes in "Microtubule Based Process" and "Synapse Organization" biological categories in T0-treated APP/E4/Abca1$^{+/-}$ mice. In conclusion, the results suggest that T0 treatment ameliorates APOE4-induced AD pathogenesis and targeting the LXR-ABCA1-APOE regulatory axis could be an effective therapy for those at risk of dementia.

# 3.0    INTRODUCTION

Alzheimer's disease (AD) is a progressive neurodegenerative disorder. Accumulation of soluble extracellular high molecular weight oligomeric Aβ species in the brain influences the onset and progression of cognitive deficits, Aβ plaques, and tangles with hyperphosphorylated tau. In general, human amyloid precursor protein (APP) transgenic mice recapitulate AD amyloid pathology and cognitive deficits [210-212]. There are two forms of AD: A relatively rare familial, early-onset form (EOAD) and sporadic LOAD that encompasses the vast majority of AD cases. Whereas genetic factors clearly cause EOAD, no single risk factor for LOAD has been identified. LOAD bears the characteristics of a multifactorial disease where the risk is a complex interplay of genetic and environmental factors [213]. Inheritance of *APOEε4* allele of Apolipoprotein E (*APOE)* is the major genetic risk factor for LOAD [134]. *APOEε4* carriers have an earlier onset of the disease and a higher level of amyloid plaques, but the mechanism by which *APOEε4* affects amyloid deposition is still unclear [139]. At the same time, homozygous *APOEε3* AD patients still account for the majority of LOAD cases, suggesting additional genetic, environmental, and lifestyle factors as risk modifiers.

Liver X Receptors (LXRα and LXRβ) are nuclear receptor transcription factors that form obligate heterodimers with retinoid X receptors (RXR) and peroxisome proliferator-activated receptors (PPAR). LXRs are critical for executing essential functions such as cholesterol regulation, fatty acid homeostasis, and the formation of high-density lipoproteins (HDL) [214].

One of the main LXR target genes is ATP-binding cassette transporter A1 (ABCA1). ABCA1 plays a critical function in cholesterol transport by regulating the efflux of lipids from cells to lipid-poor apolipoprotein A-I (ApoA-I) and apolipoprotein E (APOE) to form HDL in the periphery and HDL-like particles in the brain (reviewed in [168]). Previous data from our lab and other groups have demonstrated significantly increased amyloid plaques in different APP transgenic mice lacking *Abca1* [178, 215-217] associated with a significantly decreased ApoE protein level in the brain. In contrast, *Abca1* overexpression in PDAPP mice decreases amyloid burden [218]. We have reported that mice expressing human APOE4 were more susceptible to *Abca1* haplo-deficiency than APOE3 mice [219] suggesting that *Abca1* genotype can interact with other genetic risk factors to worsen AD phenotype. Recently, using APP/PS1dE9 transgenic mouse model crossed to *Abca1*[ko] mice we demonstrated an increased level of Aβ oligomers in APP/*Abca1*[ko] mice. We also observed that the dendritic complexity in the CA1 region of the hippocampus but not in CA2 region was significantly impaired in APP/*Abca1*[ko] mice. An unexpected finding was that lack of ABCA1 affected the performance of *Abca1*[ko] mice in contextual fear conditioning paradigm similarly in APP transgenic and wild-type mice [220].

Previous studies demonstrated that treatment with synthetic LXR ligands decreased Aβ burden and increased its clearance [149, 182, 221]. LXR agonists significantly affect the transcriptome in the brain and decrease inflammation in mouse models representative of AD [186, 222]. Since LXRs create heterodimers with RXRs, uncovering the mechanism to establish RXR therapeutic targets has also been suggested to treat AD. It has been shown that RXR agonist bexarotene can ameliorate AD phenotype in APP transgenic mice [193]. We have demonstrated that bexarotene improves cognitive deficits in APP and wild type (WT) mice expressing human APOE isoforms [194, 200]. Furthermore, our recent data suggest that

activating RXR/LXR improves neuronal differentiation and neurogenesis in APOE4 and APOE3 targeted replacement mice [223, 224]. These studies demonstrate that increasing APOE protein level and its lipidation by targeting LXR/RXR has favorable effects on cognition, Aβ oligomers and neuronal differentiation in mice expressing human APOE4 isoform.

In addition to the genetic variants, environmental and life-style factors such as stress [225], diet [226] and physical activity were shown to affect cognition [227] and could also affect the risk of LOAD. Among those environmental factors high fat/high cholesterol diet (HFD) is one obvious culprit with several possible connections. First, APOE is the major brain cholesterol transporter and an important component of the circulating lipoproteins. Second, epidemiological studies have pointed to the significant overlap between cardiovascular and LOAD risk factors such as obesity, hypertension and type 2 diabetes; likely increasing the burden of dementia [228] especially in midlife [229]. Numerous studies with mouse models of AD suggest that HFD affects amyloid pathology and cognitive performance in adult mice [183, 230-232] and prenatally exposed offspring [233], without affecting tau pathology [234]. Recent studies examining the effect of HFD on phenotype, demonstrate significant effects on both, inflammation and cognition [235, 236]. The complexity of LOAD, encompassing interactions between APOE genotype, other genetic variants and environmental factors complicates the pursuit for a detailed etiology and successful strategy for therapeutic intervention. Therefore, we hypothesize that transcriptional control of LXR target genes such as APOE and Abca1 in combination with HFD and LXR agonism influences amyloid deposition, cognitive decline in mouse models representative of AD phenotypes.

# 4.0    MATERIALS AND METHODS


## 4.1    USE OF APPROVAL FOR TRANSGENIC MICE


All experiments followed NIH guidelines for the Care and Use of Laboratory Animals and were approved by the University of Pittsburgh Institutional Animal Care and Use Committee and carried out in accordance with PHS policies on the use of animals in research.


## 4.2    MOUSE STRAINS


### 4.2.1   APP/*Abca1*^wt, APP/*Abca1*^ko, non-transgenic *Abca1*^wt, *Abca1*^ko


*Abca1*^het mice were bred to *Abca1*^het mice to yield *Abca1*^ko, *Abca1*^het, and *Abca1*^wt littermates. All mice used in this study were purchased from Jackson Laboratory and bred onto a C57BL/6J background for greater than 11 generations. APP/PS1ΔE9 (B6.Cg-Tg(APPswe, PSEN1ΔE9)85Dbo/Mmjax; referred to as APP) transgenic mice, also purchased from Jackson Laboratory, were crossbred to *Abca1*^het mice to generate APP/*Abca1*^ko, APP/ *Abca1*^het, APP/*Abca1*^wt and corresponding non-APP expressing littermates. Non-APP expressing - *Abca1*^wt littermates are referred here in as wild-type (WT) mice. The progeny were identified by PCR. All reagents purchased through Fisher Scientific unless otherwise stated.

### 4.2.2   APP/E3/*Abca1*het, APP/E4/*Abca1*het, non-transgenic E3/*Abca1*het, E4/*Abca1*het

APP/PS1ΔE9 mice [237, 238] and Abca1$^{+/-}$ heterozygous mice were purchased from The Jackson Laboratory (Bar Harbor, ME). Human *APOE4*+/+ and *APOE3*+/+ targeted replacement mice (*APOE*-TR) were originally purchased from Taconic (Germantown, NY). All mice that were either purchased or bred for at least ten generations were on C57BL/6 genetic background. APP/PS1ΔE9/APOE4+/+/Abca1$^{+/-}$ and APP/PS1ΔE9/APOE3+/+/Abca1$^{+/-}$ (referred to as APP/E4/Abca1$^{+/-}$ and APP/E3/Abca1$^{+/-}$ respectively) as well as non–transgenic, expressing endogenous APP littermates (referred to as E4/Abca1$^{+/-}$ and E3/Abca1$^{+/-}$) were bred as previously described [219].

### 4.2.3   APP23, APP/E3, APP/E4

APP23 transgenic mice (C57Bl6 background) express human APP751 familial Swedish AD mutation (APPK670N, M671L) that is driven by the murine Thy-1 promoter and restricted to neurons [239]. APP/PS1ΔE9 mice were bred to targeted replacement APOE3+/+ and APPE4+/+ mice to generate APP/PS1ΔE9/APOE3+/+ and APP/PS1ΔE9/APOE4+/+ (referred to as APP/E3 and APP/E4, respectively) [219].

## 4.3    ANIMAL DIETS

### 4.3.1   LXR Agonist T0901317

T0901317 (T0) was purchased from Cayman Chemical (Ann Arbor, MI). All other materials were purchased through Fisher Scientific, unless otherwise noted. At five–months of age, 104 APP transgenic and non–transgenic controls (APP/E4/Abca1$^{+/-}$, 11 females and 15 males; APP/E3/Abca1$^{+/-}$, 12 females and 17 males; E4/Abca1$^{+/-}$, 14 females and 9 males; E3/Abca1$^{+/-}$, 13 females and 13 males) were randomly assigned to vehicle (control) or T0 fed diet. Each diet was prepared as previously described [191]. Briefly, T0 was dissolved in dimethyl sulfoxide (DMSO), Cremophor (Sigma–Aldrich, St. Louis, MO), then double distilled water (final 0.03% DMSO in prepared food), mixed with milled standard chow (Prolab® Isopro® RMH 3000, 5P76, LabDiet®, St. Louis, MO) and divided into daily portions. The diet was dried in order to achieve a 0.028% (w/w) T0 drug concentration and a dosage of 20 to 25 mg T0/kg mouse/day. Standard chow for the vehicle group was prepared as described, but only containing DMSO and Cremophor. Mice were subjected to behavioral testing after one month (28 days) on corresponding diet. Age– and gender matched non–transgenic littermates were used as controls for behavior experiments.

### 4.3.2   High Fat Diet

Male and female APP23 mice (mean age 11.7 months) were randomly assigned to ND (Prolab Isopro RMH 3000, Lab Diet) or HFD (D12079B RD Western Diet, Research Diets). After 3 months of feeding, behavior was assessed at mean age of 14.7 months. Similarly, male and

female APP/E3 and APP/E4 mice at mean age of 3.5 months were randomly assigned to a diet and feed for a 3-month period followed by behavioral testing (mean age 6.5 months).

## 4.4 CANNULA IMPLANTATION

To examine the effects of Aβ oligomers on memory, mice were infused with Aβ oligomers directly into the hippocampus through guide cannulas. Following anesthesia with isoflurane, the head was shaven and sterilized with two separate iodine - alcohol washes. A 50% mixture of bupivacaine and lidocaine were applied to the surgical site and ophthalmic ointment applied to the eyes. The head was leveled in a stereotaxic frame and an incision made exposing the dorsal aspect of the skull. Two holes were drilled into the skull (coordinates: P=2.46 mm, L= +/-1.50 mm) and 26-gauge guide cannulas (Plastics One) were lowered into the dorsal part of the hippocampi to a depth of 1.30 mm. Cannulas were fixed to the skull with acrylic dental cement attached to two bone anchoring screws and the surgical opening sutured closed. Animals were allowed to recover for 8 days before behavioral testing started.

## 4.5 BETA-AMLOID OLIGOMER PREPARATION

Under a fume hood, 1 mg of $A\beta_{42}$ peptide (American Peptide Company) was dissolved in ice cold 1,1,1,3,3,3-Hexafluoro-2-Propanol (HFIP, Fluka) to obtain a 1 mM solution then vortex for few seconds. The solution was quickly aliquoted into 3 polypropylene vials and dried with a gentle stream of $N_2$ to obtain a clear peptide film in the bottom of the vials. Prior to use, one film

was re-suspend in anhydrous DMSO to form a 5 mM solution, sonicated in water bath for 10 min and diluted 200X with sterile PBS buffer. Aβ samples were left at room temperature for 24 hrs to form oligomer complexes and stored at –20° C until use. The same concentration of scrambled Aβ (AnaSpec) was dissolved in vehicle and utilized as a negative control.

## 4.6 BETA-AMYLOID OLIGOMER CHARACTERIZATION

### 4.6.1 Western Blot

To examine Aβ oligomers on Western blotting, proteins were resolved on 4–12% Bis-Tris gels (Invitrogen) and transferred onto nitrocellulose membranes. These membranes were probed with 6E10 antibody (1:1000; Signet) and immunoreactive signals visualized using enhanced chemiluminescence.

### 4.6.2 Dot Blot

For detection of prefibrillar Aβ oligomers, 1 μg of protein was spotted on a nitrocellulose membrane and probed with A11 antibody (1:2000, Invitrogen). The membranes were probed with anti-rabbit secondary antibody, and immunoreactive signals visualized using enhanced chemiluminescence. The exact same amount of samples was spotted on additional dot blots and probed with 6E10 antibody and Bradford reagent for normalization.

### 4.6.3 Electron Microscopy

Imaging was performed as before [240]. Briefly, time zero and 24 hr incubated Aβ oligomer aliquots were placed on freshly glow-discharged carbon-coated grids (Electron Microscopy Sciences) and incubated for 1 min. Excess sample was removed with filter paper and the sample grid was then washed with deionized water, stained with 1% uranyl acetate (w/v) solution for 3 s, and blotted. Grids were imaged using Tecnai T12 microscope (FEI Co.) operating at 120 kV and 30,000 × magnification and equipped with an ultrascan 1000 CCD camera (Gatan) with post-column magnification of 1.4×.

## 4.7    BEHAVIORAL TESTING

### 4.7.1   Morris Water Maze

Behavioral tests to assess spatial navigational learning and memory retention were performed with a modified version of the Morris water maze (MWM) as before [183]. Briefly, in a circular pool of water (diameter 122 cm, height 51 cm, temperature $21 \pm 1$ °C), we determined the ability of mice to form a spatial representation between a safe but invisible platform (10 cm diameter; submerged 1 cm below the surface or the water) and visual cues surrounding the pool. Animals were handled for two days prior to testing and received a habituation trial, during which they were allowed to explore the pool of water without the platform present for 1 min. Beginning the next day, they received four daily hidden platform training (acquisition) trials with 5 min inter-trial interval over five consecutive days. Animals were allowed 60 s to locate the platform and

39

rest there for 20 s. Mice that failed to find the platform were lead to the platform by the experimenter and allowed to rest there for 20 s. Twenty-four hours following the last acquisition trial, a single 60-s probe trial was administered to assess spatial memory retention. For the probe trial, animals were returned to the maze as during training but with no platform present. Performance was recorded with AnyMaze video tracking (Stoelting Co.) during all phases. During the acquisition trials, escape latency and path length were subsequently used to analyze and compare the performance between different genotypes. In addition, the swimming speed during the acquisition phase was analyzed (this was used to evaluate the locomotor activity), and mice with swimming speed significantly lower than the mean speed were disqualified from the analysis. The latency to reach the target quadrant and time spent in the target quadrant were recorded and analyzed during the probe trials.

### 4.7.2   Radial Water Maze

Two day radial arm water maze (RWM) was used to measure the ability of mice to form a spatial relationship between a safe, but hidden platform and visual cues surrounding the maze [219]. The RWM consisted of six arms (20 cm wide, 40 cm long, 8 cm high walls above the water) and a central area (30 cm diameter), filled with water (temperature, $21 \pm 1°C$) to a level 1 cm above the hidden platform (10 cm diameter). All animals were handled for 2 min for 2 consecutive days before behavioral testing and 1 day before testing allowed to explore the water maze without the platform present. Acquisition testing was performed over 2 consecutive days with mice trained in groups of five or six. Each day, a mouse received two 6 trial blocks and a final 3 trial block (total of 15 trials per day) with a 30 min rest between blocks. Thirty minutes prior to each training block animals were infused with the Aβ oligomer or scrambled Aβ. Briefly, the dummy cannulas

were removed and infusion cannulas, attached to microsyringe pump by polyethylene tubing, were placed in the guide cannula. Aβ oligomer or scrambled Aβ (final volume of 1 μl per hemisphere) was infused over 1 min, the cannulas left in place for 1 min to allow for diffusion of sample and finally dummy cannulas replaced. Each animal received three infusions of Aβ oligomer or scrambled Aβ prior each of the 3 training blocks (2 - 6 trial blocks and 1 - 3 trial block).

During day 1 of training, a visible platform (flag projecting 6 cm from the platform) was used during trials 1, 3, 5, 7, 9, and 11 to define the rule of a safe platform. All other trials consisted of animals finding the location of a hidden platform. Animals were allowed 60 s to find the platform and 20 s to rest on it. Mice that failed to find the platform were led there by the experimenter and allowed to rest there for 20 s. All animals in a group completed the trial before proceeding, providing a 5 min inter-trial interval. The start location was changed for each trial and the platform location was changed between groups. Performance was recorded with an automated tracking system (AnyMaze; Stoelting Co.) during training. During the acquisition phase, total number of incorrect arm entries and time errors were combined for the overall performance of an animal during a trial. An incorrect arm entry was defined as the entry of 50% of the animal's body into an arm that did not contain the hidden platform. A time error was defined as the failure of an animal to enter an arm after 15 s elapsed. For the 15 daily trials, performance during 3 consecutive trials was averaged into a block (total of 5 blocks per day). During the open pool task of training, speed and latency to the platform were used to compare the performance between genotypes.

### 4.7.3   Novel Object Recognition

Changes in long term memory were assessed utilizing a novel object recognition paradigm as before [194]. On day 1 of testing mice were acclimated to the behavioral arena (40cm X 40cm X 30cm tall- white plastic box) for 5 min. For training, 24 hrs following acclimation mice were placed into the center of the arena with two similar objects and allowed to explore the objects for 30 total visits but no longer than 10 min. The two identical objects were made of weighted plastic to prevent movement and located in the southeast and northwest quadrant, spaced equidistant from the arena walls. This training trial was completed twice separated by a 10 min interval. Twenty-four hours following the last training trial one object was replaced with a novel object, the object replaced was alternated for each mouse to avoid a side preference and mice were again placed into the arena and allowed to explore the objects for 30 total visits or 10 min. An exploratory visit was defined as the mouse sniffing, climbing on, or touching an object or within 1 cm while facing an object. Testing was recorded with automated tracking system (AnyMaze; Stoelting Co.) and the arena was cleaned with 70% alcohol between trials to eliminate olfactory cues. An increased percentage of visits exploring the novel object (number of novel object visits / total visits $\times$ 100) was considered an index for improved long term memory retention in this task.

For the publication, "Liver X Receptor Agonist Treatment Significantly Affects Phenotype and Transcriptome of APOE3 and APOE4 Abca1 Heterozygous Mice," novel object recognition (NOR) was performed as previously described with modifications [241]. On day one, mice were acclimated to the behavioral arena (White plastic box, 40–cm x 40–cm x 30–cm) for ten minutes. Twenty-four hours following acclimation, mice were placed in the center of the arena with two similar objects (Tower of Lego® bricks 8cm x 3.2cm, built in white, blue,

yellow, red and green bricks) and allowed to explore the objects for two trials lasting five minutes each, with a five-minute inter-trial interval. The similar objects were located in the east and west quadrant and spaced equidistant from the arena walls. Twenty-four hours following the habituation, one object was replaced with a novel object (large metal bolt and nut of similar size). Mice were placed in the arena and allowed to explore the objects for ten minutes. Exploratory visit was defined as the mouse sniffing, climbing on, or touching an object or within three centimeters while facing an object. Exploration time was recorded and scored with ANY-maze software (Stoelting Co., Wood Dale, IL). The arena was cleaned with 70% ethanol between animals to eliminate olfactory cues. Exploration time was calculated by dividing time exploring the novel object by total time exploring objects. Animals exhibiting memory impairments spent less time exploring the novel object.

### 4.7.4   Contextual Fear Conditioning

Contextual fear conditioning (Equipment obtained from Stoelting Co., Wood Dale, IL) was performed as previously described with minor modifications [239]. Briefly, mice were placed in a conditioning chamber for two minutes, followed by 30 seconds of tone representing the conditioned stimulus (Sound, 2800 Hz; Intensity, 85 dB). At the end of the tone, mice received a foot shock (0.7 mA) for two seconds through the floor of the chamber. The cycle was repeated once more. At the end of the second cycle, the mice remained in the chamber for 30 seconds before returning to their housing cages. Twenty-four hours after the training phase, contextual fear conditioning was assessed and consisted of measuring freezing behavior for five minutes in the original conditioning chamber. Twenty-four hours after the contextual phase, freezing behavior during the cued fear conditioning was assessed and consisted of placing mice in a novel

43

context for two minutes (plain gray walls replace by black and white stripped walls), followed by exposure to the conditioned stimulus for three minutes. Freezing behavior was defined as the absence of movement except for respiration. Freezing behavior was recorded using ANY-maze software and calculated as percent freezing of the total time spent in the chamber.

## 4.8 ANIMAL TISSUE PROCESSING

Mice were anesthetized with Avertin (250 mg/kg of body weight, i.p.) and blood was drawn from the heart. The mice were perfused transcardially with 25 ml of cold 0.1 m PBS, pH 7.4. One hemisphere was drop fixed in 4% phosphate-buffered paraformaldehyde at 4°C for 48 h before storage in 30% sucrose.

## 4.9 HISTOLOGY, IMMUNOHISTOCHEMISTRY, AND QUANTITATION

### 4.9.1 X34

Histology, X-34 and 6E10 immunohistochemistry was performed as previously described [223, 239]. Brain hemispheres were removed from the 30% sucrose solution and embedded in HistoPrep™. Brain hemispheres were cut into 30 μm coronal sections. Six sections starting at the formation of the dentate gyrus (-1.2mm from Bregma) and separated by 450 μm were used for immunohistochemistry. Sections were stored in glycol-based cryoprotectant at -20°C until staining. For X-34 staining, sections mounted on positively charged glass slides were washed in

PBS and treated with 1,4-bis(3-carboxy-4-hydroxyphenylethenyl)-benzene (X-34) for 10 min each. Slides were destained with 0.2% NaOH in 80% ethanol for 3 min and washed with PBS before and after destaining.

### 4.9.2    6E10

For 6E10 staining, sections adjacent to those used for X-34 were immunostained with biotinylated 6E10 antibody (803009, Biolegend, San Diego, CA). Antigen retrieval was done on free-floating sections with 70% formic acid. Blocking of endogenous peroxidases and avidin-biotin followed antigen retrieval. Then, sections were incubated with 6E10 biotin-labeled antibody (1:1000) overnight at 4°C and developed with Vectastain ABC Elite kit and DAB substrate (Vector Laboratories, Burlingame, CA). After staining, sections were coverslipped with Permafluor. All sections were examined under the microscope using the Nikon Eclipse 90i at 10× magnification. For quantitative analysis, percent positive staining was defined as the percent area covered by X-34 or 6E10 staining using NIS Elements software (Nikon Instruments Inc., Melville, NY).

### 4.9.3    IBA1

For identification of activated microglia, brain sections were incubated with IBA-1 primary antibody (019-19741, Wako Chemicals) followed by incubation with secondary Dylight 594 labeled antibody (Vector Labs) and counterstained with H33342[242]. For IBA-1 imaging in cortices, 2 confocal images were captured dorsal and lateral to the hilus of the dentate gyrus (Nikon A1, 40X magnification). The FilamentTracer (Imaris, version 7.1.1, Bitplane) was

utilized to determine neuronal patterning in the hippocampal CA1 region and IBA-1 positive microglia. Unbiased examination and quantitation of neurite size and length required manual introduction. Neurite length was normalized to the number of H33342 stained nuclei. The morphology of IBA-1 positive microglia was determined by seed points labeling cell bodies and dendrites and normalized to the filament count.

### 4.9.4   MAP2 and Neurite Morphology

Neurite morphometry analysis was performed as described before [220]. Coronal brain sections (30 μm thickness) were obtained with a sliding microtome. Sections were stored in cryoprotectant at -20°C until staining commenced. For immunofluorescence labeling, brain tissue sections were rinsed 3 times in PBS for 10 min and incubated with 1% Triton X-100 (permeabilizing reagent) in PBS solution for 5 h at 4°C.  The tissue was washed 3 times in PBS for 10 min each and blocked with 10% serum and 0.3% Triton X-100 in PBS solution for 30 min at RT. The sections were incubated for 72 h at 4°C with microtubule-associated protein 2 (MAP2) primary antibody (1:2000; Millipore), a cytoskeletal protein that binds to tubulin and stabilizes microtubules and is essential for the development and maintenance of neuronal morphology. Tissue was rinsed 3 times in PBS for 10 min each to remove unreacted primary antibodies. Tissue sections were incubated with Cy3-conjugated anti-sheep antibody (1:500; Jackson-ImmunoResearch) secondary antibody for 2 hr at RT. Sections were washed 2 times in PBS for 10 min and counterstained with H33342 nuclear reagent (1:3000; Sigma-Aldrich) for 5 min at RT. Sections were washed 3 times in PBS for 10 min each and then, were mounted onto plus-coated slides and coverslipped using gelvatol mounting media. The FilamentTracer module of Imaris (Bitplane), which facilitates 3D neuron reconstruction, was utilized to determine

46

neuronal patterning and connections of hippocampal brain sections. The MAP2 (Cy3) channel was used to quantify total neurite length, the number of segments, and the number of branches in the CA1 and CA2 regions of the hippocampus. 5 sections per animal starting at the beginning of the dentate gyrus and every 300 μm were used. For neurite analysis, 4-5 confocal images (considered replicates) were acquired for the CA1 region while 3-4 confocal pictures were captured for the CA2 region. Confocal fluorescence micrographs were obtained using a 60x lens magnification at very high resolution (100 μs exsposure). For unbiased examination, the size and the length of the neurites were the only parameters that required manual introduction. For parity, image assessment must use identical grid dimensions. Neurite length was normalized to the number of MAP2 neurons.

## 4.10    TRANSCRIPTOME ANALYSIS

### 4.10.1  RNA Isolation, qPCR, and Sequencing

RNA was isolated from the cortex and purified according to the RNAeasy mini kit manufacturer protocol (Qiagen, Valencia, CA) as previously described [224]. RNA quality was determined using the 2100 Bioanalyzer instrument (Agilent Technologies, Santa Clara, CA). Samples with a RIN > 8 were used for library generation and sequencing (mRNA Library Prep Reagent Set; Illumina, San Diego, CA) on the Illumina HiSeq2000 instrument at the Functional Genomics Core, University of Pennsylvania, Philadelphia, PA (http://fgc.genomics.upenn.edu/). Subread (v1.5.0, http://subread.sourceforge.net) was used to align sequencing reads to the mouse genome (mm9). EdgeR package (v3.14.0) in R environment (v3.2.4) was used to analyze the differential

gene expression. qPCR assays were performed using TaqMan™ Gene Expression Assay or Power SYBR® Green PCR Master Mix (Applied Biosystems, Foster City, CA). cDNA was synthesized using EcoDry™ Premix, Random Hexamers (Clontech, Mountain View, CA).

### 4.10.2 Functional Annotation Analysis

Functional annotation clustering was performed using two different bioinformatics databases. We first used Database for Annotation, Visualization and Integrated Discovery (DAVID; http://david.abcc.ncifcrf.gov/; Huang et al., 2009) to determine gene ontology (GO) terms. Additional analysis with data from EdgeR output tables was performed using Gene set enrichment analysis (GSEA v2.2.2, https://www.broadinstitute.org/GSEA) with a gene matrix set for Biological Process (BP) (c5.bp.v5.1.symbols.gmt) [243, 244].

## 4.11    BIOCHEMICAL ANALYSIS

### 4.11.1 Western Blot

To prepare lysate for both Western blotting and ELISA, frozen cortices were homogenized in a glass Dounce containing tissue homogenization buffer (250 mM sucrose, 20 mM Tris base, 1 mM EDTA, and 1 mM EGTA (Sigma–Aldrich, St. Louis, MO), 1 ml per 100 mg of tissue) and protease and phosphatase inhibitor cocktail (Roche, Indianapolis, IN). The Bradford assay was used to determine protein concentration of all samples. The supernatant of the initial homogenate (TBS extract) was used to determine soluble APOE (EMD Millipore, Temecula, CA) and APOJ

(Santa Cruz Biotechnology, Dallas, TX) concentration. The pellet was re-suspended, sonicated and spun with RIPA buffer containing protease and phosphatase inhibitors. 30 µg of total protein was mixed with Tris-Glycine denaturing loading buffer, loaded, and electrophoresed on 10% Tris-Glycine or 4-12% Bis-Tris gels. On nitrocellulose membranes ABCA1 was detected using polyclonal antibody, ab7360 (Abcam, Cambridge, MA), and APPfl with 6E10 antibody. β-Actin served as a loading control for all Western blots and detected using a monoclonal antibody (Sigma-Aldrich, St. Louis, MO). Membranes were incubated with respective secondary antibodies conjugated to horseradish peroxidase, and visualized by enhanced chemiluminescence Plus-ECL (PerkinElmer, Waltham, MA). Blots were imaged using the chemiluminescent setting on the Amersham Imager 600 (GE Healthcare Life Sciences, Marlborough, MA). All bands were quantified by densitometry (ImageQuant, version 5.2; GE Healthcare) and normalized to β-Actin. To quantify APPfl and ABCA1, bands were normalized to respective vehicle groups. Quantification of APOE and APOJ is represented as fold of vehicle treated APP/E3/Abca1$^{+/-}$ mice.

### 4.11.2 Aβ Dimer ELISA

Aβ dimer ELISA was performed as previously published [239] with few modifications. As a standard we used a standard curve of Aβ$_{1-40}$Ser26Cys dimer. 6E10 antibody was used as the capture antibody (10 µg/ml) to coat a 96 well Nunc MaxiSorp plate overnight at 4°C. After removing the antibody, the plate was washed with PBS and blocked with Block Ace for four hours. Following the removal of Block Ace, Aβ$_{1-40}$Ser26Cys dimer standards and RIPA fraction from the cortex were diluted in EC buffer and loaded on the plate in duplicates. Biotinylated

6E10 antibody was used as the detection antibody (0.167 µg/ml) and incubated 4 hours at room temperature. The assay was developed with HRP-labeled streptavidin (1:30,000) for 1.5 hours at RT, followed by the use of the TMB Microwell Peroxidase Substrate System (KPL, Gaithersburg, MD). Plate was read on the SpectraMax i3 (Molecular Devices, Sunnydale, CA) at 650 nm. Final values were compared to $A\beta_{1-40}$Ser26Cys dimer standard curve using linear regression analysis, normalized to the total protein concentration in each sample, and expressed as ng $A\beta$/mg protein.

### 4.11.3 Native-PAGE

Native PAGE was performed according to a previously published protocol [245] with slight modifications. TBS brain extract was mixed with 2× non-denaturing loading buffer and resolved on Novex™ 4-20% Tris-Glycine gels. TBS brain extract from $Apoe^{ko}$ mice was used as a negative control. Amersham™ HMW calibration kit was used as a native ladder (GE Healthcare, Marlborough, MA). Polyclonal anti-APOE (EMD Millipore, Temecula, CA) along with respective secondary antibody was used for incubation and developed as described for Western blot. Quantification of lipidated APOE is represented as the fold of respective vehicle groups.

## 4.12   STATISTICAL ANALYSIS

For the article, "ABCA1 deficiency affects basal cognitive deficits and dendritic density in mice," data are reported as means ± SEM. Statistical differences between mean scores during acquisition phase of training in the MWM were analyzed with two-way ANOVA and *t*-test was

used to determine difference for each trial day. One-way ANOVA followed by Tukey's post hoc analysis for multiple comparisons was used to analyze the MWM probe trial data. Performance in RWM was assessed with two-way ANOVA Repeated measure (using Genotype or Infusion Group and Trial as sources of variation) followed by Tukey's post hoc analysis. Significant differences between groups for the rest of the data were determined by t-test. All statistical analyses were performed in GraphPad Prism, version 6.0 and differences were considered significant where $p < 0.05$.

For the article, "Liver x receptor agonist treatment significantly affects phenotype and transcriptome of APOE3 and APOE4 *Abca1* haplo-deficient mice," All results are reported as means ± SEM. All data was analyzed by two-way ANOVA for genotype and treatment factors followed by Bonferroni's or Sidak's (Aβ dimer ELISA) post hoc test. One-way ANOVA followed by Tukey's post hoc analysis was applied only to contextual fear conditioning. All statistical analyses were performed in GraphPad Prism, version 6.0. Significance was determined as $p < 0.05$.

# 5.0    RESULTS AND DISCUSSION

## 5.1    ABCA1 DEFICIENCY AFFECTS BASAL COGNITIVE DEFICITS AND DENDRITIC DENSITY IN MICE

### 5.1.1    *Abca1* deficiency significantly impairs spatial memory in APP transgenic mice

Recently we showed that lack of *Abca1* increases amyloid load and worsens the performance of APP expressing mice in the contextual fear conditioning test [220]. Contextual fear condition paradigm assesses hippocampal-dependent associative learning to unconditional stimulus such as electric shock [212]. To test if ABCA1 deficiency affects other types of memory such as spatial learning and retention and long-term memory we employed MWM and novel object recognition test respectively. We used 7 month old APP mice that express wild type *Abca1* (APP/*Abca1*$^{wt}$) or *Abca1*$^{ko}$ (APP/*Abca1*$^{ko}$) and their non APP transgenic littermates (WT and *Abca1*$^{ko}$). As illustrated in Fig. 6A and B, during the acquisition phase, APP mice with intact *Abca1* performed similarly to WT mice (no significant main effect of genotype); however there was a statistical difference on the last day of testing ($p < 0.05$) suggesting impaired acquisition. In contrast, APP/*Abca1*$^{ko}$ mice performed much worse than *Abca1*$^{ko}$ (significant main effect of genotype, $p<0.001$), particularly on the last days of MWM. This suggests that the lack of ABCA1 impairs

spatial acquisition in mice expressing human APP. In the MWM probe trial, APP/$Abca1^{ko}$ mice demonstrated decreased memory retention exemplified by a longer latency time to enter the target zone compared to APP/$Abca1^{wt}$ and non-transgenic $Abca1^{ko}$ mice (Fig. 6C). APP/$Abca1^{ko}$ mice also spent the shortest time in the target quadrant compared to the other genotypes however the difference with $Abca1^{ko}$ was not significant (Fig. 6D). These changes in performance were not due to swim speeds as there was no difference in the swim speeds of the assessed genotypes.

To confirm that the memory impairment is not restricted only to MWM, the mice were also tested using the novel object recognition paradigm as before [194]. Once more, APP/$Abca1^{ko}$ mice demonstrated the worst performance (Fig. 6E, $p < 0.05$ compared are APP/$Abca1^{ko}$ and APP/$Abca1^{wt}$) with APP/$Abca1^{ko}$ mice exploring the novel object far less than the other genotypes.

The behavior experiments presented on Fig. 6 demonstrate that ABCA1 deficiency exaggerates cognitive deficits in APP transgenic mice that could be a result of either increased endogenously formed Aβ oligomers or amyloid plaques present in APP/$Abca1^{ko}$ mice.
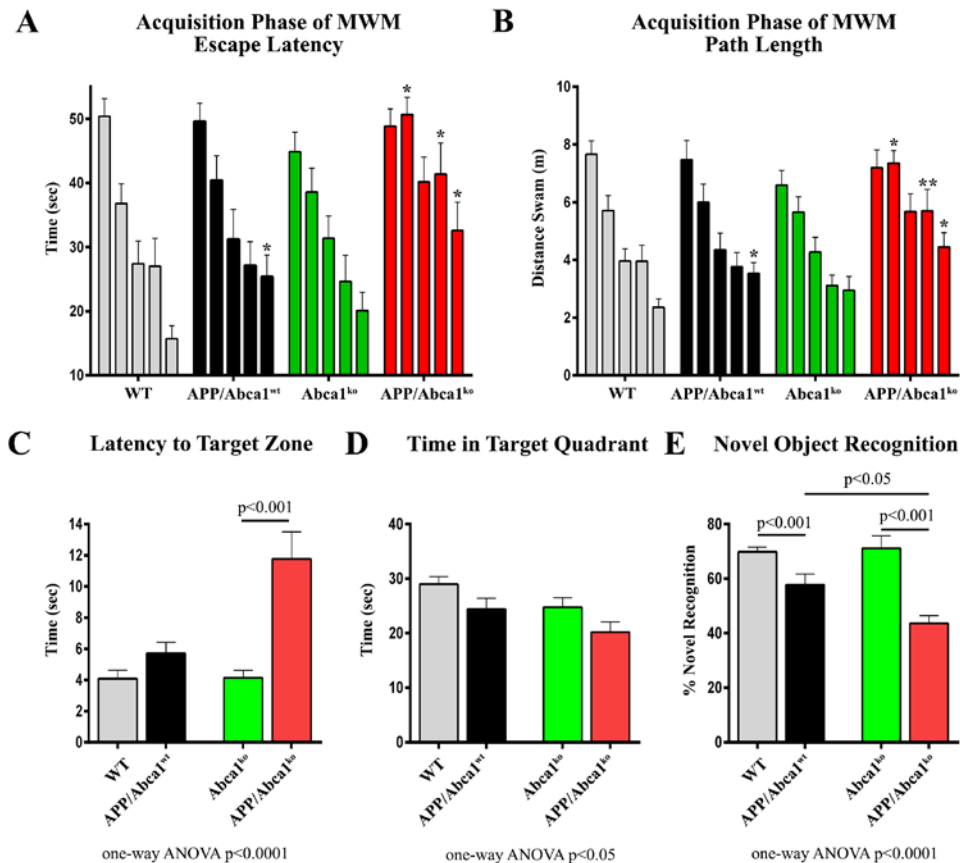
**Figure 6 *Abca1* deficiency negatively affects memory of APP transgenic mice**

On **A, B**, **C** and **D**, are presented the MWM results from 7 month old APP mice expressing mouse *Abca1* (APP/*Abca1*$^{wt}$; N=16) or *Abca1*$^{ko}$ (APP/*Abca1*$^{ko}$; N=14). Age- and gender-matched non-APP expressing *Abca1*$^{wt}$ (N=14) or *Abca1*$^{ko}$ (N=16) littermates were used as controls. Analysis is by two-way ANOVA to determine interaction and main effect of genotype or training, and t-test to determine genotype differences in performance within trial days. **A & B**, Training phase of MWM with each bar representing performance from all trials for a training day. **A**, Escape latency to the hidden platform: APP/*Abca1*$^{wt}$ vs WT, no interaction and no main effect of genotype. APP/*Abca1*$^{ko}$ vs *Abca1*$^{ko}$, no interaction and significant main effect of genotype; $F(1,140) = 22.26$, $p < 0.001$. **B**, Path length to the hidden platform: APP/*Abca1*$^{wt}$ vs WT, no interaction and no main effect of genotype. APP/*Abca1*$^{ko}$ vs *Abca1*$^{ko}$, no interaction and significant main effect of genotype; $F(1,140) = 21.09$, $p < 0.001$. For **A** and **B**, **\*\***, $p < 0.01$, **\***, $p < 0.05$ vs non-APP expressing controls by *t*-test. **C & D** represents probe trial of MWM performed 24 hrs following last training trial. Analysis is by one-way ANOVA followed by Tukey's post-test (shown on the graph). **C**, Latency to reach the target quadrant of the hidden platform. $p < 0.0001$. **D**, Time spent in the target quadrant of the hidden platform. $p < 0.05$. **E**, Novel object recognition was performed on a different group of 7 month old mice of the same genotypes. Shown is percent novel object recognition as indicated in the Methods. Analysis is by one-way ANOVA followed by Tukey's post-test. N=8-12 male and female mice per group.

54

## 5.1.2  Characterization of Aβ oligomers utilized in this study

It has been reported that Aβ oligomers affect synaptic plasticity and cognitive function [246]. Recently we have shown that amyloid load and A11-positive Aβ oligomers are significantly increased in 7 month old APP/*Abca1*[ko] mice in comparison with APP mice expressing *Abca1*[wt] [220]. To determine how the acute infusion of Aβ oligomers into hippocampus affects the memory of WT and *Abca1*[ko] mice, we used Aβ$_{42}$ peptide and employed several methods to characterize the Aβ oligomers. On Fig. 7A is shown SDS PAGE followed by Western blotting with anti-Aβ 6E10 antibody. As visible, at time 0, Aβ existed only as monomers and low MW oligomers such as dimers, trimers and tetramers. Upon oligomerization, following 24 hrs incubation, there was an increase of higher MW oligomers such as 9-mer, 12-mer etc.; however, we were unable to detect oligomers with MW higher than 100 kDa. For comparison on the right of Fig. 7A is shown WB of Aβ fibrils. Aβ oligomers were also confirmed using conformation specific A11 antibody. As seen on Fig. 7B, when the dot blot was probed with A11 there was an increase in the intensity of oligomeric Aβ from time 0 to 48 hrs incubation. Finally, on Fig. 7C are shown electron micrographs of Aβ at time 0 and 24 hrs incubation. At time 0 (Fig. 7C-a) disaggregated Aβ$_{42}$ is present as a monomer. After incubation for 24 hrs at room temperature Aβ$_{42}$ was converted into rod-shaped oligomers with diameter of approximately 10 nm and length between 20-50 nm (Fig. 7C-b).
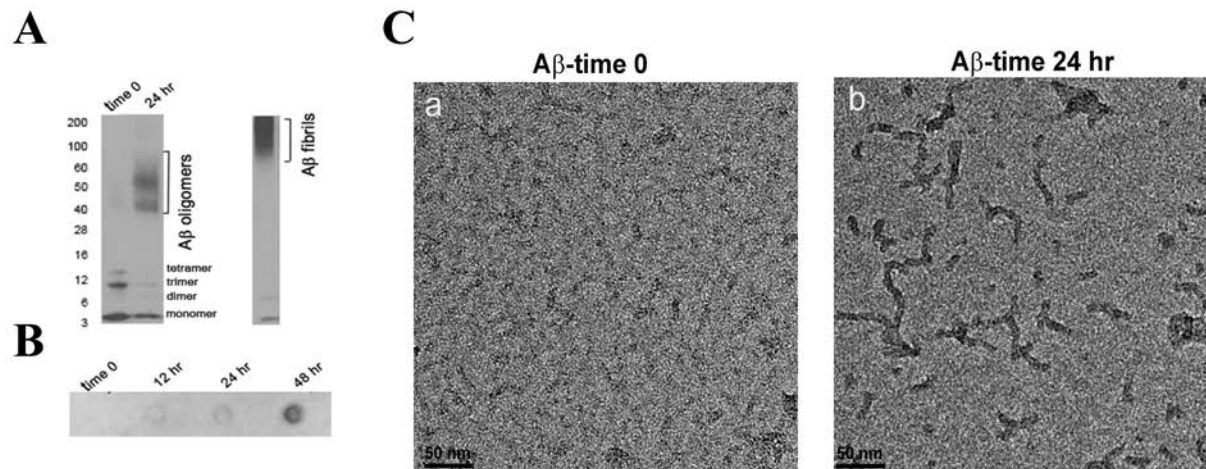
**Figure 7: Characterization of Aβ oligomer**

Disaggregated Aβ42 was incubated at room temperature for 24 hrs as indicated in the Methods. **A**, SDS PAGE of Aβ42 at time 0 and 24 hrs after the start of incubation. Western blotting was performed with anti-Aβ antibody, 6E10. On the left are shown molecular weight markers. Aβ oligomers migrate between 40 and 90 kDa marker. Western blot of Aβ fibrils is shown for comparison. **B**, Aβ oligomers were identified by dot blotting performed with A11 antibody. Notice with the dot blot an increase in Aβ oligomers with increased incubation time. **C**, Electron micrograph of Aβ42 at time 0 (**a**) and 24 hrs after the start of incubation (**b**).

### 5.1.3 Infusion of Aβ oligomers in hippocampus differentially affects cognitive deficits in WT and *Abca1*[ko] mice

To test the effect of the oligomers shown on Fig. 7 on cognition we infused WT and *Abca1*[ko] mice, which do not express human APP transgene, with the 24 hr oligomeric Aβ preparation. Young 7 month old mice were implanted with cannulas into both hippocampi (see picture on Fig. 8A) followed by a recovery period of 8 days before behavioral testing. Aβ42 oligomers were infused bilaterally into the hippocampus 30 mins prior to each of the RWM training blocks (2 - 6 trial blocks and 1 - 3 trial block) for a total of 3 infusions. RWM paradigm tests reference memory [212] and was used as a more demanding task, compared to MWM, to detect relatively subtle changes in cognitive function. Control mice were infused with scrambled Aβ. In addition,

mice were compared to naïve mice that were not subjected to surgery. As shown on Fig. 8B, in WT mice Aβ$_{42}$ oligomers significantly affected cognitive performance as compared to the control mice infused with scrambled Aβ (compare purple circles to grey squares). In contrast there was no statistical difference between naïve (no surgery) and mice infused with scrambled Aβ (Fig. 8B, compare grey squares to black triangles). This experiment suggests that surgical procedures followed by the infusion of scrambled peptide do not affect the memory of WT mice.

We next examined how Aβ oligomers infused into the hippocampus would impact cognitive performance of age-matched *Abca1*$^{ko}$ mice and compare them to controls of *Abca1*$^{ko}$ and WT mice infused with scrambled Aβ. Surprisingly, we found a statistically significant difference between WT and *Abca1*$^{ko}$ infused with control scrambled Aβ (see Fig. 8C, compare black to grey squares) suggesting that *Abca1*$^{ko}$ mice are vulnerable to the effect of stress/trauma induced by surgery and infusion of scrambled Aβ. Due to the worsened performance of the control *Abca1*$^{ko}$ mice (injected with scrambled Aβ) there was no statistical difference between their behavior and *Abca1*$^{ko}$ mice infused with Aβ oligomers (compare black squares to red circles). Our conclusion is that *Abca1*$^{ko}$ mice have basal cognitive deficits that prevent them from coping with additional stressors that do not impact performance of normal healthy WT mice.
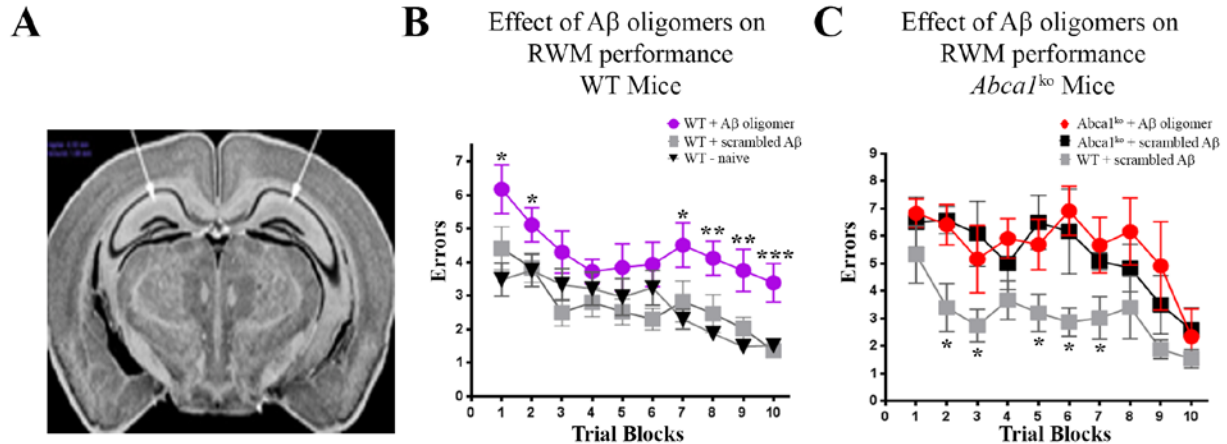
**Figure 8: Infusion of Aβ oligomers into the hippocampus differentially affects cognitive performance in WT and *Abca1*ko mice**

Aβ$_{42}$ oligomers (characterized on Fig. 2) were infused into the hippocampus of 7 month old WT or *Abca1*ko mice and cognitive performance was evaluated by Radial arm water maze (RWM) paradigm. Control mice were infused with scrambled Aβ. As additional control, we used WT naïve mice without surgery. **A**, Represents the location of cannulas implanted into the hippocampus. **B**, Cognitive performance of WT mice is significantly affected by Aβ$_{42}$ oligomers but not by scrambled Aβ. Analysis by two-way repeated measures ANOVA shows no interaction between training and treatment; however there was a significant main effect of treatment (Aβ$_{42}$ oligomers); $F_{(2,279)} = 17.84$, $p < 0.0001$ and trial block (trial block); $F_{(9,279)} = 7.99$, $p < 0.0001$. Post-test for multiple comparisons demonstrates the difference between mice infused with Aβ$_{42}$ oligomers and scrambled Aβ (compare purple circles to grey squares): ***, $p < 0.001$; **, $p < 0.01$; *, $p < 0.05$. N=11-12 mice per group. **C**, There is a significant difference in RWM performance between WT and *Abca1*ko mice infused with scrambled Aβ. In contrast there is no significant difference in RWM performance between *Abca1*ko mice infused with Aβ$_{42}$ oligomers and scrambled Aβ. Analysis by two-way repeated measures ANOVA shows no interaction between training and treatment; but a significant main effect of treatment; $F_{(2,90)} = 5.56$, $p = 0.0238$ and training $F_{(9,90)} = 6.29$, $p < 0.0001$. Post-test for multiple comparisons demonstrates the difference between WT and *Abca1*ko mice infused with scrambled Aβ (compare black to grey squares): *, $p < 0.05$. N=4-5 mice per group.

### 5.1.4 Deficiency of *Abca1* significantly impairs neurite morphology in CA1 but not in CA2 region of the hippocampus

Recently we have demonstrated that *Abca1* as well as *Apoe* deficiency significantly affects dendrite architecture in human APP transgenic mice [220]. The behavior tests shown on Fig. 8 prompted us to examine the dendritic parameters of *Abca1*ko mice that do not express human

APP transgene. To test the effect of *Abca1* deficiency we used 7 months old *Abca1*$^{ko}$ mice and compared to WT mice (the same age as in Fig. 8). For neurite morphometry of pyramidal hippocampal neurons we used MAP2 stained brain sections and performed analysis in two different regions (CA1 and CA2) of medial hippocampal sections. Since neurites form complex tree-like structures, 3D image reconstruction is necessary to obtain accurate measurements. Examination of neurites in the CA1 region (Fig. 9A) revealed a significant decrease in neurite length, number of neurite segments and number of branches (Fig. 9A & B, $p < 0.05$) in *Abca1*$^{ko}$ mice when compared to WT. These changes in neurite architecture were restricted to the CA1 region of the hippocampus as we did not observe any changes in the CA2 region when comparing *Abca1*$^{ko}$ to WT mice (Fig. 9C & D). The data were normalized to the number of neurons and there was no significant change in the numbers of counted nuclei (not shown) when comparing *Abca1*$^{ko}$ mice and WT mice in either region of the hippocampus. Our data demonstrate that the genetically engineered deletion of *Abca1* disrupts neurite morphology in the hippocampus, and this effect is specific for CA1 region.

**A**

CA1 WT

a — MAP2
b — H 33342
c — Merge
d — Neurites

CA1 Abca1ko

e
f
g
h

**B**

Neuritic Length
CA1

p < 0.05

Sum neurite length/MAP2 (μm)

1200
1100
1000
900
800

WT          Abca1ko

Neuritic Branches
CA1

p < 0.05

Neurite branches/MAP2

130
120
110
100
90
80

WT          Abca1ko

Neuritic Segments
CA1

p < 0.05

Neurite segments/MAP2

130
120
110
100
90
80
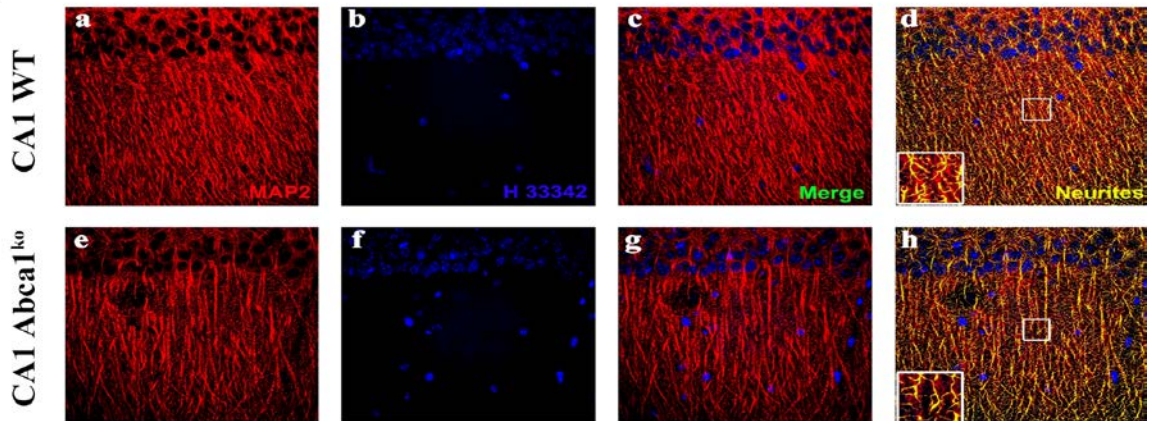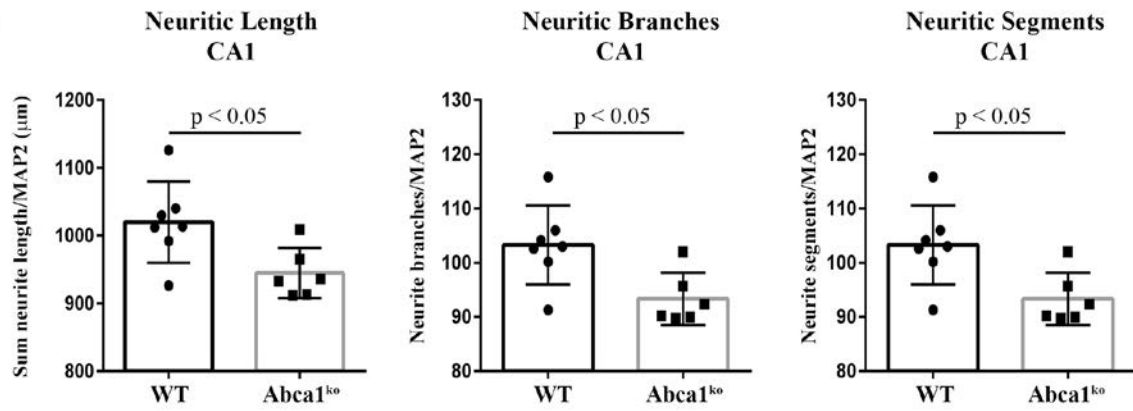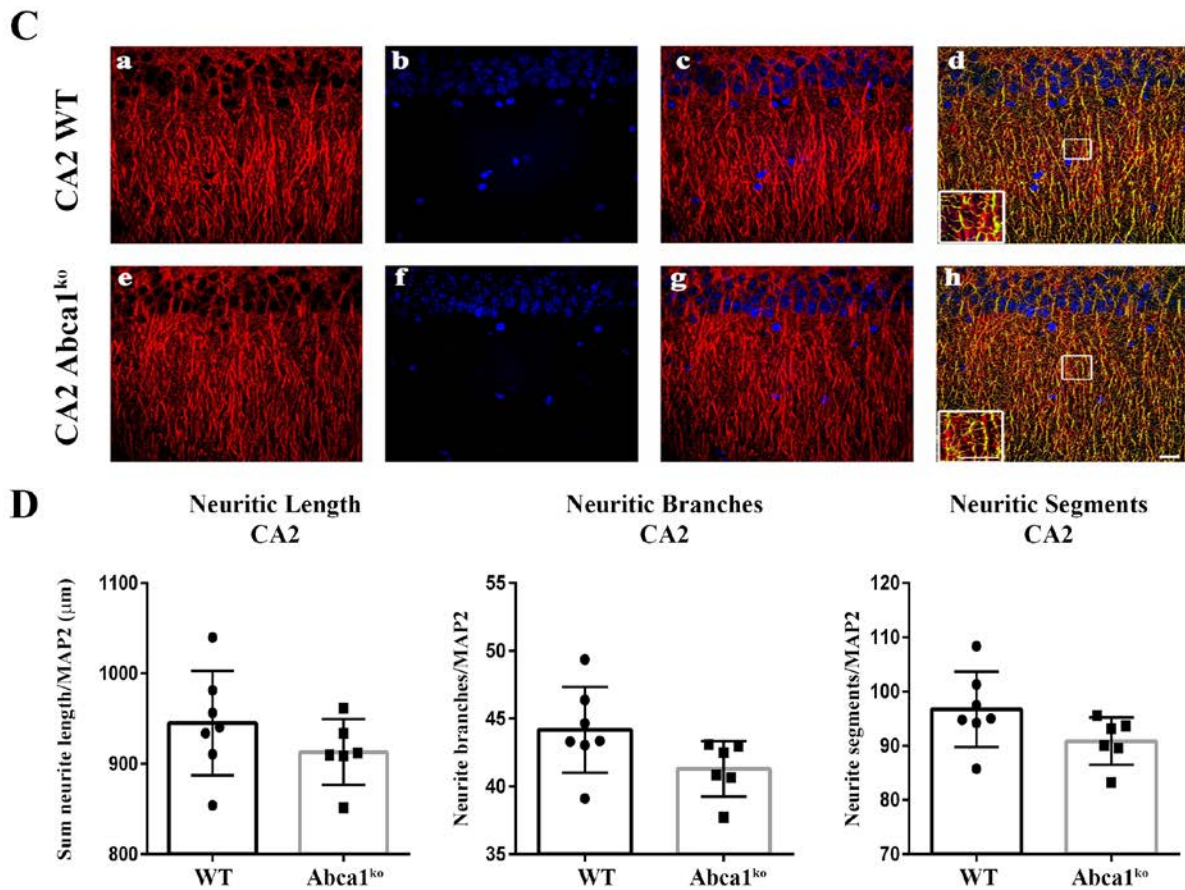
WT          Abca1ko

**Figure 9: Lack of *Abca1* significantly affects dendritic architecture in CA1 but not CA2 region of the hippocampus**

MAP2 and DAPI staining were used for dendritic tree reconstruction in the hippocampal CA1 and CA2 regions of WT and *Abca1*[ko] mice. Data were analyzed from a total of four images (60X confocal imaging) from each of the four sections for each mouse (N=5-7 mice per group; 16 images per mouse). The total dendritic length, branch points and segments were quantified using Imaris filament tracing macros and were normalized to the total DAPI positive nuclei of the CA1 and CA2 regions. Analysis by t-test**. A,** Shows representative images for CA1 region (**a** – MAP2 staining in red, **b** – DAPI staining in blue, **c** – Merged MAP2 and DAPI staining, **d** – Imaris neurite tracings in yellow); while **B**, indicates the quantification of neurite length, segments and branches. **C,** Shows representative images for CA2 region (scale bar = 100 µM); while **D**, indicates the quantification of neurite length, segments and branches in the CA2 region. Note that lack of *Abca1* significantly affects dendritic architecture in CA1 but not CA2 region of the hippocampus.

## 5.1.5 Discussion

In this study we examined the effect of global deletion of *Abca1* on cognitive performance and neurite morphology. We also determined the potential impact the deletion of *Abca1* has on cognitive impairment induced by oligomeric Aβ. In regards to cognitive performance and in correlation to the level of soluble Aβ oligomers, we have previously shown that old APP23 mice with one copy of *Abca1* performed significantly worse than mice with intact *Abca1* in a MWM paradigm [178]. Furthermore, we have reported that simultaneous deletion of *Apoe* and *Apoa1* in the AD mouse model used in the current study, significantly aggravated memory impairment, similarly to deletion of Abca1, revealed in contextual fear conditioning. Consistent with the behavior data, APP expressing mice with double - *Apoe* and *Apoa1,* or *Abca1* knockout, both demonstrated significant impairment in dendrite morphology compared to APP/WT mice. Herein, we confirmed the behavior deficits caused by *Abca1* deletion in APP/PS1ΔE9 mice at an early stage of amyloid pathology utilizing two behavioral tests – MWM and novel object recognition.

Accumulation of soluble extracellular high molecular weight oligomeric Aβ species in brain is considered pathogenic for onset and progression of cognitive deficits associated with AD. Studies have found that soluble oligomers of Aβ rapidly and potently inhibit long-term potentiation [247]. Aβ oligomers also activate glial/neuronal stress kinases and increase the production and release of nitric oxide, superoxide and other mediators [248]. It has been shown that Aβ oligomers negatively impact neuronal viability [249, 250] and synaptic plasticity [246]. We have previously shown that cognitive performance can be correlated to levels of soluble Aβ oligomers [178] and here we wanted to demonstrate that ABCA1 influences the effects of Aβ oligomers on cognitive performance. In this study we utilized mice which express endogenous

APP only and determined the effects of Aβ oligomers without the context of amyloid pathology. While we have been able to demonstrate impairments in cognitive performance in both WT and Abca1[ko] mice following infusion of Aβ oligomers into the hippocampi, we found a statistically significant difference between WT and *Abca1*[ko] mice infused with control scrambled Aβ peptide, suggesting that *Abca1*[ko] mice have basal deficits that prevent them from coping with additional stressors that do not affect performance of a normal healthy WT mouse. A possible explanation of the results could be, *Abca1*[ko] mice are, generally, unable to cope with additional stressors ultimately resulting in diminished cognitive performance. However, since ABCA1 regulates cholesterol and phospholipids efflux from cells to lipid-poor ApoE and controls the generation of HDL-like particles in brain, the overall impact could be a result of insufficient supply of cholesterol to neurons, emphasizing the regulatory role of ABCA1-ApoE axis on cholesterol homeostasis and promotion of synaptogenesis. While our study has not been designed to answer all these questions, the overall consequence of deficient, properly lipidated ApoE could explain reduced number of synapses [251], negative effects on reactive sprouting response following lesions in entorhinal cortex [252] and decreased MAP2-positive staining of neurons in the amygdala [253]. While evidence exists that adult neurons can synthesize cholesterol [254, 255], they cannot produce cholesterol efficiently, depend on an external source and rely on exogenously supplied lipids especially during periods of increased demands such as repair following additional stressors [256, 257]. Yet, another plausible explanation could be, ApoE as the main carrier of cholesterol and phospholipids in the brain, in conditions of nonfunctional ABCA1 not only inefficiently delivers cholesterol and lipids to neurons to support growth and connectivity, but indirectly influences transcriptional activity of genes, and thus the expression of

63

proteins critical for synaptogenesis, and cognitive performance. The exact molecular mechanism by which ApoE influences neuronal structure and complexity remains unresolved, however.

In conclusion, our study demonstrates behavior deficits caused by *Abca1* deletion in APP/PS1ΔE9 mouse model at an early stage of amyloid pathology. The basal deficits of *Abca1*ko, manifested by diminished cognitive performance, prevent them from coping with additional stressors which is in part due to the impairment of neurite morphology of the hippocampus. The results of this study emphasize the important role of ABCA1 in brain cholesterol homeostasis and its ability to cope with external insults: environmental, diet induced, physical trauma, or disease associated neuropathology.

## 5.2 LIVER X RECEPTOR AGONIST TREATMENT SIGNIFICANTLY AFFECTS PHENOTYPE AND TRANSCRIPTOME OF APOE3 AND APOE4 ABCA1 HAPLO-DEFICIENT MICE

Submitted on December 5, 2016 to the journal, PLOS ONE

### 5.2.1 Pharmacological Activation of LXR/RXR transcription factors improves cognitive performance of *Abca1* haplo-deficient APP/E4 mice

We have previously demonstrated that *Abca1* deficiency differentially affects AD-like phenotype in mice expressing human *APOE4* or *APOE3*. To determine if ligand activated LXR can alleviate cognitive deficits in APP/E4/Abca1$^{+/-}$ mice, we treated six-month-old APP/E4/Abca1$^{+/-}$ mice with T0 and compared changes in their AD-like phenotype to those of non-transgenic

littermates and to APP/E3/Abca1$^{+/-}$ mice. First, we examined changes in cognitive function following T0 treatment in a novel object recognition paradigm. As seen in Fig.10A, two-way ANOVA analysis revealed both main variables T0 and APOE isoform significantly affected performance in APP-expressing mice. In contrast, neither LXR ligand treatment nor APOE isoform had an effect on non-transgenic littermates (Fig.10B). To confirm the effect seen in novel object recognition, we used contextual fear conditioning paradigm that tests hippocampal-associated learning. As visible from Fig.10C, T0 treatment significantly improved the performance of both APP/E4/Abca1$^{+/-}$ mice compared to vehicle treated APP/E4/Abca1$^{+/-}$ mice (Sidak's post-test, $p < 0.05$) while in APP/E3/Abca1$^{+/-}$ the response did not reach a significant level. Interestingly, in difference to novel object test, LXR ligand treatment and *APOE* genotype had a significant main effect on the performance of WT controls (Fig.10D). Cued test demonstrated no effect of T0 and *APOE* genotype confirming that the effect of T0 is reflected by hippocampal-associative memory (Fig.10E and F). Thus, the conclusion from these experiments is that LXR ligand treatment significantly improves cognition of APP/E4/Abca1$^{+/-}$ mice.
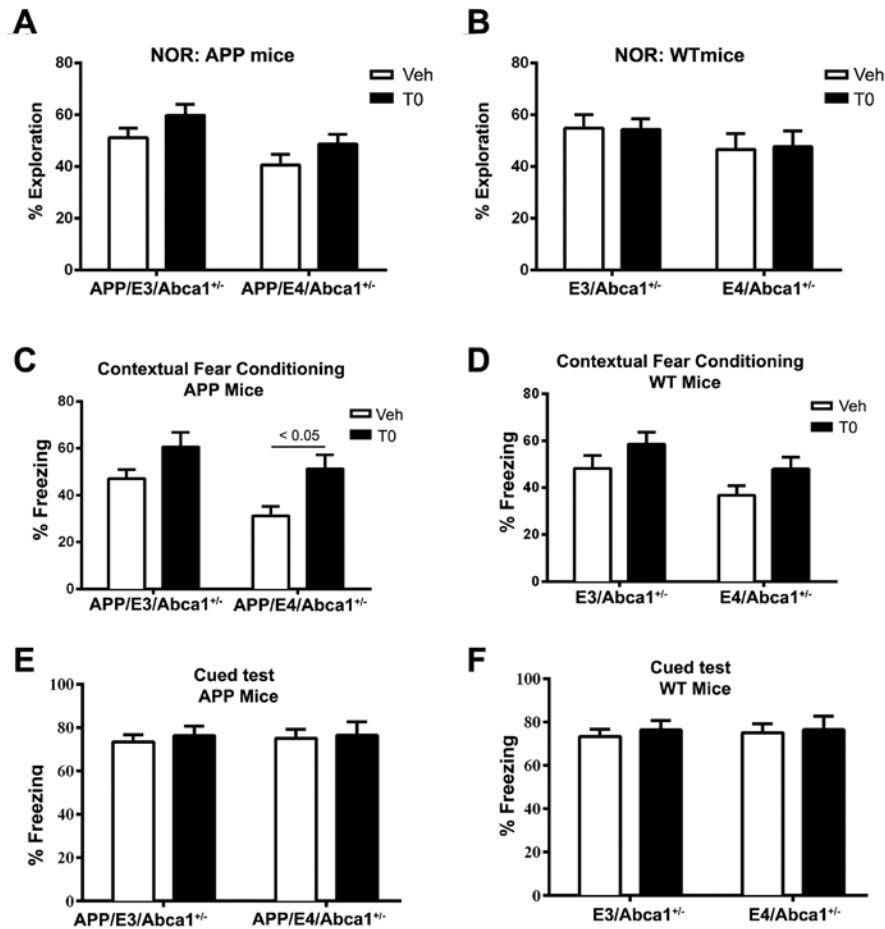
**Figure 10: LXR agonist treatment improves cognitive performance**
T0 treatment restores cognition in APP/E4/Abca1+/-. 6-month-old APP/E3/Abca1+/-, APP/E4/Abca1+/- and non-transgenic mice were treated with T0 and vehicle (control) for one month. Cognitive function was assessed with novel object recognition (A and B) and contextual fear conditioning behavioral paradigms (C and D). A, T0 affected the performance of APP transgenic mice in the novel object recognition test. Analysis by two-way ANOVA shows no interaction between APOE genotype and T0 treatment with a significant main effects of APOE genotype $(F_{(1, 51)}= 7.44, p < 0.01)$ and T0 treatment $(F_{(1, 51)}= 4.45, p< 0.05)$. B, T0 treatment did not affect the performance of non-APP littermates. APOE genotype $(F_{(1, 45)}= 1.9)$ and T0 treatment $(F_{(1, 45)}= 0.002)$. C, LXR agonist significantly improved the performance of APP/E4/Abca1+/- mice in contextual fear conditioning paradigm. Analysis by two-way ANOVA shows no interaction between APOE genotype and T0 treatment and significant main effects of T0 treatment $(F_{(1, 51)}= 5.94, p= 0.018)$ and APOE genotype $(F_{(1, 51)}= 10.6, p= 0.002)$. Sidak's multiple comparison test shows a significant difference between T0 and vehicle treated APP/E4/Abca1+/- mice $(p < 0.05)$. D, T0 also affected the behavior of non-APP controls in the contextual fear conditioning behavior paradigm. Analysis by two-way ANOVA shows no interaction and significant main effects of T0 treatment $(F_{(1, 45)}= 4.47, p= 0.03)$ and APOE genotype $(F_{(1, 45)}= 4.49, p= 0.04)$. T0 had no effect on APP (E) and non-APP mice (F) during the cued phase of fear conditioning. For all panels, N=11-15 mice per group. Data represented as means ±SEM.

**5.2.2 Ligand activated LXR/RXR do not affect amyloid plaque level but significantly decrease soluble Aβ oligomers in APP/E4/Abca1$^{+/-}$ mice**

To examine if LXR/RXR agonist treatment can alleviate amyloid plaque pathology in APP/E3/Abca1$^{+/-}$ and APP/E4/Abca1$^{+/-}$ mice, brain sections were stained with X-34 to visualize compact fibrillary amyloid plaques. Representative images of X-34 staining in the cortex and hippocampus are shown in Fig.11A. While simple comparison of areas occupied by deposited compact amyloid plaques (*t*-test) did not reveal a difference (Fig.11B), a two-way ANOVA confirmed a significant main effect of *APOE* genotype but not T0 treatment. To visualize diffuse and compact (total) amyloid plaques, brain sections were stained with anti-Aβ antibody 6E10. Representative images of 6E10 staining in the cortex and hippocampus are shown in Fig.11C. Similarly, to the results of X-34 staining, the analysis showed a significant main effect of *APOE* genotype on the total amyloid burden, regardless of the T0 treatment (Fig.11D). Next, we determined the effect of T0 on the level of soluble Aβ dimers in the cortices of APP/E3/Abca1$^{+/-}$ and APP/E4/Abca1$^{+/-}$ mice (Fig.11E). We found a statistically significant interaction between *APOE* genotype and T0 treatment and a difference in the amount of Aβ dimers in T0 and vehicle treated APP/E4/Abca1$^{+/-}$ mice (Sidak's post-hoc test $p < 0.05$). These changes were not a consequence of T0 effect on full length APP processing as its protein level was unchanged (Fig.11F). The conclusion is that LXR ligand T0 does not affect amyloid plaques but significantly decreases soluble Aβ oligomers that confirms our previous data on the effect of activated LXR/RXR on amyloid pathology.
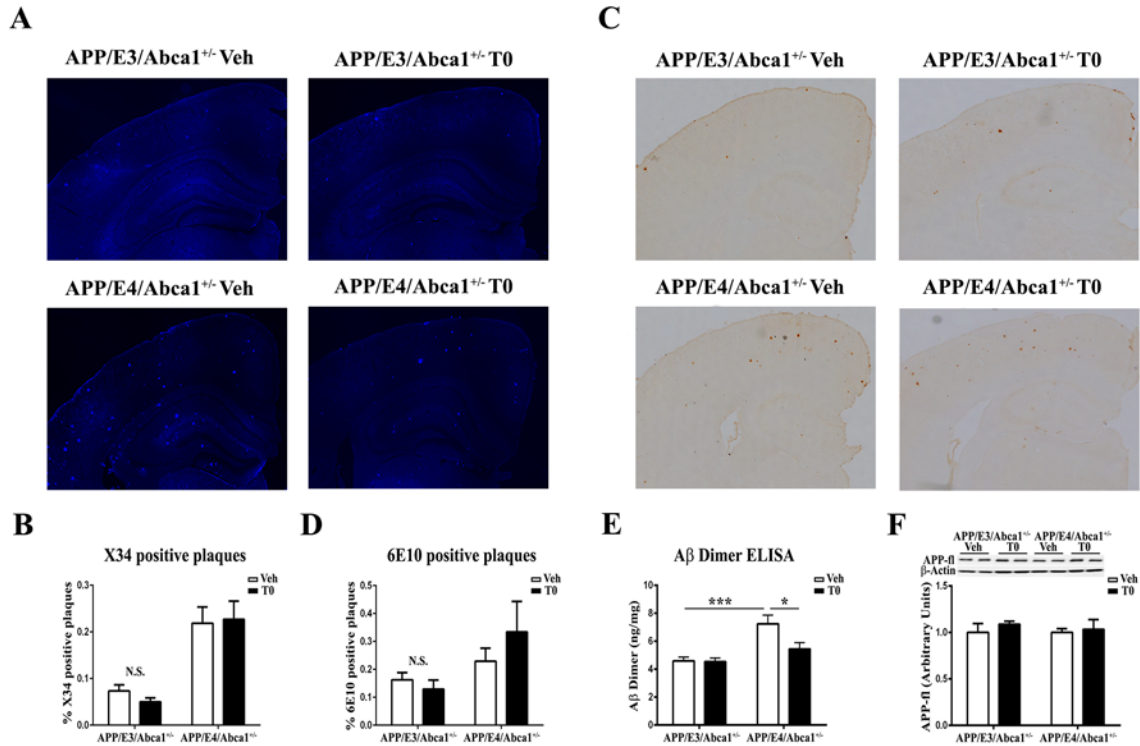
**Figure 11: T0 treatment significantly decreased soluble Aβ oligomers, not amyloid plaque pathology in APP/E4/Abca1$^{+/-}$ mice**

T0 treatment significantly decreased soluble Aβ dimers, but not amyloid plaque pathology in APP/E4/Abca1$^{+/-}$ mice. Amyloid plaque pathology was assessed by immunostaining. **A,** Brain sections were stained with X-34 to visualize compact fibrillary amyloid plaques in vehicle and T0 treated APP/E3/Abca1$^{+/-}$ and APP/E4/Abca1$^{+/-}$ mice. Representative images of X-34 staining were captured at 10× magnification. **B,** X-34 positive amyloid plaques were analyzed by two-way ANOVA. There is no interaction between *APOE* genotype and T0 treatment and a significant main effect of *APOE* genotype (F (1, 55)= 34.7, p < 0.0001), but not of T0 treatment. N=14-16 mice per group. N.S., not significant. **C,** Brain sections were stained with anti-Aβ antibody, 6E10, to visualize diffuse and compact (total) amyloid plaques in vehicle and T0 treated APP/E3/Abca1$^{+/-}$ and APP/E4/Abca1$^{+/-}$ mice. Representative images of 6E10 staining are shown (10× magnification). **D,** 6E10 positive amyloid plaque load analyzed by two-way ANOVA. There is no interaction between *APOE* genotype and T0 treatment and a significant main effect of *APOE* genotype (F(1, 19)= 4.41, p=0.049), but not of T0 treatment. N= 5-6 mice per group. **E,** T0 treatment significantly decreases Aβ oligomers in APP/E4/Abca1$^{+/-}$ mice. RIPA fraction was evaluated for soluble Aβ by dimer-specific ELISA. Analysis by two-way ANOVA revealed an interaction between *APOE* genotype and T0 treatment (F(1, 32)=4.82, p= 0.036). Sidak's post-test demonstrated a significant difference between T0 and vehicle treated APP/E4/Abca1$^{+/-}$ mice (p < 0.05). N=6-10 mice per group. **F,** T0 has no effect on full-length APP. For all panels the data are means ±SEM.

### 5.2.3 Genome-wide effects of activated LXR/RXR on brain transcriptome in *APOE*-TR mice

To determine the effect of T0 treatment on the transcriptome of APP/E3/Abca1$^{+/-}$ and APP/E4/Abca1$^{+/-}$, we performed RNA-seq using total RNA extracted from cortices of APP/E3/Abca1$^{+/-}$ and APP/E4/Abca1$^{+/-}$ male mice treated with T0 or vehicle and analyzed the sequencing datasets using edgeR v. 3.14.0 (http://bioconductor.org/). First, we evaluated the source of the variation in gene expression. We applied Principal Component Analysis (PCA) to process the abundance matrix of observed variables (static normalized expression level of genes across the genotypes and treatment) and to calculate Principal Components that account for most of the variance in the datasets. The scattered plot on Fig.12A is a two-dimensional (PC1 vs PC2) representation of T0 treatment and genotype. Interestingly, APP/E3/Abca1$^{+/-}$ and APP/E4/Abca1$^{+/-}$ mice formed two very distinct clusters encompassing the type of treatment. Thus it demonstrates that the effect of APOE isoform on gene expression is higher than the T0 treatment, yet APP/E4/Abca1$^{+/-}$ mice were more responsive to pharmacological activation of LXR/RXR.

Next we compared expression profiles of vehicle and T0 treated APP/E3/Abca1$^{+/-}$ mice and identified a total of 411 differentially expressed genes: 137 up- and 274 down-regulated by T0 at a cut-off of $p < 0.05$ (Fig.12B). Using the same criteria, we found 746 differentially expressed genes in APP/E4/Abca1$^{+/-}$ mice: 438 up- and 308 down-regulated following T0 treatment (Fig.12D). In mice expressing either APOE isoform, among common up-regulated genes known to affect brain lipoprotein metabolism and APOE lipidation were *Abca1, Abcg1* and *Lpcat3* (marked on the volcano plots shown on Fig.12B and D). Surprisingly, T0 treatment did not affect *APOE* mRNA level in mice expressing either isoform. To examine biological

categories affected by the treatment, we used DAVID. As visible from Table 1A, similarly upregulated by T0 in both APP/E3/Abca1$^{+/-}$ and APP/E4/Abca1$^{+/-}$ mice, were processes related to lipid and cholesterol metabolism, DNA repair and chromatin modifications. In contrast there was a little similarity between biological processes down regulated in *APOE3* and *E4* mice. As shown on Table 1B, in APP/E3/Abca1$^{+/-}$ mice, significantly downregulated by T0 was GO term "innate immune response" including toll like receptor 3 (*Tlr3*), bone marrow stromal cell antigen 2 (*Bst2*), as well as interferon induced genes such as *Ifit1* and *Ifit3*, and *Oas2* and *Oasl2*. In contrast, uniquely and significantly downregulated in APP/E4/Abca1$^{+/-}$ mice were transforming growth factor beta receptor signaling, cell differentiation, cell chemotaxis and synaptic transmission among others.

In validation qPCR assays we confirmed up-regulation of *Abca1, Abcg1, Scd1* and *Scd2*, *Srebf1* and *Lpcat3* using total RNA isolated from brains of male and female mice of both genotypes (Fig.12C and E). To confirm the effect of activated LXR/RXR on transcription is translated into increased protein level, we performed western blotting on ABCA1 and APOE. As visible from Fig.13A, T0 treatment increased ABCA1 protein level in both genotypes. Fig.13B, shows that pharmacological LXR/RXR activation by T0 did not change total APOE protein level which is in agreement with gene expression data. Similarly, we did not observe any significant effect of activated LXR/RXR on APOJ/CLU protein level (Fig.13B). Lastly, we examined APOE lipidation using native PAGE. As shown in Fig.13C, T0 treatment increased APOE lipidation in APP/E3/Abca1$^{+/-}$ and APP/E4/Abca1$^{+/-}$ mice. We conclude that in both isoforms, LXR treatment increased gene expression of genes related to cholesterol efflux and APOE lipidation, such as *Abca1*.
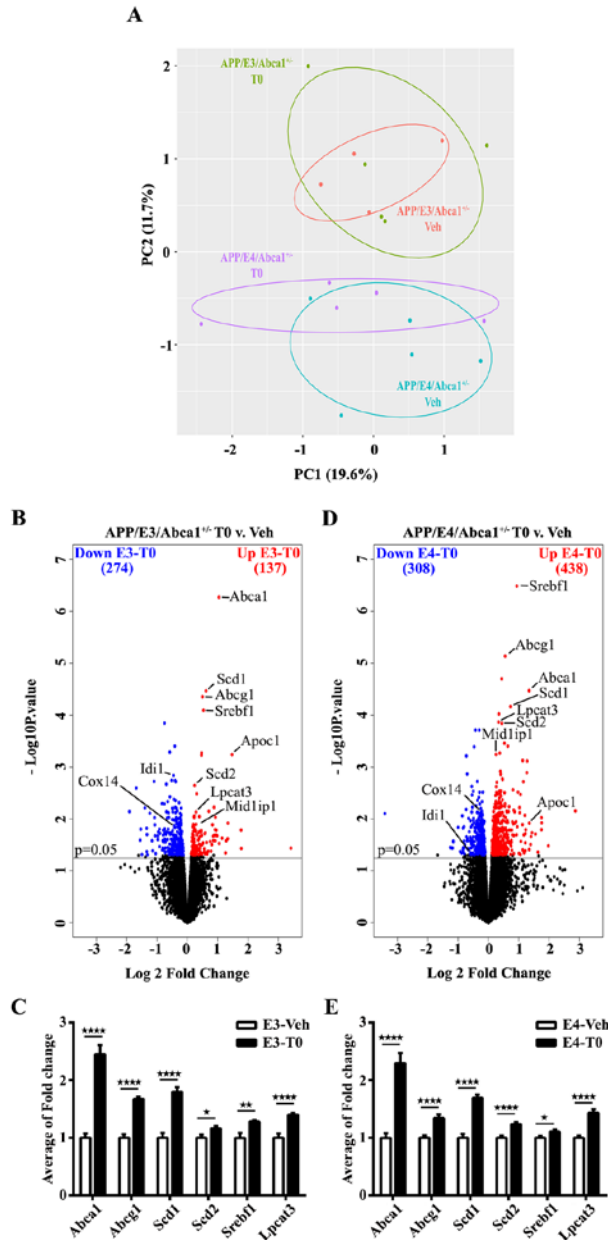
**Figure 12: Transcriptional analysis of T0 treatment from the cortices of six-month-old APP/E3/Abca1$^{+/-}$ and APP/E4/Abca1$^{+/-}$ mice**

**A,** Principle component analysis (PCA) plot shows two dimensional comparison (PC1 vs PC2) of *APOE* genotype and T0 treatment in APP/E3/Abca1$^{+/-}$ and APP/E4/Abca1$^{+/-}$ mice. **B** and **D,** The volcano plots show differential gene expression between T0 treated APP/E3/Abca1$^{+/-}$ (**B**) and APP/E4/Abca1$^{+/-}$ (**D**) mice when compared to their vehicle treated counterparts using EdgeR RNA-sequencing results analysis. The up-regulated genes are represented in red, down-regulated genes are represented in blue and the cut off is at p<0.05. Up-regulated genes represent target genes of T0 treatment. **C** and **E,** qPCR validation of upregulated genes in T0 treated APP/E3/Abca1$^{+/-}$ and APP/E4/Abca1$^{+/-}$ from the volcano plot analysis. N=12 mice per group. qPCR values are mean ± SEM. Analysis were performed by student t-test.

71

**Table 1. Gene ontology categories (GO) differentially affected by LXR agonist**

A. Up-regulated GO terms in T0 treated APP/E3/Abca1$^{+/-}$ and APP/E4/Abca1$^{+/-}$ mice

| APP/E3/Abca1$^{+/-}$: T0 vs Vehicle | | | | | |
|---|---|---|---|---|---|
| Term | Count | % | PValue | FE | Benjamini |
| **GO:0006629~lipid metabolic process** | 12 | 8.51 | 1.88E-04 | 4.01 | 0.11 |
| **GO:0006633~fatty acid biosynthetic process** | 5 | 3.55 | 0.001131 | 10.84 | 0.22 |
| **GO:0055091~phospholipid homeostasis** | 3 | 2.13 | 0.001518 | 49.88 | 0.22 |
| **GO:0006281~DNA repair** | 8 | 5.67 | 0.004104 | 3.94 | 0.32 |
| **GO:0042632~cholesterol homeostasis** | 4 | 2.84 | 0.007355 | 9.98 | 0.45 |
| GO:0006310~DNA recombination | 4 | 2.84 | 0.015530 | 7.58 | 0.64 |
| **GO:0006974~cellular response to DNA damage stimulus** | 8 | 5.67 | 0.018579 | 2.94 | 0.67 |
| **GO:0016568~chromatin modification** | 6 | 4.26 | 0.032402 | 3.36 | 0.74 |
| APP/E4/Abca1$^{+/-}$: T0 vs Vehicle | | | | | |
| Term | Count | % | PValue | FE | Benjamini |
| GO:0006355~regulation of transcription, DNA-templated | 69 | 14.90 | 2.50E-05 | 1.66 | 0.04 |
| **GO:0006974~cellular response to DNA damage stimulus** | 20 | 4.32 | 7.88E-04 | 2.39 | 0.43 |
| GO:0006351~transcription, DNA-templated | 57 | 12.31 | 0.001272 | 1.52 | 0.46 |
| **GO:0006281~DNA repair** | 14 | 3.02 | 0.010360 | 2.24 | 0.92 |
| **GO:0006633~fatty acid biosynthetic process** | 6 | 1.30 | 0.013636 | 4.22 | 0.94 |
| GO:0006810~transport | 50 | 10.80 | 0.020717 | 1.36 | 0.95 |
| GO:0000723~telomere maintenance | 4 | 0.86 | 0.034595 | 5.55 | 0.98 |
| **GO:0016568~chromatin modification** | 11 | 2.38 | 0.049604 | 2.00 | 0.99 |

In Red are shown pathways related to lipid and cholesterol metabolism

In bold are marked GO terms overlapping in both APOE isoforms

**B. Down-regulated GO terms in T0 treated APP/E3/Abca1^{+/-} and APP/E4/Abca1[+/-]mice**

| APP/E3/Abca1^{+/-}: T0 vs Vehicle | | | | | |
|---|---|---|---|---|---|
| Term | Count | % | PValue | FE | Benjamini |
| GO:0007155~cell adhesion [a] | 18 | 6.19 | 3.48E-04 | 2.72 | 0.40 |
| GO:0045087~innate immune response | 15 | 5.15 | 4.11E-04 | 3.06 | 0.26 |
| GO:0043410~positive regulation of MAPK cascade | 8 | 2.75 | 6.72E-04 | 5.44 | 0.28 |
| GO:0042127~regulation of cell proliferation | 11 | 3.78 | 9.34E-04 | 3.63 | 0.24 |
| **GO:0043065~positive regulation of apoptotic process[b]** | 13 | 4.47 | 0.001376 | 3.00 | 0.29 |
| GO:0005977~glycogen metabolic process | 5 | 1.72 | 0.001427 | 10.10 | 0.26 |
| GO:0030335~positive regulation of cell migration | 10 | 3.44 | 0.001575 | 3.70 | 0.25 |
| GO:0008284~positive regulation of cell proliferation | 15 | 5.15 | 0.004897 | 2.35 | 0.45 |
| GO:0035458~cellular response to interferon-beta | 4 | 1.37 | 0.008467 | 9.42 | 0.52 |
| GO:0055114~oxidation-reduction process | 18 | 6.19 | 0.010928 | 1.95 | 0.53 |
| APP/E4/Abca1^{+/-}: T0 vs Vehicle | | | | | |
| Term | Count | % | PValue | FE | Benjamini |
| GO:0009968~negative regulation of signal transduction | 7 | 2.16 | 1.45E-04 | 8.67 | 0.18 |
| GO:0030512~negative regulation of transforming growth factor beta receptor signaling pathway | 6 | 1.85 | 0.001225 | 7.43 | 0.57 |
| GO:0030154~cell differentiation | 23 | 7.10 | 0.002570 | 2.01 | 0.59 |
| GO:0032436~positive regulation of proteasomal ubiquitin-dependent protein catabolic process | 6 | 1.85 | 0.003043 | 6.06 | 0.57 |
| GO:0006469~negative regulation of protein kinase activity | 6 | 1.85 | 0.014215 | 4.19 | 0.92 |
| GO:0090090~negative regulation of canonical Wnt signaling pathway | 6 | 1.85 | 0.015452 | 4.10 | 0.91 |
| **GO:1901214~regulation of neuron death** | 3 | 0.93 | 0.021139 | 13.13 | 0.91 |
| GO:0060326~cell chemotaxis | 4 | 1.23 | 0.034302 | 5.59 | 0.94 |
| GO:0007268~synaptic transmission | 6 | 1.85 | 0.036113 | 3.28 | 0.94 |
| GO:0046777~protein autophosphorylation | 7 | 2.16 | 0.049486 | 2.64 | 0.97 |

[a], **In Green are shown pathways differentially downregulated in both APOE isoforms**

[b], **Bold: similar GO terms**
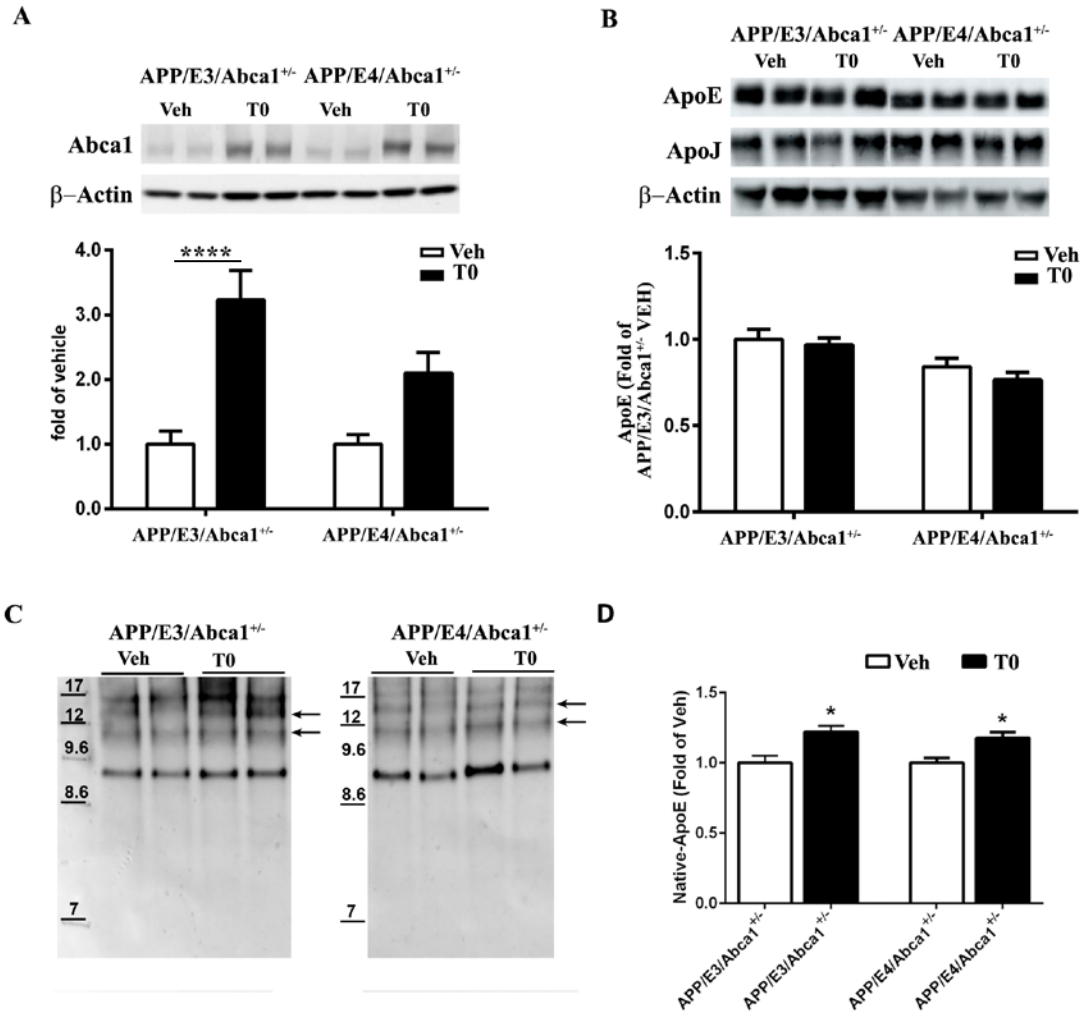
**Figure 13: T0 treatment increases ABCA1 protein level and APOE lipidation**
T0 treatment increases ABCA1 protein level and APOE lipidation. ABCA1, APOE and APOJ protein levels were determined by SDS-PAGE. Additionally, APOE lipidation was determined by Native PAGE. **A,** Representative image of ABCA1 protein level is shown above the graph. T0 significantly affected ABCA1 protein level. Analysis by two-way ANOVA shows no interaction between *APOE* genotype and T0 treatment. There is a significant main effect on T0 treatment ($F_{(1, 34)} = 26.12$, $p < 0.0001$), but not on *APOE* genotype. Bonferroni's post-test shows a significant difference between T0 and vehicle treated APP/E3/Abca1$^{+/-}$ mice (****$p<0.0001$). **B,** T0 treatment did not affect APOE or APOJ protein levels. N=9-10 mice per group. **C,** APOE lipidation state in APP/E3/Abca1$^{+/-}$ (left) and APP/E4/Abca1$^{+/-}$ (right) mice. Representative images of APOE lipidation are shown. Arrows are indicative of lipidation status. N=4-5 mice per group.

### 5.2.4 Genes commonly affected by APOE isoform regardless of treatment

Since PCA (Fig.12A) showed high isoform-dependent variability in APP/E3/Abca1$^{+/-}$ and APP/E4/Abca1$^{+/-}$ datasets, we tested the effect of *APOE* genotype in conditions of T0 or vehicle treatment. First, we compared vehicle treated APP/E3/Abca1$^{+/-}$ and APP/E4/Abca1$^{+/-}$ mice and identified 1,524 differentially expressed genes at $p \leq 0.05$ cut-off (Fig.14A). In the T0 treated APP/E3/Abca1$^{+/-}$ and APP/E4/Abca1$^{+/-}$ datasets the number of the genes above the cut-off was 1,068 (Fig.14B).

We focused on few target genes which were up- or down-regulated in APP/E4/Abca1$^{+/-}$ mice regardless of treatment. We were particularly interested in genes implicated in immune response and receptor mediated phagocytosis such as Fyn, *Cxcl10, Olig1, Oscar* and autophagy - several *Serpina* isoforms (3g, 3h, 3m, and 3n). As visible from the volcano plots on Fig.14A and B, these genes were significantly up-regulated in vehicle and T0 treated APP/E4/Abca1$^{+/-}$ mice when compared to their respective APP/E3/Abca1$^{+/-}$ counterparts (shown in Fig.5A and B as red). On Fig.14C are presented RNA-seq results from the comparison of T0 treated APP/E4/Abca1$^{+/-}$ and APP/E3/Abca1$^{+/-}$ mice. The result demonstrates that there is a significant increase of *Cxcl10, Fyn, Olig1, Oscar* and Serpina isoforms (3g, 3h, 3m, and 3n) mRNA expression in APP/E4/Abca1$^{+/-}$ when compared to APP/E3/Abca1$^{+/-}$ mice in the same T0 treated group. We also identified genes downregulated in APP/E4/Abca1$^{+/-}$ mice, regardless of the treatment, were related to lipid metabolism (Pip5kl1) and vesicular transport – *Stx17, Stx2* and *Stx3* (shown in Fig.14A and B as blue). mRNA level of these genes as determined by RNA-seq is shown on Fig. 14D.
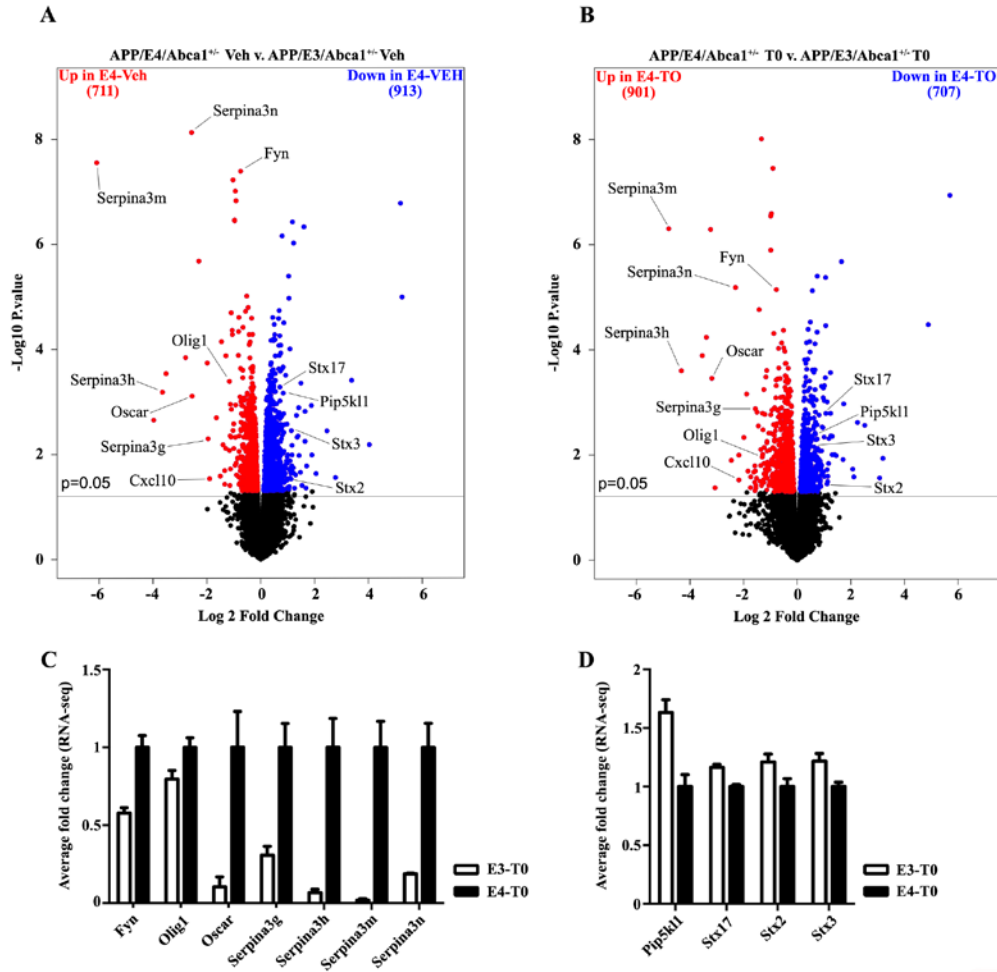
**Figure 14: Transcriptional analysis of *APOE* genotype on APP/E3/Abca1$^{+/-}$ and APP/E4/Abca1$^{+/-}$ mice transcriptome**

**A,** Comparison between vehicle treated APP/E3/Abca1$^{+/-}$ and APP/E4/Abca1$^{+/-}$ mice. **B,** Comparison between T0 treated APP/E3/Abca1$^{+/-}$ and APP/E4/Abca1$^{+/-}$ mice. Data were analyzed using EdgeR and the volcano plots are built using $p < 0.05$ cut-off. Up- and down-regulated genes are represented in red and blue respectively. On **C** and **D** are shown genes that are up- or down-regulated in APP/E4/Abca1-/+ mice regardless of the treatment. **C,** shown is RNA-seq result for genes that are significantly upregulated in APP/E4/Abca1$^{+/-}$ vs APP/E3/Abca1$^{+/-}$ mice regardless of treatment. **D,** shown is RNA-seq result for genes that are significantly down-regulated in APP/E4/Abca1$^{+/-}$ vs APP/E3/Abca1$^{+/-}$ mice regardless of treatment.

76

### 5.2.5 Differential effect of T0 treatment in APP/E4/Abca1$^{+/-}$ and APP/E3/Abca1$^{+/-}$ mice

Next, to examine if LXR treatment differentially affects biological processes in isoform-dependent manner, we applied Gene Set Enrichment Analysis (GSEA) and compared T0 treated APP/E4/Abca1$^{+/-}$ and APP/E3/Abca1$^{+/-}$ mice. We included expression data for all transcripts without setting a cut-off to avoid a bias towards the effect of highly affected genes [244]. Using GSEA we ranked the top 50 up- (Fig.15A) and down-regulated (Fig.15B) genes of the gene-ontology (GO) category "biological process". The bubble plot shown on Fig.15C represents biological processes affected by T0 treatment in APP/E3/Abca1$^{+/-}$ (right) and APP/E4/Abca1$^{+/-}$ mice (left) and is based on the number of genes in each category and the nominal p-value (see also Table 2). To further illustrate significantly enriched biological process terms, we show enrichment plots with corresponding heat maps for "Microtubule Based Process" (Fig. 15D) and "Synapse Organization and Biosynthesis" (Fig. 15F). While the morphological and functional validation of the affected biological processes in APP/E4/Abca1$^{+/-}$ is beyond the scope of this study, the results are suggesting APOE isoform specific response to LXR/RXR activation and enrichment in sets of genes that help to better understand positive effects of treatment on cognitive performance.
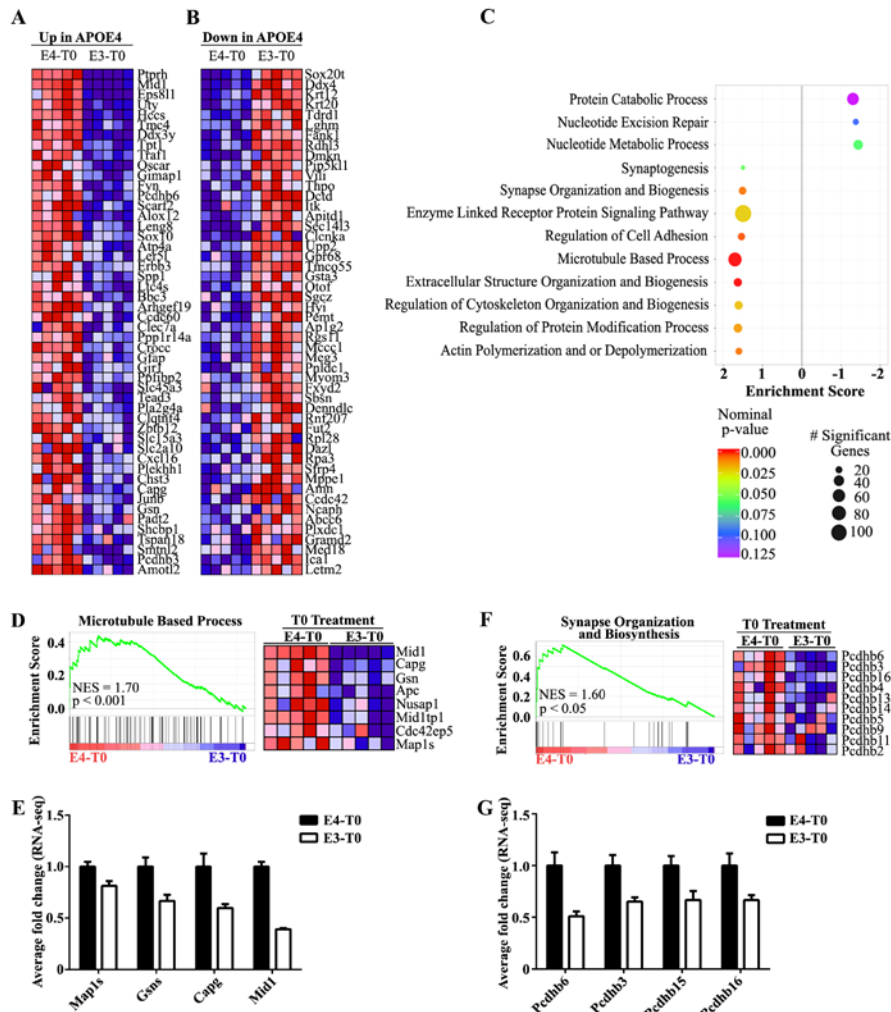
**Figure 15: APOE isoform-specific effect on gene expression in APP/E3/Abca1$^{+/-}$ and APP/E4/Abca1$^{+/-}$ mice**

Comparison between T0 treated APP/E3/Abca1$^{+/-}$ and APP/E4/Abca1$^{+/-}$ mice. Heat-maps provided by GSEA analysis were used to identify and rank the top 50 up-regulated genes (**A**) and top 50 down regulated genes (**B**) in APP/E3/Abca1$^{+/-}$ mice. **C,** Bubble plot shows top ranked "biological process" (BP) differentially affected by T0 treatment in APP/E3/Abca1$^{+/-}$ vs APP/E4/Abca1$^{+/-}$ mice. The gene lists were derived from edgeR output tables and included expression data for all transcripts. Color indicates nominalized p-value. Significant BP are represented in red to purple shades (p<0.05 and FDR≤0.25). Size of bubble indicates the number of significant genes in each represented BP. GSEA enrichment score curves and corresponding heat-maps show BP significantly enriched in T0 treated APP/E4/Abca1$^{+/-}$ mice, **D** and **E,** "Microtubule Based Process". **D,** GSEA analysis provided a heat-map (right) and enrichment score (left) for this category. **E,** RNA-seq results of significantly changed mRNA expression levels of representative genes from category "Microtubule Based Process". **F-G,** "Synapse Organization and Biosynthesis". **F,** GSEA analysis provided a heat-map (right) and enrichment score (left). **G,** RNA-seq results of significantly changed mRNA expression levels of representative genes from category "Synapse Organization and Biosynthesis".

**Table 2. Top 20 up- and down-regulated GSEA Biological Process in APP/E4/Abca1$^{+/-}$ vs APP/E3/Abca1$^{+/-}$ T0 treated mice**

| UP regulated in APP/E4/Abca1$^{+/-}$ vs APP/E3/Abca1$^{+/-}$ | | | | |
|---|---|---|---|---|
| NAME | SIZE | NES | NOM p-val | FDR q-val |
| **MICROTUBULE_CYTOSKELETON_ORGANIZATION_AND_BIOGENESIS** *a* | **31** | **-1.87** | **0.00** | **0.16** |
| **NEGATIVE_REGULATION_OF_PROTEIN_METABOLIC_PROCESS** | **31** | **-1.68** | **0.01** | **0.24** |
| ANTI_APOPTOSIS | 89 | -1.64 | 0.00 | 0.31 |
| REGULATION_OF_PROTEIN_MODIFICATION_PROCESS | 28 | -1.63 | 0.01 | 0.26 |
| **SYNAPSE_ORGANIZATION_AND_BIOGENESIS** *b* | **20** | **-1.60** | **0.01** | **0.25** |
| ONE_CARBON_COMPOUND_METABOLIC_PROCESS | 25 | -1.55 | 0.04 | 0.37 |
| REGULATION_OF_ORGANELLE_ORGANIZATION_AND_BIOGENESIS | 35 | -1.54 | 0.02 | 0.38 |
| ACTIN_POLYMERIZATION_AND_OR_DEPOLYMERIZATION | 21 | -1.54 | 0.00 | 0.36 |
| REGULATION_OF_CELL_ADHESION | 23 | -1.51 | 0.01 | 0.40 |
| PEPTIDYL_TYROSINE_PHOSPHORYLATION | 16 | -1.49 | 0.04 | 0.39 |
| CELL_CYCLE_ARREST_GO_0007050 | 46 | -1.49 | 0.05 | 0.38 |
| NEGATIVE_REGULATION_OF_PROGRAMMED_CELL_DEATH | 112 | -1.49 | 0.03 | 0.36 |
| Down regulated in APP/E4/Abca1$^{+/-}$ vs APP/E3/Abca1$^{+/-}$ | | | | |
| NAME | SIZE | NES | NOM p-val | FDR q-val |
| NUCLEOTIDE_METABOLIC_PROCESS | 34 | 1.44 | 0.06 | 1 |
| NUCLEOTIDE_EXCISION_REPAIR | 18 | 1.38 | 0.10 | 1 |
| PROTEIN_CATABOLIC_PROCESS | 55 | 1.31 | 0.13 | 1 |
| TRANSCRIPTION_INITIATION | 24 | 1.27 | 0.18 | 1 |
| PHOSPHOLIPID_METABOLIC_PROCESS | 55 | 1.24 | 0.11 | 1 |
| STRESS_ACTIVATED_PROTEIN_KINASE_SIGNALING_PATHWAY | 41 | 1.19 | 0.18 | 1 |
| REGULATION_OF_DNA_METABOLIC_PROCESS | 36 | 1.16 | 0.28 | 1 |
| PROTEIN_MODIFICATION_BY_SMALL_PROTEIN_CONJUGATION | 39 | 1.15 | 0.26 | 1 |
| PROTEIN_DNA_COMPLEX_ASSEMBLY | 36 | 1.15 | 0.27 | 1 |
| NEGATIVE_REGULATION_OF_MAP_KINASE_ACTIVITY | 16 | 1.12 | 0.27 | 1 |
| JNK_CASCADE | 39 | 1.11 | 0.32 | 1 |
| MEMBRANE_LIPID_METABOLIC_PROCESS | 79 | 1.09 | 0.31 | 1 |

*a*, With bold are marked statistically significant Biological Process (BP) (FDR≤0.25)

### 5.2.6 Discussion

In this study we analyzed the effect of LXR agonist T0 on the phenotype of *Abca1* haplo-deficient APP/E3 and APP/E4 mice. The results demonstrate that T0 significantly ameliorates cognitive deficits seen in APP/E4/Abca1$^{+/-}$ mice, as examined by Novel Object Recognition and Contextual Fear Conditioning paradigms. T0 treatment also reduced soluble Aβ oligomers without affecting amyloid plaques, confirming our recent study [191]. Importantly, RNA-seq results and the analysis of changes in the transcriptome demonstrated that commonly up-regulated genes in response to T0 induced LXR/RXR activation affect lipoprotein metabolism and APOE lipidation. We postulate that the ultimate changes in the phenotype of AD animal model used here are the result of interconnected effects T0 on molecular, cellular and organism levels.

Prior studies have demonstrated that treatment with LXR agonists ameliorates memory deficits in APP mice [182, 183, 187, 189, 191, 214, 258]. There are several explanations for this effect. First – the increased lipidation of APOE, even without an increase in *APOE* mRNA or APOE protein level. As seen on the Native-PAGE, our findings illustrate that T0 increases the level of lipidated APOE in cortical homogenates of both APP/E3/Abca1$^{+/-}$ and APP/E4/Abca1$^{+/-}$ mice (Fig. 4). Based on our transcriptomics and expression validation data we postulate that the increased APOE lipidation is a result of the upregulated expression of *Abca1*, *Abcg1*, *Scd1*, *Scd2* and *Lpcat3* genes, and thus proteins, essential for cholesterol efflux. These genes were identified as commonly up-regulated in brain of mice expressing either APOE isoform. In this respect it is important to emphasize the previous studies showing that the deficiency of ABCA1 results in lack of lipidated APOE in brain parenchyma and CSF [176, 177, 179, 259, 260].

80

We hypothesize that clearance of Aβ oligomers out of the brain via BBB or an increased phagocytosis by microglia are possible and important consequences of the increased level of fully lipidated APOE (a general discussion can be found in [168]). Whereas in this study we did not specifically examine which one of those clearance routes is affected, our data clearly show that Aβ dimers in T0-treated APP/E4/Abca1$^{+/-}$ mice are decreased. Published data from our group also demonstrated that LXR/RXR agonists decrease the level of soluble Aβ$_{40}$ and Aβ$_{42}$ in ISF [183, 191, 261], and the treatment of APP/E3 and APP/E4 mice with RXR ligand, bexarotene, decreases the level of soluble Aβ oligomers in brain parenchyma. Altogether, these data are suggesting that the effect of T0 treatment on clearance of Aβ soluble species could be a result of concerted action of activated RXR homodimers and LXR/RXR heterodimers [261]. A second consequence of increased APOE lipidation is that properly lipidated APOE can deliver cholesterol and phospholipids to neurons more efficiently. Those lipid molecules are needed for repair of axonal/neuronal damage resulting from amyloid deposition and thus for improved synaptic transmission. As extensively discussed in our previous study [239] mice lacking *Apoe* have impairments in cognition and dendritic arborization. Synaptic dysfunction in AD pathogenesis is recognized as an important mechanism and the role of APOE in affecting synaptic plasticity in an isoform-dependent manner has been repeatedly confirmed (reviewed in [262-264]).

Our results also show that there is a significant APOE isoform-specific effect on expression of genes with a role in Aβ clearance. As shown on Fig. 5, several genes associated with immune response such as *Cxcl10, Fyn, Oscar* and isoforms of *Serpina*, compared to APP/E3/Abca1$^{-/+}$ mice were up-regulated in APP/E4/Abca1$^{-/+}$ mice, even without a treatment. The analysis of differentially expressed genes also identified genes downregulated in

APP/E4/Abca1$^{+/-}$ mice regardless of the treatment; those gene were related to lipid metabolism (*Pip5kl1*) and vesicular transport – *Stx17, Stx2* and *Stx3* (shown in blue on the volcano plots on Fig. 5A and B). While specific experiments have been outside of the scope of this study, considering the growing knowledge of the role of immune receptors in Aβ clearance the transcriptional changes of the above genes and possible control of neuroinflammatory responses in AD brain are worth pursuing in the future.

When we compared only agonist treated APP/E3/Abca1$^{+/-}$ and APP/E4/Abca1$^{+/-}$mice, we identified "Microtubule Based Process" and "Synapse Organization and Biosynthesis" as GO categories uniquely enriched in APP/E4/Abca1$^{+/-}$ mice. Members of the beta-protocadherin (*Pcdh-β*) family were up-regulated in T0 treated APP/E4/Abca1$^{+/-}$ mice. *Pcdh* genes, a subfamily of cadherin adhesion molecules, are expressed in the brain (reviewed in [265]) and have been demonstrated essential in establishing synapses and synapse function [266]. *Pcdh* gene family expression has been identified in various neuronal populations and the protein localizes predominantly in synapses. An isoform of *Pcdhg-β, Pcdhβ-16* is expressed in the hippocampus and cortical layers [266] and we found isoforms of *Pcdhβ-16* up-regulated following T0. Although currently the research focuses primarily on PCDH-α and PCDH-γ and their ability to mediate cell adhesion through combinatorial expression on the surface of neurons [267, 268], it is reasonable to assume that PCDH-β could be involved in those processes, as well. PCDH-β can localize to synapses, suggesting the protein might have the potential to contribute to the formation of synaptic plasticity in the mammalian CNS. No research, however, has been conducted so far, to reveal if their function is interconnected to APOE secretion and deposition of Aβ, or cholesterol transport and its internalization at the synaptic level, or the way they

influence the cholesterol/phospholipid composition of the cell membrane, necessary and required for normal neuronal function.

In conclusion, the present findings show that LXR agonist treatment of *Abca1* haplo-deficient APP/E4 mice, ameliorates APOE4 driven brain pathology and cognitive deficits. The results are attributed to the ability of T0, through LXR/RXR activation, to reverse lipid deficiency of APOE4 particles in brain. The results of our study also suggest that an increased ABCA1 and ABCG1 expression through LXR/RXR activation, resulting in improved APOE lipidation may be an useful target for future prophylactic as well as therapeutic approaches in *APOE4* carriers.


## 5.3    INTEGRATED APPROACH REVEALS DIET AND APOE ISOFORMS DIFFERENTIALLY AFFECT IMMUNE RESPONSE IN ALZHEIMER'S MODEL MICE


Submitted on October 18, 2016 to the journal, Science Translational Medicine


### 5.3.1    High fat diet aggravates AD-like phenotype of middle-aged APP23 mice


*Effect on memory:* To examine the effect of high fat diet (HFD) on AD-like phenotype we used one-year old APP23 mice fed with HFD for three months and compared their learning and memory performance to those of mice fed normal diet (ND). As shown on Fig.16A, weight gain resulting from HFD was similar in male and female mice. To examine cognitive performance, we used Morris Water Maze (MWM). As seen from Fig. 16B, HFD significantly affected the

83

acquisition of spatial memory exemplified by the increased escape latency. Memory retention was also significantly reduced as indicated by the latency to enter the target quadrant in the probe trial of MWM (Fig. 16C). There was no significant difference in cognitive performance between male and female mice on either of the diet (Fig. 17A and B).

*High fat diet increases amyloid deposition*: Our previous data demonstrated that HFD increases amyloid deposition in APP23 mice [183]. To confirm this, total Aβ plaques (including diffuse and fibrillar) were visualized using 6E10 anti-Aβ antibody (Fig. 16D) and compact amyloid plaques assessed by X-34 staining (Fig. 16F). As visible on Fig. 16E and G, there was a significant diet and gender effect on 6E10-positive Aβ plaques as well as on X-34 labeling compact amyloid plaques, respectively. While HFD affected males and females similarly the females had significantly more amyloid irrespective of diet. The effect of diet on plaques was not a result of an increase in full length Aβ precursor protein (APP), as it was unaffected by HFD (Fig. 17C and D). We also observed a significant decrease in ABCA1 protein level following HFD (Fig. 17C) whereas APOE protein level was unchanged (Fig. 17D). Collectively these results confirm our previous study [183] and we conclude that in this model HFD aggravates AD-like phenotype.
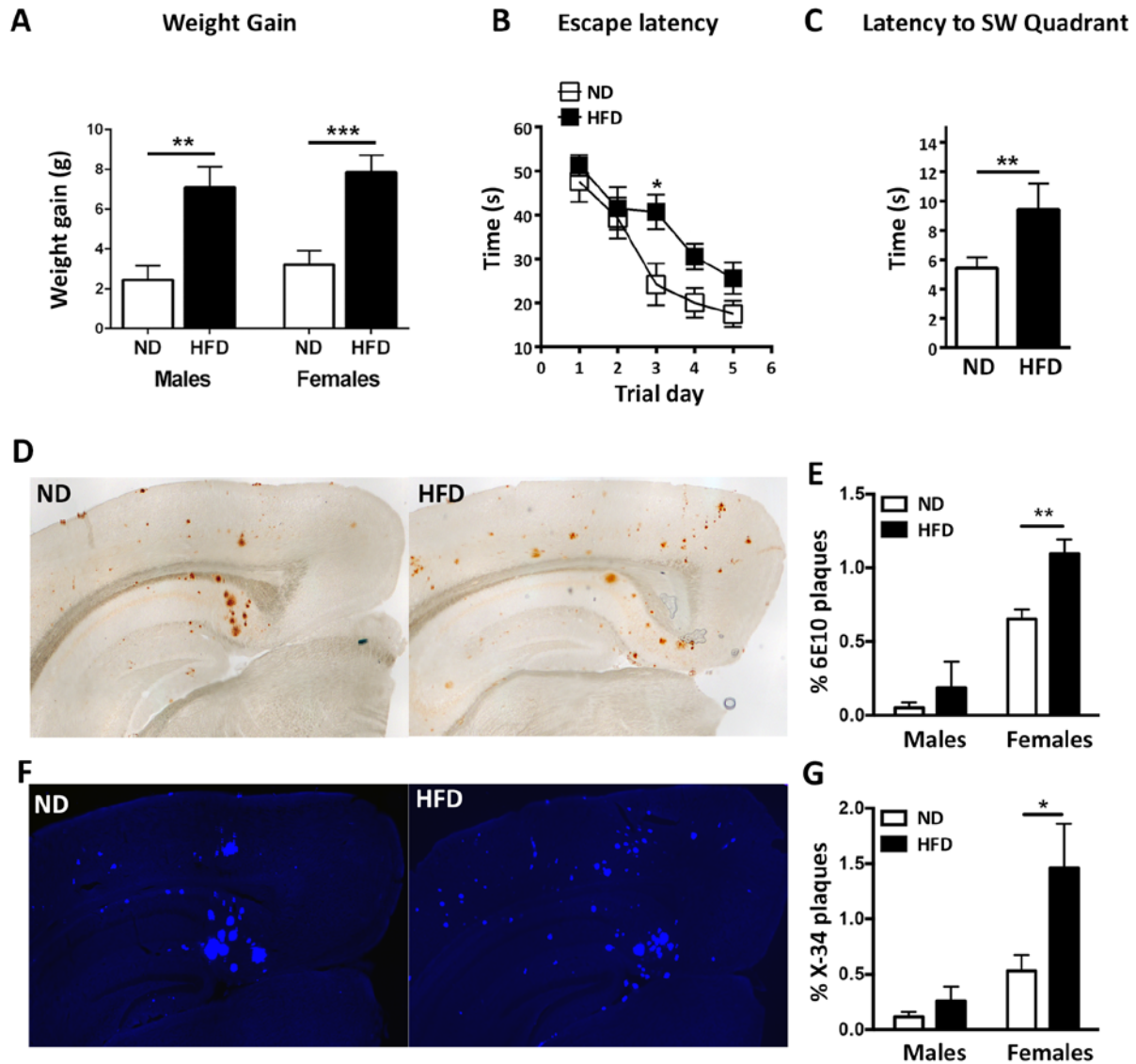
**Figure 16**: **High fat diet worsens cognitive performance and increases amyloid deposition in APP23 mice**

APP23 mice were fed with HFD for 3 months. **(A)** Weight gain in male and female mice. Student's *t*-test. N = 9 – 11 male, 13 – 14 female per group. **, p<0.01; ***, p<0.001. **(B)** Acquisition trial of MWM (Escape latency). Statistic by two-way ANOVA. No interaction between trial day and diet; significant main effect of diet ($F_{(1,110)}$ = 11.24, p = 0.0011) and trial day ($F_{(4,110)}$=12.38, p < 0.0001). **(C)** Probe trial of MWM (latency to the target). Student's *t*-test. **B-C**, N = 5 – 7 mice gender/group. **(D-G)** Amyloid plaques in cortex and hippocampus of APP23 mice on ND and HFD were analyzed by two-way ANOVA followed by Sidak's multiple comparison test. Representative images **(D)** and quantification **(E)** of Aβ deposits (6E10 staining). No interaction between diet and gender and significant effect of both diet ($F_{(1,12)}$=29.92, p=0.0001) and gender ($F_{(1,12)}$=40.58, p=0.0001). Representative images **(F)** and quantitation **(G)** of X-34 fibrillary amyloid plaques. No interaction and significant main effect of diet ($F_{(1,12)}$=5.32, p=0.004) and gender ($F_{(1,12)}$=12.11, p=0.003). For D-G N=4-5 male, 5 female mice per group. *, p < 0.05 and **, p < 0.01.

**A** MWM-Females acquisition time

| Source of Variation | % of total variation | P value | P value summary |
|---|---|---|---|
| Interaction | 3.216 | 0.6239 | ns |
| trial day | 30.94 | 0.0003 | *** |
| treatment | 4.767 | 0.0538 | ns |

**B** MWM-Males acquisition time

| Source of Variation | % of total variation | P value | P value summary |
|---|---|---|---|
| Interaction | 1.166 | 0.9293 | ns |
| trial day | 27.06 | 0.0021 | ** |
| treatment | 10.49 | 0.0080 | ** |
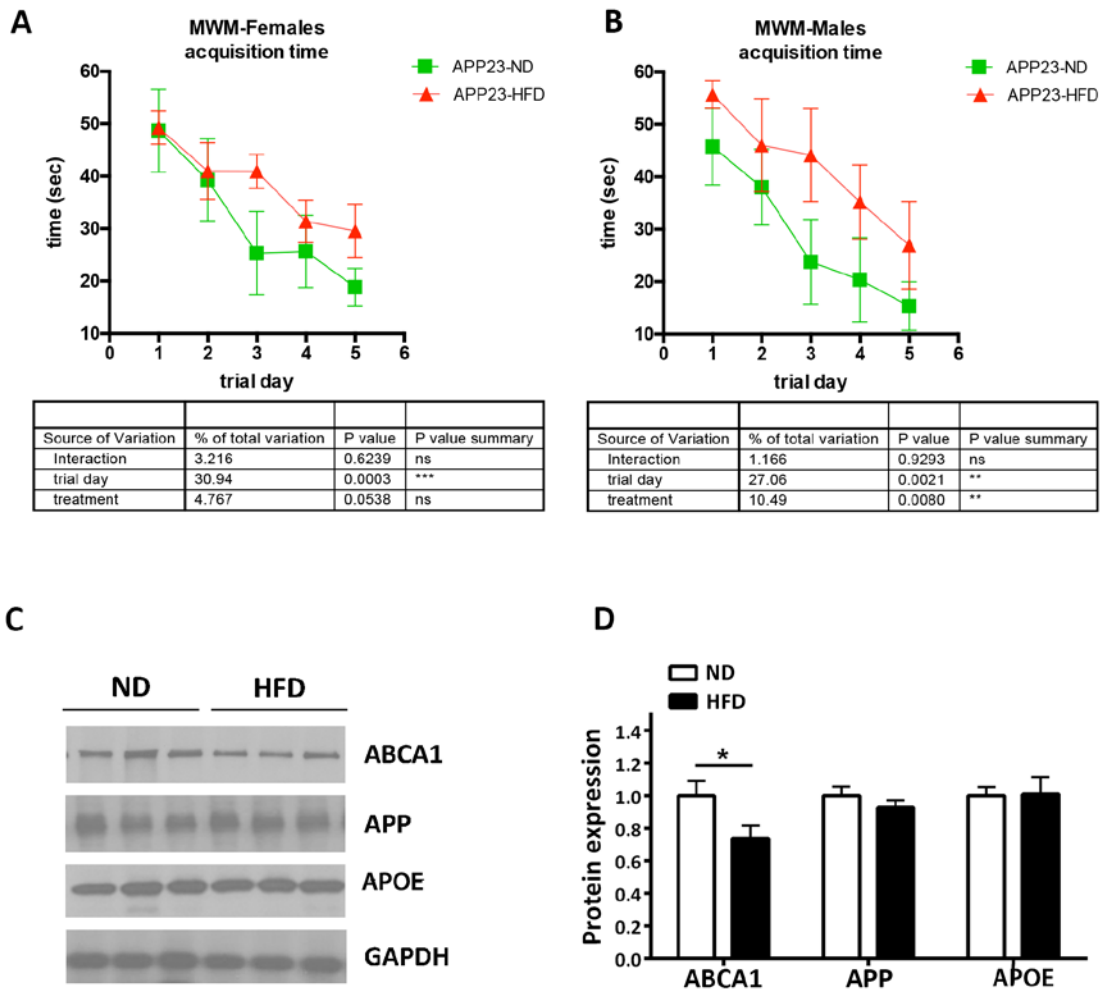
**Figure 17: MWM Behavior by gender in APP23 mice**
(A). Acquisition phase of MWM-females, N=5-7; B. Acquisition phase of MWM-males, N=5-6. C and D, HFD induces a decrease of ABCA1 protein level but does not affect APP and APOE. Representative images (C) and quantitation (D) of WB for ABCA1, APP, APOE. GAPDH is used as a loading control. Data are presented as fold of ND. N=4-5 mice/gender/group. Student's *t*-test *$p < 0.05$

## 5.3.2 Microglia morphology is altered in female APP/E4 mice

Next, we determined if the microglia morphology is similar in both genotypes. For this purpose,

we analyzed the morphology of the microglia processes on randomly chosen IBA-1 positive cells

in the cortex using IMARIS software automated filament tracer. Upon activation by reactive stimuli, microglia typically become more amoeboid with shorter and less complex processes that can be accurately quantified via unbiased IMARIS tracing [269, 270]. Confocal Z stacks were captured (Fig. 18A) from the cortex and then process length, and branching were assessed. As shown on Fig. 18B, the total process length of cortical microglia was significantly higher in APP/E3 mice and the number of branches in APP/E3 showed a strong trend toward increase when compared to APP/E4 mice (Fig. 18C). These results suggest that HFD significantly and differentially affected the activation state and microglia morphology in APP/E4 and APP/E3 mice.
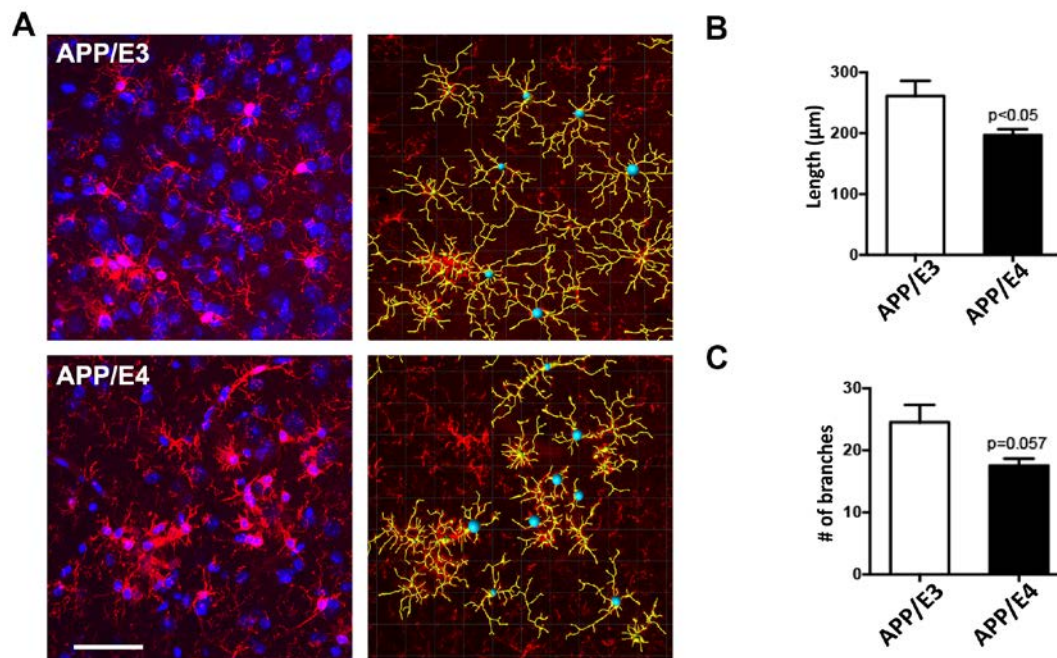


**Figure 18. Microglia morphology is altered in female APP/E4 compared to APP/E3 mice**
Compared are female APP/E4 to APP/E3 mice fed HFD. (**A**) Representative confocal images and IMARIS tracings of microglia (IBA-1 positive, red) and nuclei (blue) in the cortex of APP/E3 and APP/E4 mice fed HFD. Automated analysis using IMARIS software illustrated for each group (yellow). (**B**) Microglia process length is significantly decreased and (**C**) the number of branches shows a trend towards decrease in APP/E4 females fed HFD. Analysis was performed by Mann-Whitney test.

## 6.0 CONCLUSION

Our original hypothesis states that transcriptional control of LXR target genes such as APOE and ABCA1 in combination with environmental factors influences amyloid deposition and cognitive decline in mouse models representative of AD phenotype. Three separate aims addressed the hypothesis. To examine the first aim, we stereotaxically infused AβOs into the hippocampi of $Abca1^{ko}$ mice and assessed neurite morphology. To examine the second aim, we fed APP23, APP/E3, and APP/E4 transgenic mice a HFD and assessed the effect on the protein level of LXR targets ABCA1 and APOE, Aβ pathology, and microglial morphology. Lastly, to examine the third aim, we chronically treated APP/E3/Abca1$^{+/-}$ and APP/E4/Abca1$^{+/-}$ mice with the LXR agonist T0 and assessed Aβ pathology, mRNA expression and protein levels of ABCA1 and APOE, as well as APOE lipidation levels, and the effect on the transcriptome. The results from these studies have two far-reaching clinical implications: 1). Lifestyle or dietary and 2). Pharmacological interventions.

Cholesterol is critical for metabolic and homeostatic processes throughout the body. The brain is the most cholesterol-rich organ in the body. Cholesterol is essential for neuronal development, maintenance of synaptic plasticity, neurite outgrowth, synaptic vesicle transport, and neurotransmitter release. Cholesterol is one of the most important components of lipid rafts. Lipid rafts identified in neurons and glia further implicate cholesterol for neuronal function. Caveolin-1 is a protein present in a subset of lipid rafts involved in compartmentalization and

88

internalization of signaling complexes, neuronal differentiation, arborization, and neuroprotection. Although caveolin expression is low in neurons, caveolin-1 knockout mice present with features found in aged hippocampi like decreased levels of synaptic markers and reduced number of hippocampal synapses. In elderly human cortical samples, caveolin-1 colocalizes with APP. In aged human cortices and hippocampi, caveolin-1 is up-regulated. Enhanced BACE1 activity is a consequence of enzymatic targeting to lipid rafts. Therefore, lipid raft dysfunction may impair synapses leading to cognitive decline and AD [271-273].

The majority of cholesterol in the brain is in the active "free" unesterified form, which is primarily present in myelin and necessary to execute the functions aforementioned. An imbalance in membrane lipids, altering cholesterol biosynthesis, or any minor perturbation to brain cholesterol homeostasis can negatively affect brain function. These disruptions occur in several neurodegenerative diseases including Huntington's and Pick's disease. Neurons synthesize the majority of cholesterol for growth and synaptogenesis, however, once they are mature, neurons rely on an exogenous cholesterol supply primarily from astrocytes. Cholesterol efflux and APOE lipidation from astrocytes requires ABC transporters ABCA1 and ABCG1 to create HDL-like lipoprotein particles that neurons can then internalize. Internalized cholesterol becomes esterified and stored as lipid droplets or a source for synaptic and dendritic formation and remodeling [128, 274].

We and others previously demonstrated the role of ABCA1 in the pathogenesis of AD. APP transgenic mice lacking *Abca1* present a significant increase in amyloid plaques and decrease in APOE protein brain levels. Mice expressing human APOE4 are more susceptible to *Abca1* haplo-deficiency compared to APOE3 counterparts. Also, we previously demonstrated increased AβO levels and impairment in the CA1 region of the hippocampus in APP transgenic

mice crossed with *Abca1*<sup>ko</sup> mice [176-180, 219, 239]. However, in the current study presented here, we further supported that APP/*Abca1*<sup>ko</sup> mice have cognitive deficits in MWM and NOR behavior paradigms. However, focusing specifically on the role of ABCA1 in cognitive deficits, we infused *Abca1*<sup>ko</sup> mice with scrambled (control) Aβ into the hippocampus. Compared to wild-type counterparts, only ABCA1 not Aβ infusion affected cognitive deficits. *Abca1*<sup>ko</sup> mice presented impaired neurite morphology. Therefore *Abca1*<sup>ko</sup> mice have basal cognitive deficits that prevent coping with additional factors like Aβ. This data further implicates ABCA1 and APOE in cholesterol and lipid metabolism. Our data suggests that deleting *ABCA1* may prevent cholesterol efflux and APOE lipidation from astrocytes. Therefore, lipid-poor APOE cannot contribute to HDL-like particles in the brain and shuttle lipoproteins to neurons to support neuronal physiological functions.

High saturated fats in part characterize high-fat diet (HFD) and are problematic when eaten excessively because the brain becomes deprived of nutrients. Consumption of HFD increases AD risk, especially mid-life. We demonstrated that APP23 transgenic mice consuming HFD expressing mouse *Apoe* displayed worse cognitive performance. We examined microglia morphology in APP transgenic mice with human APOE3 and APOE4 (APP/E3 and APP/E4 respectively) fed HFD. Microglia are the brain's resident monocyte-derived cell, contributing to immune response. Activated microglia become 'ameboid' while undergoing morphological changes. These changes include increased soma size and thickened processes, suggesting that microglia may be contributing to an immune response. We demonstrated that HFD affects microglia morphology in both APOE isoforms as seen in female APP/E3 and APP/E4 mice. Importantly, we observed a decrease in number of branches and length in APP/E4 mice fed HFD when compared to APP/E3 mice fed HFD. The conversion to an activated phenotype suggests

that microglia are facilitating an overall immune response that may induce phagocytosis or inflammation, which is detrimental in AD [275].

It is important to reiterate that there is no single genetic or environmental factor that drives AD risk. Age is the greatest risk factor for AD. Chronic inflammation associated with normal aging suggests an age-related change that increases AD risk [276]. Genome-wide association studies identified immune-related genes like triggering receptor expressed on myeloid cells 2 protein (TREM2). TREM2 has functions associated with phagocytosis of Aβ deposits. Individuals haroboring heterozygous loss-of-function mutation in TREM2 have a predisposition to AD [276, 277]. Sex differences regulate the susceptibility to inflammation. Importantly, during adulthood, female sex steroid hormones protect against inflammation-related diseases. However, during aging, females become susceptible to inflammation-related diseases due to the decline in sex steroid horomone levels [276, 278].

AD is a mutlifactorial disease that can differentially affected men and women. Sex difference exist in AD, with women being predisposed to AD even after controlling for the fact that women live longer than men [276, 279]. *APOE4*, the strongest genetic risk factor for AD, is a risk factor modified by sex, with women harboring a single copy of *APOE4* at an increased risk of AD by approximately four-fold [276, 280, 281]. Similar to humans, sex bias associated with APOE4-TR mice occurs compared to APOE3-TR and increases AD-like pathology in females than male AD-transgenic mice [276, 282]. This data demonstrates the importance of factoring sex steroid hormones in modulating AD risk.

Cholesterol and lipid metabolism became the focus of AD research with indication of *APOE4* as a risk factor for LOAD. As previously stated, it is debatable whether APOE4 confers insufficient protection or deleterious effects in AD pathology; therefore, it is also debatable if

drugs should inhibit or increase APOE4 activity. Loss-of-physiological function of *APOE4* associates with decrease synaptic function, neurogenesis, lipid and cholesterol metabolism, Aβ clearance [283], suggesting that *APOE4* is not as efficient as its *APOE3* and *APOE2* counterparts. For cholesterol and lipid metabolism, this would indicate that APOE4 has impaired ability to transport fat and cholesterol via astrocytes to neurons. High serum cholesterol measured in *APOE4* occurs possibly in attempts to adjust for the poor rate of cholesterol uptake. Therefore, therapeutic interventions to increase APOE4 lipidation may be useful in AD patients.

We demonstrate that LXR agonist T0901317 improves cognition in multiple behavior paradigms, decreases AD-associated pathology, and affects the transcriptome in APP/E4/Abca1$^{+/-}$ mice that underlies cholesterol and lipid metabolism [183, 186, 191]. Importantly, T0901317 increased Abca1 expression and protein levels as restored APOE lipidation in both APP/E3/Abca1$^{+/-}$ and APP/E4/Abca1$^{+/-}$ mice, suggesting that the benefits of T0901317 may positively affect both APOE genotypes. This finding is of importance because individuals who are *APOE3* carriers also suffer from AD. Also of importance is the use of *Abca1* heterozygous mice instead of *Abca1* knockout mice. *Abca1* heterozygotes are relevant to clinical phenotypes seen in the human population because of reduced ABCA1 transport function due to genetic variants. Two non-functional copies of *ABCA1* as in Tangier disease or global deletion of *Abca1* in *Abca1* knockout mice represent extreme examples. Therefore, administering LXR agonist to individuals with *Abca1* heterozygosity may prove beneficial in treating AD [171, 178].

T0901317 did not affect insoluble Aβ plaques, but reduced soluble Aβ levels. While endogenous and synthetic LXRs like oxysterols increase *Abca1*, *Abcg1*, and *Apoe* gene expression, we also saw that T0 increased gene expression of enzymes involved in fatty-acid remodeling, such as *Scd1* and *Scd2,* and *Srebp* that positively regulates genes involved in fatty-

acid biosynthesis. Therefore, this raises doubts about the use of LXR and RXR agonists as a pharmacological agent. This effect may lead to chronic activation of these pathways, a compensatory effect, and further induce AD-related deficits. Bexarotene or Targretin®, a FDA-approved retinoid medication for the use of cutaneous T-cell lymphoma (CTCL), selectively upregulates RXRs Bexarotene proved beneficial in mouse models representative of AD [193, 194]. However, Bexarotene is associated with hypertriglyceridemia. This suggests that use of RXR and LXR agonists can be beneficial, but should not be used long-term. Although we demonstrated the perceived benefits of LXR agonist, it is still necessary to further explore LXR and RXR pathways in reducing AD-associated pathologies.

In addition to LXRs and RXRs, PPARs highly expressed in the brain are critical for lipid homeostasis by interacting with fatty acids and lipid metabolites. Activation of PPARγs induces lipid uptake and storage genes. FDA approved drugs pioglitazone (Actos™) and rosiglitazone (Avandia™) for the treatment of type II diabetes are therapeutically relevant to AD, with a phase III trial underway for pioglitazone. Although the mechanisms by which PPARγ agonist improves behavior in AD model mice is unknown, anti-inflammatory effects may in part be responsible by suppressing proinflammatory cytokine levels [214]. Chronic administration of PPARγ agonist treatment leads to reduced amyloid plaque burden due to microglial phagocytosis of Aβ deposits, which in turn may improve behavior in AD model mice [214, 284, 285].

# BIBLIOGRAPHY

1.	Alzheimer A, Stelzmann RA, Schnitzlein HN, Murtagh FR. An English translation of Alzheimer's 1907 paper, "Uber eine eigenartige Erkankung der Hirnrinde". Clin Anat. 1995;8(6):429-31.

2.	Cipriani G, Dolciotti C, Picchi L, Bonuccelli U. Alzheimer and his disease: a brief history. Neurol Sci. 2011;32(2):275-9.

3.	Ramirez-Bermudez J. Alzheimer's disease: critical notes on the history of a medical concept. Arch Med Res. 2012;43(8):595-9.

4.	McKhann G, Drachman D, Folstein M, Katzman R, Price D, Stadlan EM. Clinical diagnosis of Alzheimer's disease: report of the NINCDS-ADRDA Work Group under the auspices of Department of Health and Human Services Task Force on Alzheimer's Disease. Neurology. 1984;34(7):939-44.

5.	Albert MS, DeKosky ST, Dickson D, Dubois B, Feldman HH, Fox NC, et al. The diagnosis of mild cognitive impairment due to Alzheimer's disease: recommendations from the National Institute on Aging-Alzheimer's Association workgroups on diagnostic guidelines for Alzheimer's disease. Alzheimers Dement. 2011;7(3):270-9.

6.	McKhann GM, Knopman DS, Chertkow H, Hyman BT, Jack CR, Jr., Kawas CH, et al. The diagnosis of dementia due to Alzheimer's disease: recommendations from the National Institute on Aging-Alzheimer's Association workgroups on diagnostic guidelines for Alzheimer's disease. Alzheimers Dement. 2011;7(3):263-9.

7.	Sperling RA, Aisen PS, Beckett LA, Bennett DA, Craft S, Fagan AM, et al. Toward defining the preclinical stages of Alzheimer's disease: recommendations from the National Institute on Aging-Alzheimer's Association workgroups on diagnostic guidelines for Alzheimer's disease. Alzheimers Dement. 2011;7(3):280-92.

8.	van Harten AC, Visser PJ, Pijnenburg YA, Teunissen CE, Blankenstein MA, Scheltens P, et al. Cerebrospinal fluid Abeta42 is the best predictor of clinical progression in patients with subjective complaints. Alzheimers Dement. 2013;9(5):481-7.

9.	Thal DR, Rub U, Orantes M, Braak H. Phases of A beta-deposition in the human brain and its relevance for the development of AD. Neurology. 2002;58(12):1791-800.

10.  Braak H, Alafuzoff I, Arzberger T, Kretzschmar H, Del Tredici K. Staging of Alzheimer disease-associated neurofibrillary pathology using paraffin sections and immunocytochemistry. Acta Neuropathol. 2006;112(4):389-404.

11.  Braak H, Braak E. Neuropathological stageing of Alzheimer-related changes. Acta Neuropathol. 1991;82(4):239-59.

12.  Mirra SS, Heyman A, McKeel D, Sumi SM, Crain BJ, Brownlee LM, et al. The Consortium to Establish a Registry for Alzheimer's Disease (CERAD). Part II. Standardization of the neuropathologic assessment of Alzheimer's disease. Neurology. 1991;41(4):479-86.

13.  Hyman BT, Phelps CH, Beach TG, Bigio EH, Cairns NJ, Carrillo MC, et al. National Institute on Aging-Alzheimer's Association guidelines for the neuropathologic assessment of Alzheimer's disease. Alzheimers Dement. 2012;8(1):1-13.

14.  Thal DR, Capetillo-Zarate E, Del Tredici K, Braak H. The development of amyloid beta protein deposits in the aged brain. Sci Aging Knowledge Environ. 2006;2006(6):re1.

15.  Brettschneider J, Del Tredici K, Lee VM, Trojanowski JQ. Spreading of pathology in neurodegenerative diseases: a focus on human studies. Nat Rev Neurosci. 2015;16(2):109-20.

16.  Alzheimer's A. 2016 Alzheimer's disease facts and figures. Alzheimers Dement. 2016;12(4):459-509.

17.  Hebert LE, Weuve J, Scherr PA, Evans DA. Alzheimer disease in the United States (2010-2050) estimated using the 2010 census. Neurology. 2013;80(19):1778-83.

18.  Xu J, Murphy SL, Kochanek KD, Bastian BA. Deaths: Final Data for 2013. Natl Vital Stat Rep. 2016;64(2):1-119.

19.  Ganguli M, Dodge HH, Shen C, Pandav RS, DeKosky ST. Alzheimer disease and mortality: a 15-year epidemiological study. Arch Neurol. 2005;62(5):779-84.

20.  Waring SC, Doody RS, Pavlik VN, Massman PJ, Chan W. Survival among patients with dementia from a large multi-ethnic population. Alzheimer Dis Assoc Disord. 2005;19(4):178-83.

21.  Brookmeyer R, Corrada MM, Curriero FC, Kawas C. Survival following a diagnosis of Alzheimer disease. Arch Neurol. 2002;59(11):1764-7.

22.  Larson EB, Shadlen MF, Wang L, McCormick WC, Bowen JD, Teri L, et al. Survival after initial diagnosis of Alzheimer disease. Ann Intern Med. 2004;140(7):501-9.

23.  Helzner EP, Scarmeas N, Cosentino S, Tang MX, Schupf N, Stern Y. Survival in Alzheimer disease: a multiethnic, population-based study of incident cases. Neurology. 2008;71(19):1489-95.

24. Xie J, Brayne C, Matthews FE, Medical Research Council Cognitive F, Ageing Study c. Survival times in people with dementia: analysis from population based cohort study with 14 year follow-up. BMJ. 2008;336(7638):258-62.

25. Wasco W, Gurubhagavatula S, Paradis MD, Romano DM, Sisodia SS, Hyman BT, et al. Isolation and characterization of APLP2 encoding a homologue of the Alzheimer's associated amyloid beta protein precursor. Nat Genet. 1993;5(1):95-100.

26. Wasco W, Bupp K, Magendantz M, Gusella JF, Tanzi RE, Solomon F. Identification of a mouse brain cDNA that encodes a protein related to the Alzheimer disease-associated amyloid beta protein precursor. Proc Natl Acad Sci U S A. 1992;89(22):10758-62.

27. Yoshikai S, Sasaki H, Doh-ura K, Furuya H, Sakaki Y. Genomic organization of the human amyloid beta-protein precursor gene. Gene. 1990;87(2):257-63.

28. Kang J, Lemaire HG, Unterbeck A, Salbaum JM, Masters CL, Grzeschik KH, et al. The precursor of Alzheimer's disease amyloid A4 protein resembles a cell-surface receptor. Nature. 1987;325(6106):733-6.

29. Rohan de Silva HA, Jen A, Wickenden C, Jen LS, Wilkinson SL, Patel AJ. Cell-specific expression of beta-amyloid precursor protein isoform mRNAs and proteins in neurons and astrocytes. Brain Res Mol Brain Res. 1997;47(1-2):147-56.

30. Puig KL, Combs CK. Expression and function of APP and its metabolites outside the central nervous system. Exp Gerontol. 2013;48(7):608-11.

31. O'Brien RJ, Wong PC. Amyloid precursor protein processing and Alzheimer's disease. Annu Rev Neurosci. 2011;34:185-204.

32. Bayer TA, Cappai R, Masters CL, Beyreuther K, Multhaup G. It all sticks together--the APP-related family of proteins and Alzheimer's disease. Mol Psychiatry. 1999;4(6):524-8.

33. Tang K, Wang C, Shen C, Sheng S, Ravid R, Jing N. Identification of a novel alternative splicing isoform of human amyloid precursor protein gene, APP639. Eur J Neurosci. 2003;18(1):102-8.

34. Sisodia SS. Beta-amyloid precursor protein cleavage by a membrane-bound protease. Proc Natl Acad Sci U S A. 1992;89(13):6075-9.

35. Dawkins E, Small DH. Insights into the physiological function of the beta-amyloid precursor protein: beyond Alzheimer's disease. J Neurochem. 2014;129(5):756-69.

36. Nicolas M, Hassan BA. Amyloid precursor protein and neural development. Development. 2014;141(13):2543-8.

37. van der Kant R, Goldstein LS. Cellular functions of the amyloid precursor protein from development to dementia. Dev Cell. 2015;32(4):502-15.

38. Hayashi Y, Kashiwagi K, Ohta J, Nakajima M, Kawashima T, Yoshikawa K. Alzheimer amyloid protein precursor enhances proliferation of neural stem cells from fetal rat brain. Biochem Biophys Res Commun. 1994;205(1):936-43.

39. Ohsawa I, Takamura C, Morimoto T, Ishiguro M, Kohsaka S. Amino-terminal region of secreted form of amyloid precursor protein stimulates proliferation of neural stem cells. Eur J Neurosci. 1999;11(6):1907-13.

40. Demars MP, Bartholomew A, Strakova Z, Lazarov O. Soluble amyloid precursor protein: a novel proliferation factor of adult progenitor cells of ectodermal and mesodermal origin. Stem Cell Res Ther. 2011;2(4):36.

41. Freude KK, Penjwini M, Davis JL, LaFerla FM, Blurton-Jones M. Soluble amyloid precursor protein induces rapid neural differentiation of human embryonic stem cells. J Biol Chem. 2011;286(27):24264-74.

42. Baratchi S, Evans J, Tate WP, Abraham WC, Connor B. Secreted amyloid precursor proteins promote proliferation and glial differentiation of adult hippocampal neural progenitor cells. Hippocampus. 2012;22(7):1517-27.

43. Chasseigneaux S, Dinc L, Rose C, Chabret C, Coulpier F, Topilko P, et al. Secreted amyloid precursor protein beta and secreted amyloid precursor protein alpha induce axon outgrowth in vitro through Egr1 signaling pathway. PLoS One. 2011;6(1):e16301.

44. Zhou F, Gong K, Song B, Ma T, van Laar T, Gong Y, et al. The APP intracellular domain (AICD) inhibits Wnt signalling and promotes neurite outgrowth. Biochim Biophys Acta. 2012;1823(8):1233-41.

45. Koo EH, Sisodia SS, Archer DR, Martin LJ, Weidemann A, Beyreuther K, et al. Precursor of amyloid protein in Alzheimer disease undergoes fast anterograde axonal transport. Proc Natl Acad Sci U S A. 1990;87(4):1561-5.

46. Hornsten A, Lieberthal J, Fadia S, Malins R, Ha L, Xu X, et al. APL-1, a Caenorhabditis elegans protein related to the human beta-amyloid precursor protein, is essential for viability. Proc Natl Acad Sci U S A. 2007;104(6):1971-6.

47. Wiese M, Antebi A, Zheng H. Intracellular trafficking and synaptic function of APL-1 in Caenorhabditis elegans. PLoS One. 2010;5(9).

48. Luo L, Tully T, White K. Human amyloid precursor protein ameliorates behavioral deficit of flies deleted for Appl gene. Neuron. 1992;9(4):595-605.

49. Torroja L, Packard M, Gorczyca M, White K, Budnik V. The Drosophila beta-amyloid precursor protein homolog promotes synapse differentiation at the neuromuscular junction. J Neurosci. 1999;19(18):7793-803.

50.    von Koch CS, Zheng H, Chen H, Trumbauer M, Thinakaran G, van der Ploeg LH, et al. Generation of APLP2 KO mice and early postnatal lethality in APLP2/APP double KO mice. Neurobiol Aging. 1997;18(6):661-9.

51.    Zheng H, Jiang M, Trumbauer ME, Sirinathsinghji DJ, Hopkins R, Smith DW, et al. beta-Amyloid precursor protein-deficient mice show reactive gliosis and decreased locomotor activity. Cell. 1995;81(4):525-31.

52.    Magara F, Muller U, Li ZW, Lipp HP, Weissmann C, Stagljar M, et al. Genetic background changes the pattern of forebrain commissure defects in transgenic mice underexpressing the beta-amyloid-precursor protein. Proc Natl Acad Sci U S A. 1999;96(8):4656-61.

53.    Dawson GR, Seabrook GR, Zheng H, Smith DW, Graham S, O'Dowd G, et al. Age-related cognitive deficits, impaired long-term potentiation and reduction in synaptic marker density in mice lacking the beta-amyloid precursor protein. Neuroscience. 1999;90(1):1-13.

54.    Seabrook GR, Smith DW, Bowery BJ, Easter A, Reynolds T, Fitzjohn SM, et al. Mechanisms contributing to the deficits in hippocampal synaptic plasticity in mice lacking amyloid precursor protein. Neuropharmacology. 1999;38(3):349-59.

55.    Kamal A, Almenar-Queralt A, LeBlanc JF, Roberts EA, Goldstein LS. Kinesin-mediated axonal transport of a membrane compartment containing beta-secretase and presenilin-1 requires APP. Nature. 2001;414(6864):643-8.

56.    Smith KD, Kallhoff V, Zheng H, Pautler RG. In vivo axonal transport rates decrease in a mouse model of Alzheimer's disease. Neuroimage. 2007;35(4):1401-8.

57.    Smith KD, Peethumnongsin E, Lin H, Zheng H, Pautler RG. Increased Human Wildtype Tau Attenuates Axonal Transport Deficits Caused by Loss of APP in Mouse Models. Magn Reson Insights. 2010;4:11-8.

58.    Goldstein LS. Axonal transport and neurodegenerative disease: can we see the elephant? Prog Neurobiol. 2012;99(3):186-90.

59.    Heber S, Herms J, Gajic V, Hainfellner J, Aguzzi A, Rulicke T, et al. Mice with combined gene knock-outs reveal essential and partially redundant functions of amyloid precursor protein family members. J Neurosci. 2000;20(21):7951-63.

60.    Cacace R, Sleegers K, Van Broeckhoven C. Molecular genetics of early-onset Alzheimer's disease revisited. Alzheimers Dement. 2016;12(6):733-48.

61.    Glenner GG, Wong CW. Alzheimer's disease and Down's syndrome: sharing of a unique cerebrovascular amyloid fibril protein. Biochem Biophys Res Commun. 1984;122(3):1131-5.

62.    St George-Hyslop PH, Tanzi RE, Polinsky RJ, Haines JL, Nee L, Watkins PC, et al. The genetic defect causing familial Alzheimer's disease maps on chromosome 21. Science. 1987;235(4791):885-90.

63.    Goate AM, Haynes AR, Owen MJ, Farrall M, James LA, Lai LY, et al. Predisposing locus for Alzheimer's disease on chromosome 21. Lancet. 1989;1(8634):352-5.

64.    Hardy J, Goate A, Owen M, Rossor M. Presenile dementia associated with mosaic trisomy 21 in a patient with a Down syndrome child. Lancet. 1989;2(8665):743.

65.    Mullan M, Houlden H, Windelspecht M, Fidani L, Lombardi C, Diaz P, et al. A locus for familial early-onset Alzheimer's disease on the long arm of chromosome 14, proximal to the alpha 1-antichymotrypsin gene. Nat Genet. 1992;2(4):340-2.

66.    Schellenberg GD, Bird TD, Wijsman EM, Orr HT, Anderson L, Nemens E, et al. Genetic linkage evidence for a familial Alzheimer's disease locus on chromosome 14. Science. 1992;258(5082):668-71.

67.    St George-Hyslop P, Haines J, Rogaev E, Mortilla M, Vaula G, Pericak-Vance M, et al. Genetic evidence for a novel familial Alzheimer's disease locus on chromosome 14. Nat Genet. 1992;2(4):330-4.

68.    Van Broeckhoven C, Backhovens H, Cruts M, De Winter G, Bruyland M, Cras P, et al. Mapping of a gene predisposing to early-onset Alzheimer's disease to chromosome 14q24.3. Nat Genet. 1992;2(4):335-9.

69.    Clark RF, Cruts M, Korenblat KM, He C, Talbot C, Van Broeckhoven C, et al. A yeast artificial chromosome contig from human chromosome 14q24 spanning the Alzheimer's disease locus AD3. Hum Mol Genet. 1995;4(8):1347-54.

70.    Cruts M, Backhovens H, Theuns J, Clark RF, Le Paslier D, Weissenbach J, et al. Genetic and physical characterization of the early-onset Alzheimer's disease AD3 locus on chromosome 14q24.3. Hum Mol Genet. 1995;4(8):1355-64.

71.    Mitsunaga Y, Takahashi K, Tabira T, Tasaki H, Watanabe S. Assignment of a familial Alzheimer's disease locus between D14S289 and D14S53. Lancet. 1994;344(8930):1154-5.

72.    Levy-Lahad E, Wasco W, Poorkaj P, Romano DM, Oshima J, Pettingell WH, et al. Candidate gene for the chromosome 1 familial Alzheimer's disease locus. Science. 1995;269(5226):973-7.

73.    Rogaev EI, Sherrington R, Rogaeva EA, Levesque G, Ikeda M, Liang Y, et al. Familial Alzheimer's disease in kindreds with missense mutations in a gene on chromosome 1 related to the Alzheimer's disease type 3 gene. Nature. 1995;376(6543):775-8.

74.    Laudon H, Hansson EM, Melen K, Bergman A, Farmery MR, Winblad B, et al. A nine-transmembrane domain topology for presenilin 1. J Biol Chem. 2005;280(42):35352-60.

75. De Strooper B, Iwatsubo T, Wolfe MS. Presenilins and gamma-secretase: structure, function, and role in Alzheimer Disease. Cold Spring Harb Perspect Med. 2012;2(1):a006304.

76. Scheuner D, Eckman C, Jensen M, Song X, Citron M, Suzuki N, et al. Secreted amyloid beta-protein similar to that in the senile plaques of Alzheimer's disease is increased in vivo by the presenilin 1 and 2 and APP mutations linked to familial Alzheimer's disease. Nat Med. 1996;2(8):864-70.

77. Borchelt DR, Thinakaran G, Eckman CB, Lee MK, Davenport F, Ratovitsky T, et al. Familial Alzheimer's disease-linked presenilin 1 variants elevate Abeta1-42/1-40 ratio in vitro and in vivo. Neuron. 1996;17(5):1005-13.

78. Citron M, Westaway D, Xia W, Carlson G, Diehl T, Levesque G, et al. Mutant presenilins of Alzheimer's disease increase production of 42-residue amyloid beta-protein in both transfected cells and transgenic mice. Nat Med. 1997;3(1):67-72.

79. Borchelt DR, Ratovitski T, van Lare J, Lee MK, Gonzales V, Jenkins NA, et al. Accelerated amyloid deposition in the brains of transgenic mice coexpressing mutant presenilin 1 and amyloid precursor proteins. Neuron. 1997;19(4):939-45.

80. Duff K, Eckman C, Zehr C, Yu X, Prada CM, Perez-tur J, et al. Increased amyloid-beta42(43) in brains of mice expressing mutant presenilin 1. Nature. 1996;383(6602):710-3.

81. Flood DG, Reaume AG, Dorfman KS, Lin YG, Lang DM, Trusko SP, et al. FAD mutant PS-1 gene-targeted mice: increased A beta 42 and A beta deposition without APP overproduction. Neurobiol Aging. 2002;23(3):335-48.

82. Siman R, Reaume AG, Savage MJ, Trusko S, Lin YG, Scott RW, et al. Presenilin-1 P264L knock-in mutation: differential effects on abeta production, amyloid deposition, and neuronal vulnerability. J Neurosci. 2000;20(23):8717-26.

83. Brouwers N, Sleegers K, Van Broeckhoven C. Molecular genetics of Alzheimer's disease: an update. Ann Med. 2008;40(8):562-83.

84. Hardy JA, Higgins GA. Alzheimer's disease: the amyloid cascade hypothesis. Science. 1992;256(5054):184-5.

85. Selkoe DJ. The molecular pathology of Alzheimer's disease. Neuron. 1991;6(4):487-98.

86. Haass C, Selkoe DJ. Soluble protein oligomers in neurodegeneration: lessons from the Alzheimer's amyloid beta-peptide. Nat Rev Mol Cell Biol. 2007;8(2):101-12.

87. Erten-Lyons D, Woltjer RL, Dodge H, Nixon R, Vorobik R, Calvert JF, et al. Factors associated with resistance to dementia despite high Alzheimer disease pathology. Neurology. 2009;72(4):354-60.

88.     Petersen RC, Aisen P, Boeve BF, Geda YE, Ivnik RJ, Knopman DS, et al. Mild cognitive impairment due to Alzheimer disease in the community. Ann Neurol. 2013;74(2):199-208.

89.     Sengupta U, Nilson AN, Kayed R. The Role of Amyloid-beta Oligomers in Toxicity, Propagation, and Immunotherapy. EBioMedicine. 2016;6:42-9.

90.     Sloane JA, Pietropaolo MF, Rosene DL, Moss MB, Peters A, Kemper T, et al. Lack of correlation between plaque burden and cognition in the aged monkey. Acta Neuropathol. 1997;94(5):471-8.

91.     Harper JD, Lansbury PT, Jr. Models of amyloid seeding in Alzheimer's disease and scrapie: mechanistic truths and physiological consequences of the time-dependent solubility of amyloid proteins. Annu Rev Biochem. 1997;66:385-407.

92.     Benilova I, Karran E, De Strooper B. The toxic Abeta oligomer and Alzheimer's disease: an emperor in need of clothes. Nat Neurosci. 2012;15(3):349-57.

93.     Iannuzzi C, Maritato R, Irace G, Sirangelo I. Misfolding and amyloid aggregation of apomyoglobin. Int J Mol Sci. 2013;14(7):14287-300.

94.     Chang YJ, Chen YR. The coexistence of an equal amount of Alzheimer's amyloid-beta 40 and 42 forms structurally stable and toxic oligomers through a distinct pathway. FEBS J. 2014;281(11):2674-87.

95.     Jarrett JT, Berger EP, Lansbury PT, Jr. The C-terminus of the beta protein is critical in amyloidogenesis. Ann N Y Acad Sci. 1993;695:144-8.

96.     Serpell LC, Sunde M, Benson MD, Tennent GA, Pepys MB, Fraser PE. The protofilament substructure of amyloid fibrils. J Mol Biol. 2000;300(5):1033-9.

97.     Serpell LC, Sunde M, Blake CC. The molecular basis of amyloidosis. Cell Mol Life Sci. 1997;53(11-12):871-87.

98.     Li H, Wei Y. Application of APP/PS1 Transgenic Mouse Model for Alzheimer Disease. Journal of Alzheimer's Disease & Parkinsonism. 2015;05(03).

99.     Mullan M, Crawford F, Axelman K, Houlden H, Lilius L, Winblad B, et al. A pathogenic mutation for probable Alzheimer's disease in the APP gene at the N-terminus of beta-amyloid. Nat Genet. 1992;1(5):345-7.

100.    Weggen S, Beher D. Molecular consequences of amyloid precursor protein and presenilin mutations causing autosomal-dominant Alzheimer's disease. Alzheimers Res Ther. 2012;4(2):9.

101.    Borchelt DR, Davis J, Fischer M, Lee MK, Slunt HH, Ratovitsky T, et al. A vector for expressing foreign genes in the brains and hearts of transgenic mice. Genet Anal. 1996;13(6):159-63.

102. Savonenko AV, Xu GM, Price DL, Borchelt DR, Markowska AL. Normal cognitive behavior in two distinct congenic lines of transgenic mice hyperexpressing mutant APP SWE. Neurobiol Dis. 2003;12(3):194-211.

103. Bilkei-Gorzo A. Genetic mouse models of brain ageing and Alzheimer's disease. Pharmacol Ther. 2014;142(2):244-57.

104. Sturchler-Pierrat C, Abramowski D, Duke M, Wiederhold KH, Mistl C, Rothacher S, et al. Two amyloid precursor protein transgenic mouse models with Alzheimer disease-like pathology. Proc Natl Acad Sci U S A. 1997;94(24):13287-92.

105. Webster SJ, Bachstetter AD, Nelson PT, Schmitt FA, Van Eldik LJ. Using mice to model Alzheimer's dementia: an overview of the clinical disease and the preclinical behavioral changes in 10 mouse models. Front Genet. 2014;5:88.

106. Sturchler-Pierrat C, Staufenbiel M. Pathogenic mechanisms of Alzheimer's disease analyzed in the APP23 transgenic mouse model. Ann N Y Acad Sci. 2000;920:134-9.

107. Bondolfi L, Calhoun M, Ermini F, Kuhn HG, Wiederhold KH, Walker L, et al. Amyloid-associated neuron loss and gliogenesis in the neocortex of amyloid precursor protein transgenic mice. J Neurosci. 2002;22(2):515-22.

108. Bornemann KD, Staufenbiel M. Transgenic mouse models of Alzheimer's disease. Ann N Y Acad Sci. 2000;908:260-6.

109. Cao D, Lu H, Lewis TL, Li L. Intake of sucrose-sweetened water induces insulin resistance and exacerbates memory deficits and amyloidosis in a transgenic mouse model of Alzheimer disease. J Biol Chem. 2007;282(50):36275-82.

110. Ding Y, Qiao A, Wang Z, Goodwin JS, Lee ES, Block ML, et al. Retinoic acid attenuates beta-amyloid deposition and rescues memory deficits in an Alzheimer's disease transgenic mouse model. J Neurosci. 2008;28(45):11622-34.

111. Reiserer RS, Harrison FE, Syverud DC, McDonald MP. Impaired spatial learning in the APPSwe + PSEN1DeltaE9 bigenic mouse model of Alzheimer's disease. Genes Brain Behav. 2007;6(1):54-65.

112. Savonenko A, Xu GM, Melnikova T, Morton JL, Gonzales V, Wong MP, et al. Episodic-like memory deficits in the APPswe/PS1dE9 mouse model of Alzheimer's disease: relationships to beta-amyloid deposition and neurotransmitter abnormalities. Neurobiol Dis. 2005;18(3):602-17.

113. Takeda S, Hashimoto T, Roe AD, Hori Y, Spires-Jones TL, Hyman BT. Brain interstitial oligomeric amyloid beta increases with age and is resistant to clearance from brain in a mouse model of Alzheimer's disease. FASEB J. 2013;27(8):3239-48.

114. Ferreira ST, Lourenco MV, Oliveira MM, De Felice FG. Soluble amyloid-beta oligomers as synaptotoxins leading to cognitive impairment in Alzheimer's disease. Front Cell Neurosci. 2015;9:191.

115. Herskovits AZ, Locascio JJ, Peskind ER, Li G, Hyman BT. A Luminex assay detects amyloid beta oligomers in Alzheimer's disease cerebrospinal fluid. PLoS One. 2013;8(7):e67898.

116. Viola KL, Sbarboro J, Sureka R, De M, Bicca MA, Wang J, et al. Towards non-invasive diagnostic imaging of early-stage Alzheimer's disease. Nat Nanotechnol. 2015;10(1):91-8.

117. Giau VV, Bagyinszky E, An SS, Kim SY. Role of apolipoprotein E in neurodegenerative diseases. Neuropsychiatr Dis Treat. 2015;11:1723-37.

118. Mahley RW. Apolipoprotein E: cholesterol transport protein with expanding role in cell biology. Science. 1988;240(4852):622-30.

119. Mahley RW. Apolipoprotein E: from cardiovascular disease to neurodegenerative disorders. J Mol Med (Berl). 2016;94(7):739-46.

120. Wilson C, Mau T, Weisgraber KH, Wardell MR, Mahley RW, Agard DA. Salt bridge relay triggers defective LDL receptor binding by a mutant apolipoprotein. Structure. 1994;2(8):713-8.

121. Wilson C, Wardell MR, Weisgraber KH, Mahley RW, Agard DA. Three-dimensional structure of the LDL receptor-binding domain of human apolipoprotein E. Science. 1991;252(5014):1817-22.

122. Fredrickson DS, Levy RI, Lees RS. Fat transport in lipoproteins--an integrated approach to mechanisms and disorders. N Engl J Med. 1967;276(4):215-25 contd.

123. Di Paolo G, Kim TW. Linking lipids to Alzheimer's disease: cholesterol and beyond. Nat Rev Neurosci. 2011;12(5):284-96.

124. Dong HK, Gim JA, Yeo SH, Kim HS. Integrated late onset Alzheimer's disease (LOAD) susceptibility genes: Cholesterol metabolism and trafficking perspectives. Gene. 2016.

125. Leduc V, Jasmin-Belanger S, Poirier J. APOE and cholesterol homeostasis in Alzheimer's disease. Trends Mol Med. 2010;16(10):469-77.

126. Riedel BC, Thompson PM, Brinton RD. Age, APOE and sex: Triad of risk of Alzheimer's disease. J Steroid Biochem Mol Biol. 2016;160:134-47.

127. Boyles JK, Pitas RE, Wilson E, Mahley RW, Taylor JM. Apolipoprotein E associated with astrocytic glia of the central nervous system and with nonmyelinating glia of the peripheral nervous system. J Clin Invest. 1985;76(4):1501-13.

128. Vance JE. Dysregulation of cholesterol balance in the brain: contribution to neurodegenerative diseases. Dis Model Mech. 2012;5(6):746-55.

129. Heyman A, Wilkinson WE, Hurwitz BJ, Schmechel D, Sigmon AH, Weinberg T, et al. Alzheimer's disease: genetic aspects and associated clinical disorders. Ann Neurol. 1983;14(5):507-15.

130. Roses AD. On the discovery of the genetic association of Apolipoprotein E genotypes and common late-onset Alzheimer disease. J Alzheimers Dis. 2006;9(3 Suppl):361-6.

131. Roses AD, Pericak-Vance MA, Yamaoka L, Haynes C, Speer M, Gaskell P, et al. Linkage studies in familial Alzheimer's disease. Prog Clin Biol Res. 1989;317:201-15.

132. Strittmatter WJ, Saunders AM, Schmechel D, Pericak-Vance M, Enghild J, Salvesen GS, et al. Apolipoprotein E: high-avidity binding to beta-amyloid and increased frequency of type 4 allele in late-onset familial Alzheimer disease. Proc Natl Acad Sci U S A. 1993;90(5):1977-81.

133. Corder EH, Saunders AM, Strittmatter WJ, Schmechel DE, Gaskell PC, Small GW, et al. Gene dose of apolipoprotein E type 4 allele and the risk of Alzheimer's disease in late onset families. Science. 1993;261(5123):921-3.

134. Saunders AM, Strittmatter WJ, Schmechel D, George-Hyslop PH, Pericak-Vance MA, Joo SH, et al. Association of apolipoprotein E allele epsilon 4 with late-onset familial and sporadic Alzheimer's disease. Neurology. 1993;43(8):1467-72.

135. Van Cauwenberghe C, Van Broeckhoven C, Sleegers K. The genetic landscape of Alzheimer disease: clinical implications and perspectives. Genet Med. 2016;18(5):421-30.

136. Meyer MR, Tschanz JT, Norton MC, Welsh-Bohmer KA, Steffens DC, Wyse BW, et al. APOE genotype predicts when--not whether--one is predisposed to develop Alzheimer disease. Nat Genet. 1998;19(4):321-2.

137. Tiraboschi P, Hansen LA, Masliah E, Alford M, Thal LJ, Corey-Bloom J. Impact of APOE genotype on neuropathologic and neurochemical markers of Alzheimer disease. Neurology. 2004;62(11):1977-83.

138. Verghese PB, Castellano JM, Holtzman DM. Apolipoprotein E in Alzheimer's disease and other neurological disorders. Lancet Neurol. 2011;10(3):241-52.

139. Kanekiyo T, Xu H, Bu G. ApoE and Abeta in Alzheimer's disease: accidental encounters or partners? Neuron. 2014;81(4):740-54.

140. Golabek AA, Soto C, Vogel T, Wisniewski T. The interaction between apolipoprotein E and Alzheimer's amyloid beta-peptide is dependent on beta-peptide conformation. J Biol Chem. 1996;271(18):10602-6.

141. Tai LM, Bilousova T, Jungbauer L, Roeske SK, Youmans KL, Yu C, et al. Levels of soluble apolipoprotein E/amyloid-beta (Abeta) complex are reduced and oligomeric Abeta increased with APOE4 and Alzheimer disease in a transgenic mouse model and human samples. J Biol Chem. 2013;288(8):5914-26.

142. Wood SJ, Chan W, Wetzel R. An ApoE-Abeta inhibition complex in Abeta fibril extension. Chem Biol. 1996;3(11):949-56.

143. Bales KR, Liu F, Wu S, Lin S, Koger D, DeLong C, et al. Human APOE isoform-dependent effects on brain beta-amyloid levels in PDAPP transgenic mice. J Neurosci. 2009;29(21):6771-9.

144. Fryer JD, Simmons K, Parsadanian M, Bales KR, Paul SM, Sullivan PM, et al. Human apolipoprotein E4 alters the amyloid-beta 40:42 ratio and promotes the formation of cerebral amyloid angiopathy in an amyloid precursor protein transgenic model. J Neurosci. 2005;25(11):2803-10.

145. Youmans KL, Tai LM, Nwabuisi-Heath E, Jungbauer L, Kanekiyo T, Gan M, et al. APOE4-specific changes in Abeta accumulation in a new transgenic mouse model of Alzheimer disease. J Biol Chem. 2012;287(50):41774-86.

146. Bales KR, Verina T, Dodel RC, Du Y, Altstiel L, Bender M, et al. Lack of apolipoprotein E dramatically reduces amyloid beta-peptide deposition. Nat Genet. 1997;17(3):263-4.

147. Irizarry MC, Rebeck GW, Cheung B, Bales K, Paul SM, Holzman D, et al. Modulation of A beta deposition in APP transgenic mice by an apolipoprotein E null background. Ann N Y Acad Sci. 2000;920:171-8.

148. Yoon SS, Jo SA. Mechanisms of Amyloid-beta Peptide Clearance: Potential Therapeutic Targets for Alzheimer's Disease. Biomol Ther (Seoul). 2012;20(3):245-55.

149. Jiang Q, Lee CY, Mandrekar S, Wilkinson B, Cramer P, Zelcer N, et al. ApoE promotes the proteolytic degradation of Abeta. Neuron. 2008;58(5):681-93.

150. Tarasoff-Conway JM, Carare RO, Osorio RS, Glodzik L, Butler T, Fieremans E, et al. Clearance systems in the brain-implications for Alzheimer disease. Nat Rev Neurol. 2015;11(8):457-70.

151. Cudaback E, Li X, Montine KS, Montine TJ, Keene CD. Apolipoprotein E isoform-dependent microglia migration. FASEB J. 2011;25(6):2082-91.

152. Deane R, Sagare A, Hamm K, Parisi M, Lane S, Finn MB, et al. apoE isoform-specific disruption of amyloid beta peptide clearance from mouse brain. J Clin Invest. 2008;118(12):4002-13.

153. Dietschy JM, Turley SD. Cholesterol metabolism in the brain. Curr Opin Lipidol. 2001;12(2):105-12.

154. Vance JE, Hayashi H, Karten B. Cholesterol homeostasis in neurons and glial cells. Semin Cell Dev Biol. 2005;16(2):193-212.

155. Hirsch-Reinshagen V, Burgess BL, Wellington CL. Why lipids are important for Alzheimer disease? Mol Cell Biochem. 2009;326(1-2):121-9.

156. Tall AR. Cholesterol efflux pathways and other potential mechanisms involved in the athero-protective effect of high density lipoproteins. J Intern Med. 2008;263(3):256-73.

157. Maulik M, Westaway D, Jhamandas JH, Kar S. Role of cholesterol in APP metabolism and its significance in Alzheimer's disease pathogenesis. Mol Neurobiol. 2013;47(1):37-63.

158. Sparks DL, Scheff SW, Hunsaker JC, 3rd, Liu H, Landers T, Gross DR. Induction of Alzheimer-like beta-amyloid immunoreactivity in the brains of rabbits with dietary cholesterol. Exp Neurol. 1994;126(1):88-94.

159. Hartmann T, Kuchenbecker J, Grimm MO. Alzheimer's disease: the lipid connection. J Neurochem. 2007;103 Suppl 1:159-70.

160. Vetrivel KS, Thinakaran G. Membrane rafts in Alzheimer's disease beta-amyloid production. Biochim Biophys Acta. 2010;1801(8):860-7.

161. Simons M, Keller P, De Strooper B, Beyreuther K, Dotti CG, Simons K. Cholesterol depletion inhibits the generation of beta-amyloid in hippocampal neurons. Proc Natl Acad Sci U S A. 1998;95(11):6460-4.

162. Ehehalt R, Keller P, Haass C, Thiele C, Simons K. Amyloidogenic processing of the Alzheimer beta-amyloid precursor protein depends on lipid rafts. J Cell Biol. 2003;160(1):113-23.

163. Hattori C, Asai M, Onishi H, Sasagawa N, Hashimoto Y, Saido TC, et al. BACE1 interacts with lipid raft proteins. J Neurosci Res. 2006;84(4):912-7.

164. Riddell DR, Christie G, Hussain I, Dingwall C. Compartmentalization of beta-secretase (Asp2) into low-buoyant density, noncaveolar lipid rafts. Curr Biol. 2001;11(16):1288-93.

165. Marquer C, Devauges V, Cossec JC, Liot G, Lecart S, Saudou F, et al. Local cholesterol increase triggers amyloid precursor protein-Bace1 clustering in lipid rafts and rapid endocytosis. FASEB J. 2011;25(4):1295-305.

166. Urano Y, Hayashi I, Isoo N, Reid PC, Shibasaki Y, Noguchi N, et al. Association of active gamma-secretase complex with lipid rafts. J Lipid Res. 2005;46(5):904-12.

167. Wahrle S, Das P, Nyborg AC, McLendon C, Shoji M, Kawarabayashi T, et al. Cholesterol-dependent gamma-secretase activity in buoyant cholesterol-rich membrane microdomains. Neurobiol Dis. 2002;9(1):11-23.

168. Koldamova R, Fitz NF, Lefterov I. ATP-binding cassette transporter A1: from metabolism to neurodegeneration. Neurobiol Dis. 2014;72 Pt A:13-21.

169. Koldamova R, Fitz NF, Lefterov I. The role of ATP-binding cassette transporter A1 in Alzheimer's disease and neurodegeneration. Biochim Biophys Acta. 2010;1801(8):824-30.

170. Singaraja RR, Brunham LR, Visscher H, Kastelein JJ, Hayden MR. Efflux and atherosclerosis: the clinical and biochemical impact of variations in the ABCA1 gene. Arterioscler Thromb Vasc Biol. 2003;23(8):1322-32.

171. Oram JF, Vaughan AM. ATP-Binding cassette cholesterol transporters and cardiovascular disease. Circ Res. 2006;99(10):1031-43.

172. Tang C, Oram JF. The cell cholesterol exporter ABCA1 as a protector from cardiovascular disease and diabetes. Biochim Biophys Acta. 2009;1791(7):563-72.

173. Nagao K, Kimura Y, Mastuo M, Ueda K. Lipid outward translocation by ABC proteins. FEBS Lett. 2010;584(13):2717-23.

174. Frikke-Schmidt R, Nordestgaard BG, Stene MC, Sethi AA, Remaley AT, Schnohr P, et al. Association of loss-of-function mutations in the ABCA1 gene with high-density lipoprotein cholesterol levels and risk of ischemic heart disease. JAMA. 2008;299(21):2524-32.

175. McNeish J, Aiello RJ, Guyot D, Turi T, Gabel C, Aldinger C, et al. High density lipoprotein deficiency and foam cell accumulation in mice with targeted disruption of ATP-binding cassette transporter-1. Proc Natl Acad Sci U S A. 2000;97(8):4245-50.

176. Hirsch-Reinshagen V, Maia LF, Burgess BL, Blain JF, Naus KE, McIsaac SA, et al. The absence of ABCA1 decreases soluble ApoE levels but does not diminish amyloid deposition in two murine models of Alzheimer disease. J Biol Chem. 2005;280(52):43243-56.

177. Koldamova R, Staufenbiel M, Lefterov I. Lack of ABCA1 considerably decreases brain ApoE level and increases amyloid deposition in APP23 mice. J Biol Chem. 2005;280(52):43224-35.

178. Lefterov I, Fitz NF, Cronican A, Lefterov P, Staufenbiel M, Koldamova R. Memory deficits in APP23/Abca1+/- mice correlate with the level of Abeta oligomers. ASN Neuro. 2009;1(2).

179. Wahrle SE, Jiang H, Parsadanian M, Hartman RE, Bales KR, Paul SM, et al. Deletion of Abca1 increases Abeta deposition in the PDAPP transgenic mouse model of Alzheimer disease. J Biol Chem. 2005;280(52):43236-42.

180.	Wahrle SE, Jiang H, Parsadanian M, Kim J, Li A, Knoten A, et al. Overexpression of ABCA1 reduces amyloid deposition in the PDAPP mouse model of Alzheimer disease. J Clin Invest. 2008;118(2):671-82.

181.	Karasinska JM, Rinninger F, Lutjohann D, Ruddle P, Franciosi S, Kruit JK, et al. Specific loss of brain ABCA1 increases brain cholesterol uptake and influences neuronal structure and function. J Neurosci. 2009;29(11):3579-89.

182.	Donkin JJ, Stukas S, Hirsch-Reinshagen V, Namjoshi D, Wilkinson A, May S, et al. ATP-binding cassette transporter A1 mediates the beneficial effects of the liver X receptor agonist GW3965 on object recognition memory and amyloid burden in amyloid precursor protein/presenilin 1 mice. J Biol Chem. 2010;285(44):34144-54.

183.	Fitz NF, Cronican A, Pham T, Fogg A, Fauq AH, Chapman R, et al. Liver X receptor agonist treatment ameliorates amyloid pathology and memory deficits caused by high-fat diet in APP23 mice. J Neurosci. 2010;30(20):6862-72.

184.	Jiang Q, Heneka M, Landreth GE. The role of peroxisome proliferator-activated receptor-gamma (PPARgamma) in Alzheimer's disease: therapeutic implications. CNS Drugs. 2008;22(1):1-14.

185.	Koldamova RP, Lefterov IM, Staufenbiel M, Wolfe D, Huang S, Glorioso JC, et al. The liver X receptor ligand T0901317 decreases amyloid beta production in vitro and in a mouse model of Alzheimer's disease. J Biol Chem. 2005;280(6):4079-88.

186.	Lefterov I, Bookout A, Wang Z, Staufenbiel M, Mangelsdorf D, Koldamova R. Expression profiling in APP23 mouse brain: inhibition of Abeta amyloidosis and inflammation in response to LXR agonist treatment. Mol Neurodegener. 2007;2:20.

187.	Riddell DR, Zhou H, Comery TA, Kouranova E, Lo CF, Warwick HK, et al. The LXR agonist TO901317 selectively lowers hippocampal Abeta42 and improves memory in the Tg2576 mouse model of Alzheimer's disease. Mol Cell Neurosci. 2007;34(4):621-8.

188.	Terwel D, Steffensen KR, Verghese PB, Kummer MP, Gustafsson JA, Holtzman DM, et al. Critical role of astroglial apolipoprotein E and liver X receptor-alpha expression for microglial Abeta phagocytosis. J Neurosci. 2011;31(19):7049-59.

189.	Vanmierlo T, Rutten K, Dederen J, Bloks VW, van Vark-van der Zee LC, Kuipers F, et al. Liver X receptor activation restores memory in aged AD mice without reducing amyloid. Neurobiol Aging. 2011;32(7):1262-72.

190.	Wesson DW, Borkowski AH, Landreth GE, Nixon RA, Levy E, Wilson DA. Sensory network dysfunction, behavioral impairments, and their reversibility in an Alzheimer's beta-amyloidosis mouse model. J Neurosci. 2011;31(44):15962-71.

191.	Fitz NF, Castranio EL, Carter AY, Kodali R, Lefterov I, Koldamova R. Improvement of memory deficits and amyloid-beta clearance in aged APP23 mice treated with a

combination of anti-amyloid-beta antibody and LXR agonist. J Alzheimers Dis. 2014;41(2):535-49.

192.    Katz A, Udata C, Ott E, Hickey L, Burczynski ME, Burghart P, et al. Safety, pharmacokinetics, and pharmacodynamics of single doses of LXR-623, a novel liver X-receptor agonist, in healthy participants. J Clin Pharmacol. 2009;49(6):643-9.

193.    Cramer PE, Cirrito JR, Wesson DW, Lee CY, Karlo JC, Zinn AE, et al. ApoE-directed therapeutics rapidly clear beta-amyloid and reverse deficits in AD mouse models. Science. 2012;335(6075):1503-6.

194.    Fitz NF, Cronican AA, Lefterov I, Koldamova R. Comment on "ApoE-directed therapeutics rapidly clear beta-amyloid and reverse deficits in AD mouse models". Science. 2013;340(6135):924-c.

195.    Tesseur I, Lo AC, Roberfroid A, Dietvorst S, Van Broeck B, Borgers M, et al. Comment on "ApoE-directed therapeutics rapidly clear beta-amyloid and reverse deficits in AD mouse models". Science. 2013;340(6135):924-e.

196.    Price AR, Xu G, Siemienski ZB, Smithson LA, Borchelt DR, Golde TE, et al. Comment on "ApoE-directed therapeutics rapidly clear beta-amyloid and reverse deficits in AD mouse models". Science. 2013;340(6135):924-d.

197.    Veeraraghavalu K, Zhang C, Miller S, Hefendehl JK, Rajapaksha TW, Ulrich J, et al. Comment on "ApoE-directed therapeutics rapidly clear beta-amyloid and reverse deficits in AD mouse models". Science. 2013;340(6135):924-f.

198.    Lilley JS, Linton MF, Fazio S. Oral retinoids and plasma lipids. Dermatol Ther. 2013;26(5):404-10.

199.    Tontonoz P, Mangelsdorf DJ. Liver X receptor signaling pathways in cardiovascular disease. Mol Endocrinol. 2003;17(6):985-93.

200.    Boehm-Cagan A, Michaelson DM. Reversal of apoE4-driven brain pathology and behavioral deficits by bexarotene. J Neurosci. 2014;34(21):7293-301.

201.    Beilharz JE, Maniam J, Morris MJ. Diet-Induced Cognitive Deficits: The Role of Fat and Sugar, Potential Mechanisms and Nutritional Interventions. Nutrients. 2015;7(8):6719-38.

202.    Kanoski SE, Davidson TL. Western diet consumption and cognitive impairment: links to hippocampal dysfunction and obesity. Physiol Behav. 2011;103(1):59-68.

203.    Morris MC, Tangney CC. Dietary fat composition and dementia risk. Neurobiol Aging. 2014;35 Suppl 2:S59-64.

204.    Morris MC, Evans DA, Bienias JL, Tangney CC, Bennett DA, Aggarwal N, et al. Dietary fats and the risk of incident Alzheimer disease. Arch Neurol. 2003;60(2):194-200.

205.    Morris MC, Evans DA, Tangney CC, Bienias JL, Schneider JA, Wilson RS, et al. Dietary copper and high saturated and trans fat intakes associated with cognitive decline. Arch Neurol. 2006;63(8):1085-8.

206.    Eskelinen MH, Ngandu T, Helkala EL, Tuomilehto J, Nissinen A, Soininen H, et al. Fat intake at midlife and cognitive impairment later in life: a population-based CAIDE study. Int J Geriatr Psychiatry. 2008;23(7):741-7.

207.    Morris MC, Evans DA, Bienias JL, Tangney CC, Wilson RS. Dietary fat intake and 6-year cognitive change in an older biracial community population. Neurology. 2004;62(9):1573-9.

208.    Takechi R, Galloway S, Pallebage-Gamarallage MM, Lam V, Dhaliwal SS, Mamo JC. Probucol prevents blood-brain barrier dysfunction in wild-type mice induced by saturated fat or cholesterol feeding. Clin Exp Pharmacol Physiol. 2013;40(1):45-52.

209.    Grimm MO, Rothhaar TL, Grosgen S, Burg VK, Hundsdorfer B, Haupenthal VJ, et al. Trans fatty acids enhance amyloidogenic processing of the Alzheimer amyloid precursor protein (APP). J Nutr Biochem. 2012;23(10):1214-23.

210.    Webster SJ, Bachstetter AD, Nelson PT, Schmitt FA, Van Eldik LJ. Using mice to model Alzheimer's dementia: an overview of the clinical disease and the preclinical behavioral changes in 10 mouse models. Front Genet. 2014;5:88.(doi):10.3389/fgene.2014.00088. eCollection 2014.

211.    Bilkei-Gorzo A. Genetic mouse models of brain ageing and Alzheimer's disease. Pharmacol Ther. 2014;142(2):244-57. doi: 10.1016/j.pharmthera.2013.12.009. Epub Dec 19.

212.    Puzzo D, Lee L, Palmeri A, Calabrese G, Arancio O. Behavioral assays with mouse models of Alzheimer's disease: practical considerations and guidelines. Biochem Pharmacol. 2014;88(4):450-67. doi: 10.1016/j.bcp.2014.01.011. Epub Jan 21.

213.    Gaiteri C, Mostafavi S, Honey CJ, De Jager PL, Bennett DA. Genetic variants in Alzheimer disease - molecular and brain network approaches. Nat Rev Neurol. 2016;12(7):413-27.

214.    Skerrett R, Malm T, Landreth G. Nuclear receptors in neurodegenerative diseases. Neurobiol Dis. 2014;72 Pt A:104-16.

215.    Hirsch-Reinshagen V, Maia LF, Burgess BL, Blain JF, Naus KE, McIsaac SA, et al. The Absence of ABCA1 Decreases Soluble ApoE Levels but Does Not Diminish Amyloid Deposition in Two Murine Models of Alzheimer Disease. Journal of Biological Chemistry. 2005;280(52):43243-56.

216.    Wahrle SE, Jiang H, Parsadanian M, Hartman RE, Bales KR, Paul SM, et al. Deletion of Abca1 Increases A{beta} Deposition in the PDAPP Transgenic Mouse Model of Alzheimer Disease. Journal of Biological Chemistry. 2005;280(52):43236-42.

217.  Koldamova R, Staufenbiel M, Lefterov I. Lack of ABCA1 Considerably Decreases Brain ApoE Level and Increases Amyloid Deposition in APP23 Mice. Journal of Biological Chemistry. 2005;280(52):43224-35.

218.  Wahrle SE, Jiang H, Parsadanian M, Kim J, Li A, Knoten A, et al. Overexpression of ABCA1 reduces amyloid deposition in the PDAPP mouse model of Alzheimer disease. JClinInvest. 2008;118(2):671-82.

219.  Fitz NF, Cronican AA, Saleem M, Fauq AH, Chapman R, Lefterov I, et al. Abca1 deficiency affects Alzheimer's disease-like phenotype in human ApoE4 but not in ApoE3-targeted replacement mice. J Neurosci. 2012;32(38):13125-36.

220.  Fitz NF, Tapias V, Cronican AA, Castranio EL, Saleem M, Carter AY, et al. Opposing effects of Apoe/Apoa1 double deletion on amyloid-beta pathology and cognitive performance in APP mice. Brain : a journal of neurology. 2015.

221.  Koldamova RP, Lefterov IM, Staufenbiel M, Wolfe D, Huang S, Glorioso JC, et al. The Liver X Receptor Ligand T0901317 Decreases Amyloid {beta} Production in Vitro and in a Mouse Model of Alzheimer's Disease. Journal of Biological Chemistry. 2005;280(6):4079-88.

222.  Zelcer N, Khanlou N, Clare R, Jiang Q, Reed-Geaghan EG, Landreth GE, et al. Attenuation of neuroinflammation and Alzheimer's disease pathology by liver x receptors. Proc Natl Acad Sci U S A. 2007;104(25):10601-6.

223.  Mounier A, Georgiev D, Nam KN, Fitz NF, Castranio E, Wolfe C, et al. Bexarotene-Activated Retinoid X Receptors Regulate Neuronal Differentiation and Dendritic Complexity. Journal of Neuroscience. 2015;35(34):11862-76.

224.  Nam KN, Mounier A, Fitz NF, Wolfe C, Schug J, Lefterov I, et al. RXR controlled regulatory networks identified in mouse brain counteract deleterious effects of Abeta oligomers. Sci Rep. 2016;6:24048.

225.  Sindi S, Hagman G, Hakansson K, Kulmala J, Nilsen C, Kareholt I, et al. Midlife Work-Related Stress Increases Dementia Risk in Later Life: The CAIDE 30-Year Study. J Gerontol B Psychol Sci Soc Sci. 2016.

226.  Ngandu T, Lehtisalo J, Solomon A, Levalahti E, Ahtiluoto S, Antikainen R, et al. A 2 year multidomain intervention of diet, exercise, cognitive training, and vascular risk monitoring versus control to prevent cognitive decline in at-risk elderly people (FINGER): a randomised controlled trial. Lancet. 2015;385(9984):2255-63.

227.  Merrill DA, Siddarth P, Raji CA, Emerson ND, Rueda F, Ercoli LM, et al. Modifiable Risk Factors and Brain Positron Emission Tomography Measures of Amyloid and Tau in Nondemented Adults with Memory Complaints. Am J Geriatr Psychiatry. 2016;24(9):729-37.

228. Kalaria RN, Maestre GE, Arizaga R, Friedland RP, Galasko D, Hall K, et al. Alzheimer's disease and vascular dementia in developing countries: prevalence, management, and risk factors. The Lancet Neurology. 2008;7(9):812-26.

229. Strand BH, Langballe EM, Hjellvik V, Handal M, Naess O, Knudsen GP, et al. Midlife vascular risk factors and their association with dementia deaths: results from a Norwegian prospective study followed up for 35 years. J Neurol Sci. 2013;324(1-2):124-30.

230. Ettcheto M, Petrov D, Pedros I, Alva N, Carbonell T, Beas-Zarate C, et al. Evaluation of Neuropathological Effects of a High-Fat Diet in a Presymptomatic Alzheimer's Disease Stage in APP/PS1 Mice. J Alzheimers Dis. 2016;54(1):233-51.

231. Lin B, Hasegawa Y, Takane K, Koibuchi N, Cao C, Kim-Mitsuyama S. High-Fat-Diet Intake Enhances Cerebral Amyloid Angiopathy and Cognitive Impairment in a Mouse Model of Alzheimer's Disease, Independently of Metabolic Disorders. Journal of the American Heart Association. 2016;5(6).

232. Refolo LM, Malester B, LaFrancois J, Bryant-Thomas T, Wang R, Tint GS, et al. Hypercholesterolemia accelerates the Alzheimer's amyloid pathology in a transgenic mouse model. Neurobiol Dis. 2000;7(4):321-31.

233. Nizari S, Carare RO, Hawkes CA. Increased Abeta pathology in aged Tg2576 mice born to mothers fed a high fat diet. Sci Rep. 2016;6:21981.

234. Gratuze M, Julien J, Morin F, Calon F, Hebert SS, Marette A, et al. High-fat, high-sugar, and high-cholesterol consumption does not impact tau pathogenesis in a mouse model of Alzheimer's disease-like tau pathology. Neurobiol Aging. 2016;47:71-3.

235. Janssen CI, Jansen D, Mutsaers MP, Dederen PJ, Geenen B, Mulder MT, et al. The Effect of a High-Fat Diet on Brain Plasticity, Inflammation and Cognition in Female ApoE4-Knockin and ApoE-Knockout Mice. PLoS One. 2016;11(5):e0155307.

236. Graham LC, Harder JM, Soto I, de Vries WN, John SW, Howell GR. Chronic consumption of a western diet induces robust glial activation in aging mice and in a mouse model of Alzheimer's disease. Sci Rep. 2016;6:21568.

237. Jankowsky JL, Savonenko A, Schilling G, Wang J, Xu G, Borchelt DR. Transgenic mouse models of neurodegenerative disease: opportunities for therapeutic development. Current neurology and neuroscience reports. 2002;2(5):457-64.

238. Jankowsky JL, Slunt HH, Ratovitski T, Jenkins NA, Copeland NG, Borchelt DR. Co-expression of multiple transgenes in mouse CNS: a comparison of strategies. Biomol Eng. 2001;17(6):157-65.

239. Fitz NF, Tapias V, Cronican AA, Castranio EL, Saleem M, Carter AY, et al. Opposing effects of Apoe/Apoa1 double deletion on amyloid-beta pathology and cognitive performance in APP mice. Brain. 2015;138(Pt 12):3699-715.

240. Lefterov I, Fitz NF, Cronican AA, Fogg A, Lefterov P, Kodali R, et al. Apolipoprotein A-I deficiency increases cerebral amyloid angiopathy and cognitive deficits in APP/PS1DeltaE9 mice. Journal of Biological Chemistry. 2010;285(47):36945-57.

241. Cronican AA, Fitz NF, Carter A, Saleem M, Shiva S, Barchowsky A, et al. Genome-wide alteration of histone H3K9 acetylation pattern in mouse offspring prenatally exposed to arsenic. PLoS One. 2013;8(2):e53478.

242. Corona AW, Kodoma N, Casali BT, Landreth GE. ABCA1 is Necessary for Bexarotene-Mediated Clearance of Soluble Amyloid Beta from the Hippocampus of APP/PS1 Mice. J Neuroimmune Pharmacol. 2016;11(1):61-72.

243. Mootha VK, Lindgren CM, Eriksson KF, Subramanian A, Sihag S, Lehar J, et al. PGC-1alpha-responsive genes involved in oxidative phosphorylation are coordinately downregulated in human diabetes. Nat Genet. 2003;34(3):267-73.

244. Subramanian A, Tamayo P, Mootha VK, Mukherjee S, Ebert BL, Gillette MA, et al. Gene set enrichment analysis: a knowledge-based approach for interpreting genome-wide expression profiles. Proc Natl Acad Sci U S A. 2005;102(43):15545-50.

245. Corona AW, Kodoma N, Casali BT, Landreth GE. ABCA1 is Necessary for Bexarotene-Mediated Clearance of Soluble Amyloid Beta from the Hippocampus of APP/PS1 Mice. J Neuroimmune Pharmacol. 2015.

246. Tu S, Okamoto S, Lipton SA, Xu H. Oligomeric Abeta-induced synaptic dysfunction in Alzheimer's disease. Mol Neurodegener. 2014;9:48.(doi):10.1186/750-326-9-48.

247. Wang Q, Walsh DM, Rowan MJ, Selkoe DJ, Anwyl R. Block of long-term potentiation by naturally secreted and synthetic amyloid beta-peptide in hippocampal slices is mediated via activation of the kinases c-Jun N-terminal kinase, cyclin-dependent kinase 5, and p38 mitogen-activated protein kinase as well as metabotropic glutamate receptor type 5. The Journal of neuroscience : the official journal of the Society for Neuroscience. 2004;24(13):3370-8.

248. Rowan MJ, Klyubin I, Wang Q, Anwyl R. Mechanisms of the inhibitory effects of amyloid beta-protein on synaptic plasticity. Exp Gerontol. 2004;39(11-12):1661-7.

249. Dahlgren KN, Manelli AM, Stine WB, Jr., Baker LK, Krafft GA, LaDu MJ. Oligomeric and fibrillar species of amyloid-beta peptides differentially affect neuronal viability. The Journal of biological chemistry. 2002;277(35):32046-53.

250. Hoshi M, Sato M, Matsumoto S, Noguchi A, Yasutake K, Yoshida N, et al. Spherical aggregates of beta-amyloid (amylospheroid) show high neurotoxicity and activate tau protein kinase I/glycogen synthase kinase-3beta. Proc Natl Acad Sci U S A. 2003;100(11):6370-5.

251. Diaz-Cintra S, Yong A, Aguilar A, Bi X, Lynch G, Ribak CE. Ultrastructural analysis of hippocampal pyramidal neurons from apolipoprotein E-deficient mice treated with a cathepsin inhibitor. Journal of neurocytology. 2004;33(1):37-48.

252. Champagne D, Rochford J, Poirier J. Effect of apolipoprotein E deficiency on reactive sprouting in the dentate gyrus of the hippocampus following entorhinal cortex lesion: role of the astroglial response. Experimental neurology. 2005;194(1):31-42.

253. Robertson J, Curley J, Kaye J, Quinn J, Pfankuch T, Raber J. apoE isoforms and measures of anxiety in probable AD patients and Apoe-/- mice. NeurobiolAging. 2005;26(5):637-43.

254. Dietschy JM. Central nervous system: cholesterol turnover, brain development and neurodegeneration. Biol Chem. 2009;390(4):287-93.

255. Huang Y, Mahley RW. Apolipoprotein E: structure and function in lipid metabolism, neurobiology, and Alzheimer's diseases. Neurobiology of disease. 2014;72 Pt A:3-12.

256. Nieweg K, Schaller H, Pfrieger FW. Marked differences in cholesterol synthesis between neurons and glial cells from postnatal rats. Journal of neurochemistry. 2009;109(1):125-34.

257. Pfrieger FW, Barres BA. Synaptic efficacy enhanced by glial cells in vitro. Science (New York, NY). 1997;277(5332):1684-7.

258. Casali BT, Corona AW, Mariani MM, Karlo JC, Ghosal K, Landreth GE. Omega-3 Fatty Acids Augment the Actions of Nuclear Receptor Agonists in a Mouse Model of Alzheimer's Disease. J Neurosci. 2015;35(24):9173-81.

259. Wahrle SE, Jiang H, Parsadanian M, Legleiter J, Han X, Fryer JD, et al. ABCA1 is required for normal central nervous system ApoE levels and for lipidation of astrocyte-secreted apoE. J Biol Chem. 2004;279(39):40987-93.

260. Hirsch-Reinshagen V, Zhou S, Burgess BL, Bernier L, McIsaac SA, Chan JY, et al. Deficiency of ABCA1 impairs apolipoprotein E metabolism in brain. J Biol Chem. 2004;279(39):41197-207.

261. Fitz NF, Cronican AA, Lefterov I, Koldamova R. Comment on "ApoE-directed therapeutics rapidly clear β-amyloid and reverse deficits in AD mouse models". Science. 2013;340(6135):924-c.

262. Kim J, Yoon H, Basak J, Kim J. Apolipoprotein E in synaptic plasticity and Alzheimer's disease: potential cellular and molecular mechanisms. Mol Cells. 2014;37(11):767-76.

263. Selkoe DJ. Alzheimer's disease is a synaptic failure. Science. 2002;298(5594):789-91.

264. Kim J, Basak JM, Holtzman DM. The role of apolipoprotein E in Alzheimer's disease. Neuron. 2009;63(3):287-303.

265. Yagi T. Clustered protocadherin family. Dev Growth Differ. 2008;50 Suppl 1:S131-40.

266. Junghans D, Heidenreich M, Hack I, Taylor V, Frotscher M, Kemler R. Postsynaptic and differential localization to neuronal subtypes of protocadherin beta16 in the mammalian central nervous system. Eur J Neurosci. 2008;27(3):559-71.

267. Frank M, Ebert M, Shan W, Phillips GR, Arndt K, Colman DR, et al. Differential expression of individual gamma-protocadherins during mouse brain development. Mol Cell Neurosci. 2005;29(4):603-16.

268. Obata S, Sago H, Mori N, Rochelle JM, Seldin MF, Davidson M, et al. Protocadherin Pcdh2 shows properties similar to, but distinct from, those of classical cadherins. J Cell Sci. 1995;108 ( Pt 12):3765-73.

269. Marsh SE, Abud EM, Lakatos A, Karimzadeh A, Yeung ST, Davtyan H, et al. The adaptive immune system restrains Alzheimer's disease pathogenesis by modulating microglial function. Proc Natl Acad Sci U S A. 2016;113(9):E1316-25.

270. Mosher KI, Wyss-Coray T. Microglial dysfunction in brain aging and Alzheimer's disease. Biochem Pharmacol. 2014;88(4):594-604.

271. Cordy JM, Hussain I, Dingwall C, Hooper NM, Turner AJ. Exclusively targeting beta-secretase to lipid rafts by GPI-anchor addition up-regulates beta-site processing of the amyloid precursor protein. Proc Natl Acad Sci U S A. 2003;100(20):11735-40.

272. Kang MJ, Chung YH, Hwang CI, Murata M, Fujimoto T, Mook-Jung IH, et al. Caveolin-1 upregulation in senescent neurons alters amyloid precursor protein processing. Exp Mol Med. 2006;38(2):126-33.

273. Sebastiao AM, Colino-Oliveira M, Assaife-Lopes N, Dias RB, Ribeiro JA. Lipid rafts, synaptic transmission and plasticity: impact in age-related neurodegenerative diseases. Neuropharmacology. 2013;64:97-107.

274. Sun JH, Yu JT, Tan L. The role of cholesterol metabolism in Alzheimer's disease. Mol Neurobiol. 2015;51(3):947-65.

275. Malm TM, Jay TR, Landreth GE. The evolving biology of microglia in Alzheimer's disease. Neurotherapeutics. 2015;12(1):81-93.

276. Uchoa MF, Moser VA, Pike CJ. Interactions between inflammation, sex steroids, and Alzheimer's disease risk factors. Front Neuroendocrinol. 2016;43:60-82.

277. Guerreiro R, Wojtas A, Bras J, Carrasquillo M, Rogaeva E, Majounie E, et al. TREM2 variants in Alzheimer's disease. N Engl J Med. 2013;368(2):117-27.

278. Greendale GA, Derby CA, Maki PM. Perimenopause and cognition. Obstet Gynecol Clin North Am. 2011;38(3):519-35.

279.    Li R, Singh M. Sex differences in cognitive impairment and Alzheimer's disease. Front Neuroendocrinol. 2014;35(3):385-403.

280.    Farrer LA, Cupples LA, Haines JL, Hyman B, Kukull WA, Mayeux R, et al. Effects of age, sex, and ethnicity on the association between apolipoprotein E genotype and Alzheimer disease. A meta-analysis. APOE and Alzheimer Disease Meta Analysis Consortium. JAMA. 1997;278(16):1349-56.

281.    Payami H, Montee KR, Kaye JA, Bird TD, Yu CE, Wijsman EM, et al. Alzheimer's disease, apolipoprotein E4, and gender. JAMA. 1994;271(17):1316-7.

282.    Cacciottolo M, Christensen A, Moser A, Liu J, Pike CJ, Smith C, et al. The APOE4 allele shows opposite sex bias in microbleeds and Alzheimer's disease of humans and mice. Neurobiol Aging. 2016;37:47-57.

283.    Liu CC, Kanekiyo T, Xu H, Bu G. Apolipoprotein E and Alzheimer disease: risk, mechanisms and therapy. Nat Rev Neurol. 2013;9(2):106-18.

284.    O'Reilly JA, Lynch M. Rosiglitazone improves spatial memory and decreases insoluble Abeta(1-42) in APP/PS1 mice. J Neuroimmune Pharmacol. 2012;7(1):140-4.

285.    Searcy JL, Phelps JT, Pancani T, Kadish I, Popovic J, Anderson KL, et al. Long-term pioglitazone treatment improves learning and attenuates pathological markers in a mouse model of Alzheimer's disease. J Alzheimers Dis. 2012;30(4):943-61.